

Functional Asymmetry Within the Sec61 Translocon

with the addendum

Disulfide Loops of Peptide Hormones as a Motif for Protein Aggregation

Inauguraldissertation

zur

Erlangung der Würde eines Doktors der Philosophie
vorgelegt der
Philosophisch-Naturwissenschaftlichen Fakultät
der Universität Basel

von

Erhan Demirci
aus Aachen, Deutschland

Basel, 2017

Originaldokument gespeichert auf dem Dokumentenserver der Universität Basel
edoc.unibas.ch

Genehmigt von der Philosophisch-Naturwissenschaftlichen Fakultät

auf Antrag von

Prof. Dr. Martin Spiess

Prof. Dr. Anne Spang

Basel, den 19.09.2017

Prof. Dr. Martin Spiess

Dekan

“Everything in life is just for a while.”

Philip K. Dick
A Scanner Darkly

To my wife

Acknowledgements

I wish to extend my deepest gratitude to Prof. Dr. Martin Spiess, who continuously has supported and encouraged me especially in times of hardship.

Special thanks to Nicole Beuret and Tina Junne, who always offered a helping hand, shared their expertise and relentlessly combated entropy in the lab.

My appreciation to all members of the Spiess group: Cristina Baschong, Anna Brunauer, Dominik Buser, Marco Janoschke, Dr. Valentina Millarte, Mirjam Pennauer, Jennifer Reck, Simon Schlienger and Dr. Daniela Stadel, for both the world's most meaningful and the most senseless conversations and for creating a unique and great atmosphere.

1.	FUNCTIONAL ASYMMETRY WITHIN THE SEC61 TRANSLOCON	7
1.1	GENERAL INTRODUCTION	8
1.1.1	<i>Common Structural Principles of Membrane Proteins.....</i>	8
1.1.2	<i>Co-translational Translocation.....</i>	9
1.1.3	<i>SRP-independent translocation.....</i>	13
1.1.4	<i>The Translocon.....</i>	19
1.1.5	<i>Membrane Insertion at the Sec61 translocon.....</i>	26
1.2	AIM OF PART I	38
1.3	SUMMARY	40
1.4	INTRODUCTION	40
1.5	RESULTS.....	43
1.5.1	<i>Integration Efficiency Depends on the Distribution of Leucines in the H Segment.....</i>	43
1.5.2	<i>Hydrophobicity at the Apolar Constriction in Sec61p Lowers Membrane Integration.....</i>	47
1.5.3	<i>The 6A Translocon Mutant Retains Asymmetry of Integration.....</i>	50
1.5.4	<i>Hydration Profile of Wild-type and Mutant Translocons</i>	50
1.6	DISCUSSION	52
1.7	MATERIALS AND METHODS.....	54
1.8	CONCLUDING REMARKS.....	56
2.	SHORT DISULFIDE LOOPS OF PEPTIDE HORMONES AS A MOTIF FOR PROTEIN AGGREGATION	59
2.1	GENERAL INTRODUCTION	60
2.1.1	<i>ER Quality Control Ensures Correct Folding.....</i>	60
2.1.2	<i>Misfolded Proteins are Degraded by the Ubiquitin/Proteasome System.....</i>	61
2.1.3	<i>ER Stress Triggers the Unfolded Protein Response</i>	63
2.1.4	<i>Transport between ER and Golgi is bidirectional</i>	65
2.1.5	<i>Two Non-Exclusive Models Describe Transit through the Golgi Apparatus.....</i>	68
2.1.6	<i>Secretory Granules Store their Cargo in the Regulated Secretion Pathway.....</i>	69
2.2	DIABETES INSIPIDUS	71
2.2.1	<i>Vasopressin Regulates Water Homeostasis</i>	71
2.2.2	<i>Mutations in the Vasopressin Precursor cause Diabetes Insipidus.....</i>	74
2.2.3	<i>Amyloids as a Storage Mechanism in Secretory Granules</i>	77
2.2.4	<i>Several Peptide Hormones Share a Structural Similarity.....</i>	78
2.3	AIM OF PART II	81
2.4	SUMMARY	82
2.5	INTRODUCTION	82
2.6	RESULTS.....	85
2.6.1	<i>Disulfide Loops Mediate Aggregation of a Misfolded Provasopressin Carrier in Neuronal Cell Lines</i>	86
2.6.2	<i>Disulfide Loops are Sufficient to Drive Protein Aggregation in Constitutively Secreting Cells</i>	89
2.6.3	<i>Constructs Containing the N-Terminal Disulfide Loop of Prolactin Exit Frequently Exit the ER.....</i>	92
2.7	DISCUSSION	93
2.8	MATERIALS AND METHODS.....	96
3.	REFERENCES.....	99

1. Functional Asymmetry Within the Sec61 Translocon

1.1 General Introduction

1.1.1 Common Structural Principles of Membrane Proteins

Proteins are macromolecules composed of 20 different amino acids as building blocks that are covalently linked via peptide bonds. The sequence of amino acids is specific for every protein and is referred to as the primary structure. The primary sequence contains all information required for the protein to reach its native conformation. In live cells, this process is assisted by chaperones that bind to partly folded polypeptides to prevent aggregation until the protein has reached its state of minimized free energy.

While every protein embodies a final unique structure, specific folding patterns within parts of it can be found regularly. Both the α -helix and the β -sheet were described in the early 1950s (Pauling and Corey, 1951; Pauling, et al., 1951) and have been found to be particularly common folding motifs. The reason for this lies within the structure: since these motifs are the result of hydrogen bonds forming between the backbone amino- and carbonyl-groups, no amino acid side chains are involved and the helix or sheet can thus include nearly all amino acids.

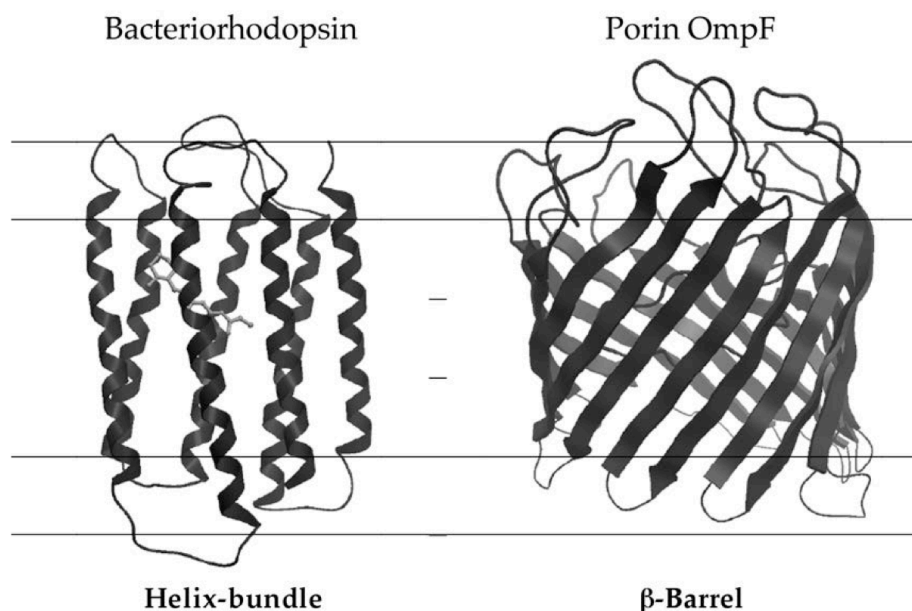


Figure 1: Multispanning membrane proteins arrange their α -helices as helix-bundles (left), while β -sheets form a barrel-like structure (right). Every 3.6 residues, the helix fulfils a turn with a length of 0.54nm. In the β -sheet, every third residue is 0.7nm apart. Spiess, personal correspondence.

In the α -helix, the polypeptide chain assumes a cylindrical shape due to the backbone performing a twist. The structure is stabilized by hydrogen bonds forming regularly between every fourth peptide bond, allowing the helix to reach a complete turn every 3.6 amino acids. The amino acid side chains are facing towards the outside of this helix. The β -sheet is stabilized by hydrogen bonds forming between the polypeptide backbones of several almost completely extended strands, which can be both parallel or antiparallel. The amino acid side chains stick out of this plane alternatingly facing upwards or downwards. α -helices, β -sheets and β -turns assemble to soluble proteins that fold by sidechain interactions and the hydrophobic effect, concealing hydrophobic parts inside the protein and exposing hydrophilic parts on the surface. Membrane proteins, in contrast, have a hydrophobic surface which is embedded in the hydrophobic core of the lipid bilayer. The majority of membrane proteins traverse the membrane with multiple segments. In these multispanning proteins, two principal architectures can be found: helix-bundles and β -barrels (**Figure 1**), formed by bundles of hydrophobic transmembrane α -helices (left) or a closed β -sheet (right) with antiparallel transmembrane strands, where every second residue is hydrophobic and faces the lipid environment.

1.1.2 Co-translational Translocation

Eukaryotic cells are divided into several membrane-enclosed organelles. This allows the cell to maintain several specialized compartments, each with a repertoire of distinct enzymes and functionalities. To achieve and maintain this degree of specificity, proteins have to be targeted to their destination organelles and may have to be translocated across membranes during the process (Palade, 1975). This is promoted via the recognition of specific signal sequences.

The predominant pathway for translocation in eukaryotic cells is co-translational. This process depends on recognition of the ribosome-nascent chain complex (RNC) and its relocation to the endoplasmic reticulum (ER) membrane and the Sec61 translocon (**Figure 2**).

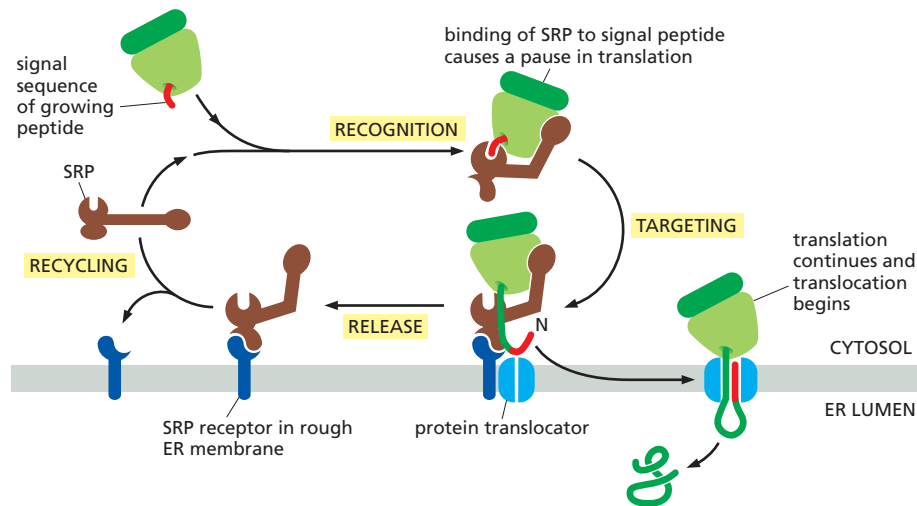


Figure 2: SRP binds a signal sequence as it emerges from the ribosome and stalls translation. The SRP-ribosome complex is then targeted to the ER membrane, where SRP engages with its receptor SR at the translocon. The nascent chain is inserted into the the protein translocator Sec61. Subsequently, SRP dissociates from SR and is recycled. Alberts (2016).

A typical signal sequence for co-translational ER import is localized at the N-terminus of a protein, 15-30 residues long and hydrophobic. While this motif does not seem to display conservation in its sequence, it characteristically presents five to seven residues counting downstream the potential cleavage site that are called “c-region”, followed by the “h-region”, usually containing 6-8 hydrophobic residues (Leu, Ala, Met, Val, Ile, Phe, Trp) that form a hydrophobic core with a helical conformation, and the N-terminal “n-region” with positively charged residues (von Heijne, 1983). While the length and composition are variable, the hydrophobicity and a net positive charge are hallmarks of signal sequences (Gierasch, 1989).

The signal sequence, as it emerges from the ribosomal exit site, is recognized by a conserved ribonucleoprotein complex called SRP (signal recognition particle). In mammals, SRP is comprised of six proteins (SRP9, SRP14, SRP19, SRP 54, SRP68 and SRP72, named after their apparent molecular weight) and one RNA molecule (7S or SRP RNA, 4.5S in bacteria) (Walter and Blobel, 1980; Walter and Blobel, 1982). SRP contains two domains: the Alu domain and the S domain (**Figure 3**). The Alu domain (formed by SRP9, SRP14 and domain I of the 7S RNA, while protein free in prokaryotes; Kempf et al., 2014) is responsible for an elongation arrest of nascent chains that occurs after SRP binding. This halt in translation ensures a time frame large enough to relocate the translation machinery to the ER, preventing a growing

peptide chain from misfolding in the cytosol and ensuring correct insertion into the translocation complex (Blobel and Sabatini, 1971; Mason et al., 2000; Thomas et al., 1997; Walter and Blobel, 1981). It is suggested that the Alu domain extends to the active site of the ribosome and competes with elongation factors at the ribosomal elongation factor binding site (Halic et al., 2004; Ogg and Walter, 1995).

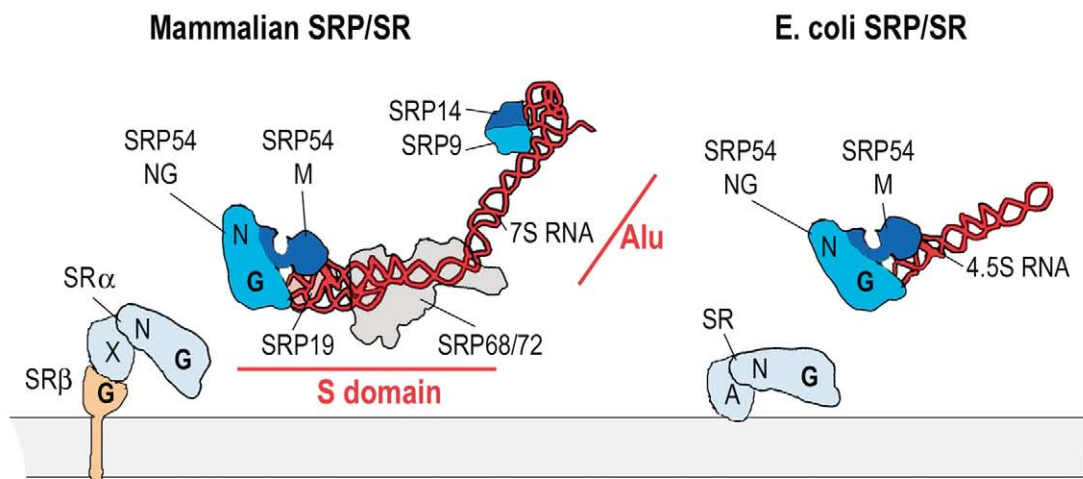


Figure 3: SRP in both *E. coli* and mammals consist of an M domain and a NG domain. The latter interacts with the corresponding domains of its homologous domain of SR. Bacterial SRP is comprised of fewer subunits and shorter RNA. Halic and Beckmann (2005).

SRP54 (Ffh in bacteria) as part of the S domain has been identified as the subunit to bind the ribosome-nascent chain complex (Kurzchalia et al., 1986). The fact that the signal sequence itself is not conserved gave rise to a model that suggests a methionine-rich domain (M-domain) of SRP54 to provide a hydrophobic binding pocket that can accommodate many different signal sequences due to the flexibility of methionine side chains (Bernstein et al., 1989) and is occupied by a short helix in the unbound state (Voorhees and Hegde, 2015). This overall interaction was confirmed by crystallography studies of different SRP54-signal peptide fusions (Hainzl et al., 2011; Janda et al., 2010). While the binding of SRP to the signal peptide is not dependent on the length of the nascent chain (Flanagan et al., 2003) and is overall rather weak (Bradshaw et al., 2009), RNC-SRP complex formation appears to be additionally stabilized by interactions of ribosomal proteins with SRP54 (Akopian et al., 2013; Halic et al., 2004).

Since SRP recognizes and binds a variety of sequences, elucidating the patterns of cargo fidelity has been of large interest. Cargo binding alone appears not to be sufficient to reliably discriminate correct from incorrect cargo. However, additional checkpoints besides cargo binding have been discovered, such as during SRP-SR assembly, control of the kinetic activity of GTP hydrolysis occurring prior to translocation, and further rejection of incorrect signal sequences by Sec61p (Jungnickel and Rapoport, 1995; Zhang et al., 2010).

The targeting of the SRP-bound RNC occurs via the SRP receptor (SR, FtsY in bacteria), a heterodimer that is bound to the ER membrane and composed of SR α and SR β . SR α is a homolog of SRP54 (Miller et al., 1995), and both protein domains contain a N-terminal four-helix bundle (N-domain) and a GTPase domain (G domain) which are closely associated and referred to as the NG domain. The interaction of the SRP-RNC complex with SR is facilitated through an interaction of their respective NG domains and regulated through GTP hydrolysis: bound GTP on both SRP54 and SR α is a prerequisite to the formation of the complex, whereas its dissociation is initiated after GTP hydrolysis. The SRP/SR-GTPase interaction is however distinct from classical GTPase switches, where external factors are required (Saraogi et al., 2011). When GTP is bound, both protein domains are found in an “open” state where their affinity to each other is very low. Complex formation is in contrast favored over 10000-fold once cargo is bound to SRP (Shen et al., 2011). Conformational changes during this process lead to interaction of SRP and SR via an intermediate “early” state to the “closed” state, which permits the GTPase domains to form contact sites and to subsequently release the cargo to the nearby translocon. This in turn allows reciprocal hydrolysis of their bound GTPs at the respective active sites, favoring disassembly and recycling of both SRP and SR (Zhang et al., 2009). It is believed that this mode of multistate GTPase regulation grants efficient control and coordination of cargo selection and targeting (Zhang et al., 2010). In this regard, the GTP-bound form of SR β is required to mediate the association with SR α (Schwartz and Blobel, 2003) and the Sec61 β subunit of the translocon may act as a nucleotide exchange factor (Helmers et al., 2003).

1.1.3 SRP-independent translocation

1.1.3.1 SecA is Involved in Post-Translational Translocation in Bacteria

In parallel to the co-translational pathway, proteins may also be translocated or integrated into the membrane post-translationally. While this is more common in prokaryotes, a substantial fraction of secretory proteins is probably conveyed in a SRP-independent manner in eukaryotes as well (Ast et al., 2013). Post-translationally translocated proteins may be too short to engage the SRP machinery (Goder et al., 2000; Zimmermann et al., 1990) or may not be hydrophobic enough to guarantee proper SRP interaction (Ng et al., 1996). The post-translational translocation pathway therefore depends on alternative modes as opposed to direction of the RNC to the ER. Calmodulin (Shao and Hegde, 2011), TRC40 (Johnson et al., 2012) and cytosolic Hsp40/Hsp70 (Ngosuwan et al., 2003) are known to act as chaperones during recognition, in that they prevent misfolding and interact with specialized ER-bound receptors for targeting the fully synthesized protein to the Sec61 translocon.

In bacteria, the SecA dependent pathway mediates translocation of fully synthesized polypeptides. While dimerization has been observed, the suggested mode of action is as a monomer (Or et al., 2005; Zimmer et al., 2008). It is comprised of several domains: two nucleotide-binding domains (NBD1 and NBD2) that together bind one molecule of ATP (Hunt et al., 2002; Papanikolaou, 2007), a helical scaffold domain (HSD, containing the “two-helix finger”), one polypeptide-cross-linking domain (PPXD) over which SecA interacts with the polypeptide chain, and a helical wing domain (HWD) (**Figure 4**).

During polypeptide binding, the PPXD domain tilts in an 80-degree angle and applies grip on the substrate. PPXD, NBD2 and parts of HSD are involved and form a structure dubbed as “clamp”. Interaction and recognition with polypeptides appears to be orchestrated by opening and closing of this clamp. For this, a highly conserved tyrosine residue in the two-helix finger domain is supposed to be a key feature (Erlandson et al., 2008). Recognition of β -strands in the substrate that complement a β -sheet at the clamp is also proposed for substrate recognition (Zimmer et al., 2009).

With the bound substrate, one molecule of SecA interacts with one molecule of SecY. The clamp is positioned directly over the translocon pore, which enables the polypeptide to be pushed into the opening (Bauer and Rapoport, 2009). This is believed to occur via insertion of the two-helix finger into the cytosolic cavity and the polypeptide along with it. Subsequent ATP hydrolysis leads to a conformational change that positions the substrate deeper in the translocon. Upon ATP regeneration, SecA reverts to its open state and both the clamp and the two-helix finger are reset. SecA-mediated translocation is assisted by the multispanning SecD/F complex that is believed to apply a pulling force at the periplasmic side, utilizing the influx of protons over aspartate and arginine residues to couple conformational changes with active pulling of the substrate (Tsukazaki et al., 2011).

Prior to SecA-mediated translocation, chaperone binding to the polypeptide is a prerequisite to prevent misfolding and aggregation. The homotetrameric SecB protein is a chaperone known to present this feature (Xu et al., 2000), although it is apparently not essential for viability and only a small number of *E. coli* proteins have been identified to rely on SecB (van der Sluis and Driessen, 2006). It specifically recognizes unfolded polypeptides, however not exclusively at defined sequences, but rather at short stretches rich in aromatic and basic residues. The engagement into either the SRP-dependent pathway or SecB-mediated translocation is decided during synthesis by Trigger Factor. This ribosome-associated chaperone is the first factor known to interact with the nascent chain (Beck et al., 2000; Valent et al., 1995). While SRP has a strong affinity to bind hydrophobic signals as they emerge from the ribosome, Trigger Factor is believed to delay the folding of non-SRP bound polypeptides and grant SecB a longer timespan to interact with it, eventually leading to localization towards the Sec translocon and post-translational translocation (Driessen et al., 2008).

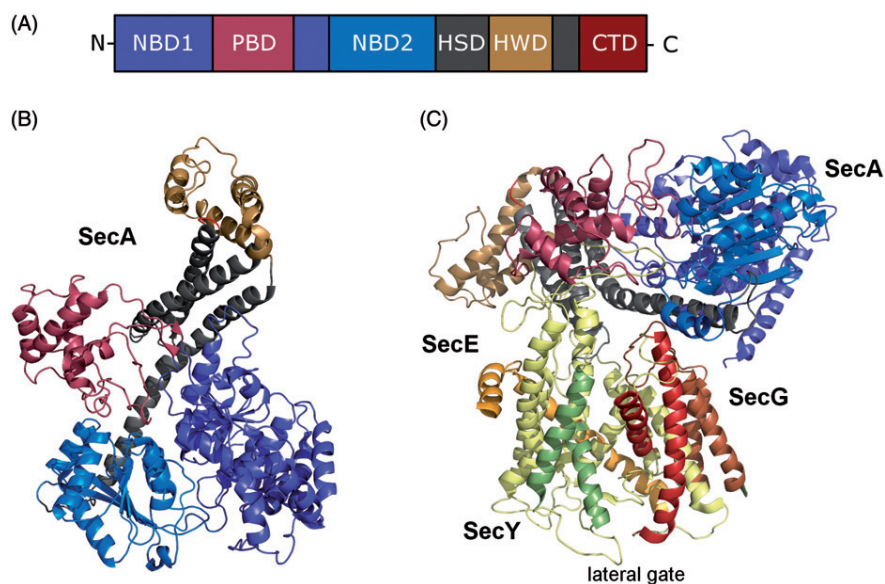


Figure 4: Structure of SecA. (A) Overview of the domain organisation. NBD: nucleotide binding domain, PBD: peptide-cross-linking domain, HSD: helical scaffold domain, HWD: helical wing domain, CTD: C-terminal domain. (B) Crystal structure. (C) SecA-SecYEG-complex, with the lateral gate for membrane insertion facing frontwards. Denks et al. (2014).

1.1.3.2 The Eukaryotic Sec62/Sec63 Complex is Involved in Post-Translational Translocation

In yeast, Sec61 is known to interact with the tetrameric Sec62/63 complex during post-translational translocation, with which it forms a functional complex comprised of seven components (Deshaies et al., 1991), including Sec71p and Sec72p which are not present in mammals (Meyer et al., 2000). Furthermore, Kar2p (BiP in mammals) is involved (Panzner et al., 1995). After the initiation of translocation and the shedding of bound chaperones (Plath et al., 2000), ATP-dependent BiP binding and release cycles in the lumen act as a ratchet that introduces directional pull and prevents the polypeptide from exiting the channel back into the cytosol due to brownian motion (Matlack et al., 1999). The hydrolysis of ATP is supported by a specific luminal domain of Sec63, the J-domain. The ADP-bound form of BiP interacts tightly with the polypeptide chain and prevents its backward movement, whereas the ATP-bound state has a weaker affinity and allows BiP to dissociate. In the meantime, other BiP molecules may bind the polypeptide chain (Misselwitz et al., 1999) (**Figure 5**). Because of the dependence on its activation by the J-domain, BiP binding may only occur in the proximity of the channel, which further enhances the

efficiency of preventing the polypeptide's movement back to the cytosol (Osborne et al., 2005).

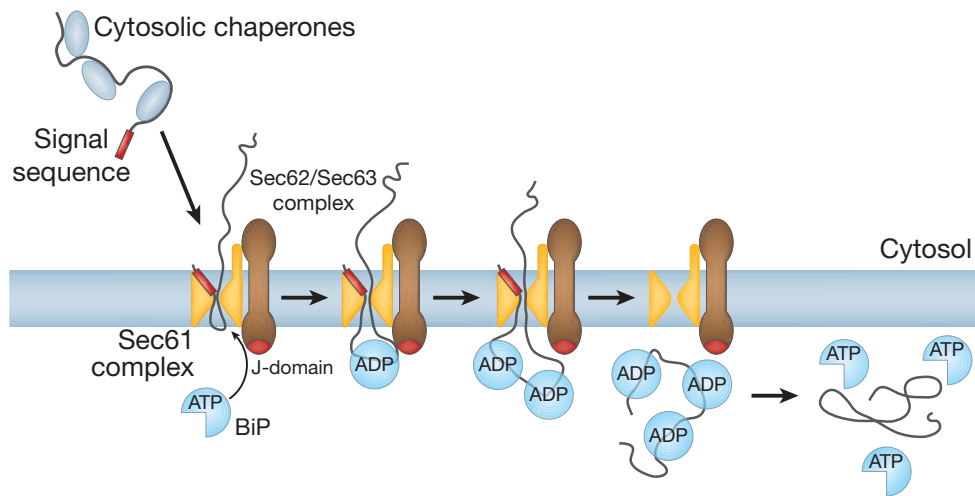


Figure 5: Model of post-translational translocation in eukaryotes. The Sec62/63-complex accepts chaperone-bound cargo and hands it over to the Sec61 complex, where it is inserted into the pore and translocated. On the luminal side, Kar2/Bip interacts with the translocated chain and is activated by the J-domain of Sec63. Rapoport (2007).

1.1.3.3 The GET Machinery Inserts Tail-Anchored Proteins into the Membrane

Tail-anchored proteins lack a classical signal sequence and are characterized by a single transmembrane segment near the C-terminal region. Long N-terminal domains project into the cytosol, while the part exposed to the lumen is approximately 30-40 amino acids long (Borgese et al., 2003). Tail-anchored proteins can be found in all organisms and carry out various functions in the cell, with an estimation of 200-400 genes coding for this type of proteins (Kalbfleisch et al., 2007). Well-known examples are proteins of the SNARE family or Sec61 β /Sec61 γ .

The class of tail-anchored proteins was early recognized to follow a pathway different from SRP-mediated targeting and Sec61-mediated membrane integration. Instead, this occurs post-translationally utilizing a different machinery (Kim et al., 1997; Kim et al., 1999; Kutay et al., 1993; Kutay et al., 1995). In parallel to the co-translational pathway, it was assumed that the hydrophobic domain must be shielded in a chaperone-mediated manner. Hsp40/Hsc70 were found to recognize these sequences, to interact and to be sufficient to mediate membrane insertion. However,

the mechanisms are unknown and the interaction with Hsp40/Hsc70 only accounts for a minority of tail-anchored proteins (Abell et al., 2007; Rabu et al., 2008). In parallel, a novel pathway with the ATPase Get3 (TRC40 in mammals, TMD recognition complex of 40kD) was identified in yeast to interact with hydrophobic substrate domains in a ribosome-free manner (Stefanovic and Hegde, 2007). Get1 and Get2 serve as a docking complex at the ER membrane and are responsible for the recruitment of Get3 without the necessity of ATP hydrolysis. When either of these two factors is absent, Get3 loses its ability to target to the ER (Schuldiner et al., 2008).

Get3 was shown to form a homodimer over distinct helical domains that can rearrange upon ATP hydrolysis. They then reveal a methionine-rich hydrophobic pocket that can accommodate an α -helical structure of approximately 20 residues. This is reminiscent of the M-domain of SRP54 binding a signal sequence (Bozkurt et al., 2009; Mateja et al., 2009). A complex of Get4 and Get5 is thought to facilitate and improve the recognition and interaction between Get3 and the substrate. This is achieved by the recruitment of Sgt2 (SGTA in mammals), which binds the substrate sequence and transfers it to Get3. Get4/Get5/Sgt2 are believed to act as a loading complex towards Get3 (Jonikas et al., 2009; Wang et al., 2010).

In mammals, TRC35 and Ubl4A are homologs of Get4 and Get5. The TRC35/Ubl4A/SGTA complex acts like Get4/Get5/Sgt2 in yeast (Leznicki et al., 2010; Mariappan et al., 2010) (**Figure 6**). Bag6 in mammals (no known yeast homolog) and Sgt2 supposedly provide additional fidelity during the recognition of substrate sequences by associating with ribosomes at their exit site and capturing the substrate after its synthesis. This is especially important in regard to the presence of other chaperones in the cytosol that might also interact with the hydrophobic domain. Furthermore, Bag6 and SGTA are proposed to create a link to protein degradation, as they can recruit ubiquitination complexes (Hessa et al., 2011; Xu et al., 2012). The precise mechanisms of these functions remain elusive.

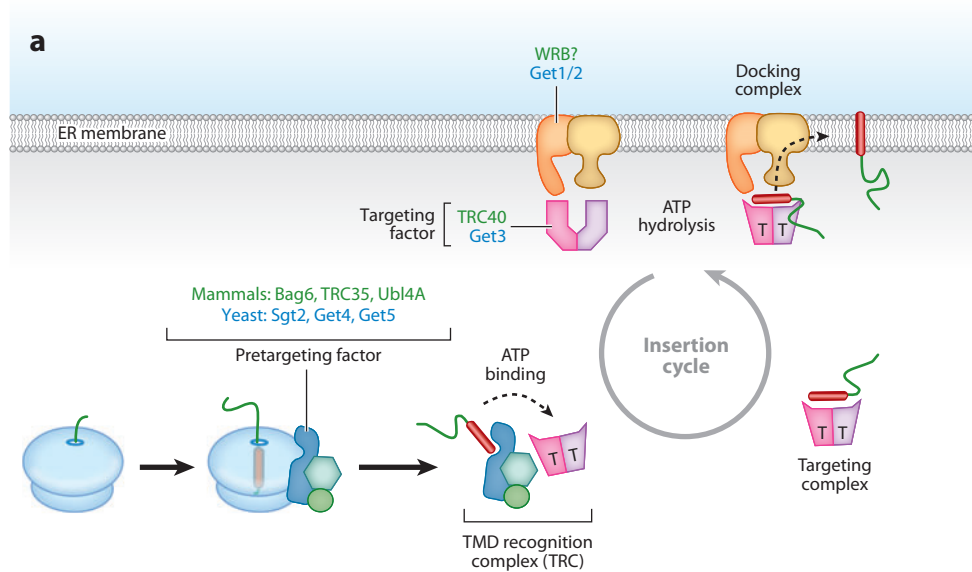


Figure 6: Insertion of tail-anchored proteins is facilitated by the GET pathway. The pretargeting factor associates with the ribosome during the synthesis of a tail-anchored protein. After translation, the protein is transferred to the targeting complex, consisting of Get3 in yeast and TRC40 in mammals. Get3/TRC40 has ATPase activity and substrate interaction is believed to occur when ATP is bound (represented by T). The protein is targeted to a receptor at the ER membrane and inserted into the membrane. After ATP hydrolysis, the targeting factor is recycled. Shao and Hegde (2011).

1.1.3.4 SND proteins mediate SRP-independent targeting to the endoplasmic reticulum

In parallel to GET and SRP-mediated pathways, proteins may also be targeted to the ER via SND proteins (SRP-independent targeting), which are believed to act complementary to these mechanisms. Snd1, Snd2 and Snd3 were shown to back up the aforementioned targeting pathways when made unavailable. Snd1 is localized in the cytosol as a suggested peripheral ribosomal interactor. Snd2 and Snd3 are transmembrane proteins localized at the ER, where they are associated with auxiliary components of the translocon complex (Ghaemmaghami et al., 2003). Aviram et al. (2016) suggested that, in yeast, SRP, GET and SND targeting work in concert, with gradual affinities for each pathway displayed by the substrates. The precise underlying mechanisms as well as means of regulation are yet unclear.

1.1.4 The Translocon

1.1.4.1 Several Subunits Form the Translocon Complex

The Sec61 translocon consists of three subunits and is conserved among eukaryotes, bacteria and archaea (**Figure 7A**). The largest α unit (Sec61 α in mammals, Sec61p in *S. cerevisiae*, SecY in archaea and bacteria) forms the protein-conducting channel with its ten membrane-spanning helices and is divided into two pseudosymmetrical clam-like halves with the loop between transmembrane helices (TMs) 5 and 6 acting as a connecting hinge. Membrane proteins can leave the channel over a lateral gate and be inserted into the lipid bilayer. The pore contains a constriction ring of six hydrophobic residues and a plug that is formed by the helix 2A in the luminal cavity (**Figure 7B**). The γ unit (Sec61 γ in mammals, Sss1p in *S. cerevisiae*, SecE in archaea and bacteria) contains a single-spanning transmembrane segment and an amphipathic helix that lies on the cytosolic surface and connects with both halves of the α unit. These subunits show strong homology between all organisms and are essential for survival in *E. coli* and *S. cerevisiae*. In contrast, the β subunit (Sec61 β in mammals, Sbh1p in *S. cerevisiae*, SecB in archaea, SecG in bacteria) shows homology in eukaryotes and archaea, but no strong similarity in bacteria and is not essential for viability. The crystal structure of the SecY complex of *M. jannaschii* has contributed much to the understanding of protein translocation (van den Berg et al., 2004) and it has been shown that the overall architecture of the translocon is identical in *E. coli* (Jomaa et al., 2016) and mammals (Voorhees and Hegde, 2015).

It has been theorized in the past that Sec61/SecY complexes may require oligomerization for translocation to occur, and indeed there is evidence for a ring-line structure composed of four Sec61 complexes (Beckmann et al., 2001; Menetret et al., 2005). Oligomers in bacteria also have been proven to exist (Deville et al., 2011). Here, it has been debated that one SecY molecule might assist the translocation of a peptide through a neighboring unit by providing a binding site for SecA, which then pushes the chain through the second channel (Osborne and Rapoport, 2007), but it is also known that one copy of SecY (Kedrow et al., 2011) or a single Sec61 complex

(Kalies et al., 2008) is sufficient for translocation. The latter work showed that a nascent chain even destabilizes the Sec61 complex tetramer. Via crosslinking both a nascent chain and its signal peptide to one SecY molecule, it was shown that both initiation of translocation and translocation itself is handled by one and the same translocon unit (Osborne and Rapoport, 2007). EM studies also revealed complex formation of both idle and translating ribosomes with a single translocon copy (Becker et al., 2009; Menetret et al., 2008). Therefore, there is strong evidence that the functional protein-conducting channel is formed by one single copy. The role of the observed oligomer complexes is unclear.

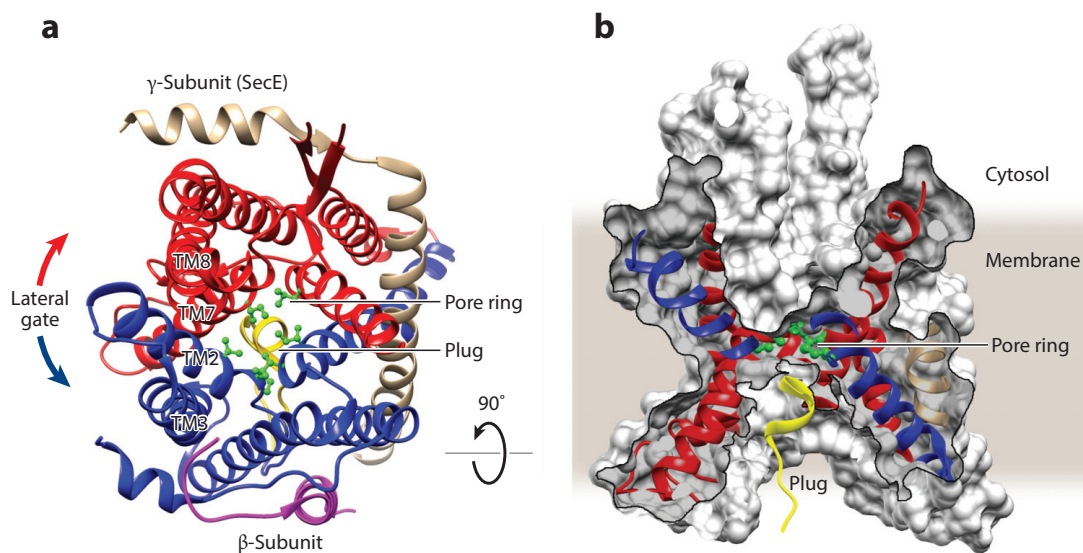


Figure 7: SecY crystal structure of the idle channel, *M. jannaschii* (PDB: 1RH5). (A) Cytosolic view. The N- and C-terminal pseudosymmetrical halves are shown in blue and red. The lateral gate allows transit of transmembrane domains into the lipid surroundings. The pore ring residues are shown in green, the plug helix in yellow. (B) Side view. Rapoport et al. (2017).

1.1.4.2 The Translocon Interacts with Various Proteins

An overview of interacting partners in eukaryotes was provided by Denks et al. (2014). Recent progresses in cryo-electron tomography could identify Sec61, TRAP (translocon associated protein complex) and OST (oligosaccharyl transferase) forming a large complex (Pfeffer et al., 2014). This does not imply that there are no other interacting partners, but that these might not be part of a stable complex and instead are transiently recruited during co- or post-translational translocation in a

dynamic and substrate-dependent manner, as suggested by Conti et al. (2015) and Pfeffer et al. (2016).

- Sec62 and Sec63 (homologous in yeast and mammals, essential in yeast) (Rothblatt et al., 1989) are involved in post-translational translocation. Sec63 interacts over its luminal J-domain with BiP. Sec63 also influences co-translational translocation; the mammalian variant has a ribosome interaction site (Müller et al., 2010).
- Besides Sec62 and Sec63, Sec71 and Sec72 (yeast) facilitate both co- and posttranslational translocation via Sec61. The Sec71/Sec72 complex can recruit cytosolic members of the Hsp70 family: Ssa1, which is believed to be involved in substrate interaction in post-translational translocation, and Ssb1 for co-translational translocation. The mechanisms are largely unknown (Tripathi et al., 2017).
- Kar2/BiP (binding protein, homologous in yeast and mammals) is a luminal protein of the Hsp70-family. Its best-studied function is the interaction with the translocated nascent chain and the function as a molecular ratchet (Nicchitta & Blobel, 1993). The J-domain of Sec63 mediates BiP activity (Lyman and Schekman, 1995). BiP was shown to interact with loop 7 of Sec61 α and prevent Ca²⁺ leakage (Alder et al., 2005; Schäuble et al., 2012).
- While BiP lumenally provides a means of calcium efflux inhibition, calmodulin (homologous in yeast and mammals) does the same on the cytosolic side over the N-terminal part of Sec61 α (Erdmann et al., 2011). A role in the targeting of substrates during post-translational translocation has been proposed (Shao and Hegde, 2011).
- The chaperone calnexin (homologous in yeast and mammals) fulfils functions during the quality control of glycoproteins (Benyair et al., 2011). It is preferentially located in the perinuclear rough ER, where it was shown to interact with the ribosome-translocon complex and recruit the actin skeleton, potentially to improve its stability (Lakkaraju et al., 2012).
- TRAM (translocating chain-associated membrane protein, mammals) interacts with nascent chains during translocation and is thought to assist during the topogenesis of multispanning membrane proteins (Shao and Hegde, 2011).

- TRAP (translocon associated protein complex, mammals) acts in heterotetrameric complexes that bind Sec61 (Hartmann et al., 1993). A role in the topogenesis of transmembrane segments has been proposed by Sommer et al. (2013), where it was found to favor their C-terminal translocation while moderating flanking charges and the positive-inside rule, but not hydrophobicity. TRAP binds to the ribosomal protein L38 and to rRNA as well as to Sec61 at its hinge region, suggesting the ability to influence its conformation and to interact with nascent chains (Pech et al., 2010).
- OST (oligosaccharyl transferase, homologous in yeast, mammals and some prokaryotes) (**Figure 8**). It co-translationally glycosylates at Asn-X-Ser/Thr (with X for any amino acid except proline) in that it transfers a branched $\text{Glc}_3\text{Man}_9\text{GlcNAc}_2$ molecule *en bloc* from the donor dolichol via introducing a N-glycosidic bond. In yeast, OST is represented as a hetero-oligomer with at least eight known subunits, of which SST3 shows catalytic activity. In mammals, its isoforms SST3A and SST3B are responsible for co- and post-translational glycosylation (Ruiz-Canada et al., 2009). Interactions with the ribosomal exit site and the Sec61 complex have been demonstrated (Harada et al., 2009; Karaoglu et al., 1997; Pfeffer et al., 2014). The association with the translocon appears to show cell type dependence (Mahamid et al., 2016).
- Signal peptidases (universally conserved). After targeting a nascent chain to the ER, cleavable signals are recognized and removed. In bacteria, SPases are categorized into three groups (Auclair et al., 2012), of which SPase I (LepB in *E. coli*) is involved in the processing of proteins in the secretory pathway. The groups II and IV mediate signal cleavage of lipoproteins and prepilin proteins. SPase I in bacteria acts as a monomer over a Ser-Lys dyad catalyzing the cleavage, classifying it as a serine protease, whereas eukaryotes show multimeric signal peptidase complexes (SPC). Their catalytic activity originates from a subunit that is homologous to LepB, namely Sec11 in yeast (van Valkenburgh et al., 1999) and Spc18/Spc21 in mammals (Liang et al., 2003). In contrast to SPase I, eukaryotic signal peptidases act with a Ser-His-Asp triad. The cleaved signal peptide is degraded and recycled by signal peptide peptidase (Nam and Paetzel, 2013).

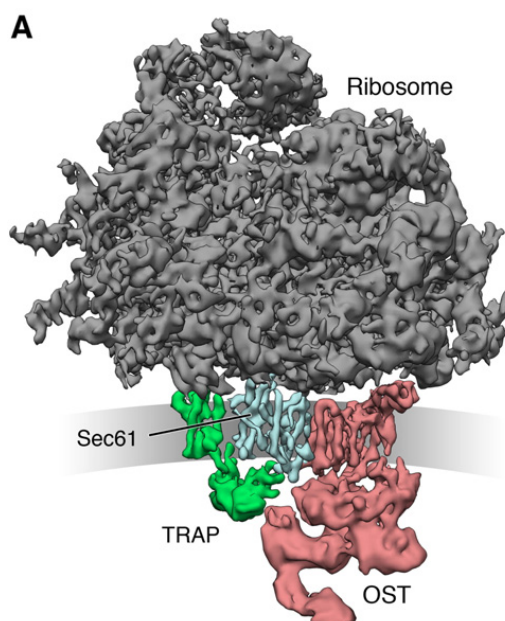


Figure 8: The structure of the ribosome-bound Sec61 translocon associated with interacting proteins. Tomographic densities of the ribosome, Sec61, TRAP and OST are shown. Modified from Pfeffer et al. (2016).

1.1.4.3 The Translocon is Primed and Opened by RNC Interactions

Recent studies characterized the effects of Sec61 interaction with the ribosome regarding its role in the activation of the translocon. Upon interaction, the ribosome initiates slight conformational changes referred to as “priming” of the channel for the following translocation process. It is known that ribosome binding to Sec61/SecY occurs at its cytosolic loops, formed between the transmembrane segments TM8 and TM9 and between TM6 and TM7, both of which are on the C-terminal half of the pseudosymmetrical channel (Gogala et al., 2014; Park et al., 2014). The nature of this interaction has been elucidated by Voorhees and Hegde (2014), stating the involvement of the ribosomal proteins uL23 and eL29 and the backbone of the 28s rRNA in the binding of loop 8/9. This occurs at conserved residues, and mutations in these decrease the efficient anchoring of the translocon to the ribosomal exit site (Cheng et al., 2005). In contrast, loop 6/7 does not appear to contribute significantly to ribosomal binding via 28s rRNA and eL39, not only because the number of affiliated hydrogen bonds is smaller compared to the binding at loop 8/9, but also because mutations did not severely affect ribosomal binding. The effects of ribosomal binding to the structure of Sec61 were analyzed by comparing the newly presented

data of ribosome-translocon-complexes with known structures, especially from van den Berg et al. (2004). It was found that both these loops take part in the “priming” of the channel upon ribosomal contact, as they are rotated and shifted and relay this distortion to the helices of the Sec61 channel. Since the lateral gate helices are believed to form relatively weak contacts with each other, helices 2 and 7/8 slightly open on the luminal side of the channel, possibly forming a binding site for signal peptides at the lateral gate to an extent that can facilitate the incorporation of a signal sequence into the membrane in an energetically favorable fashion. The plug domain and the helices that comprise the residues for the constriction ring appear to remain unaffected in the “primed” state by ribosomal binding (**Figure 9**).

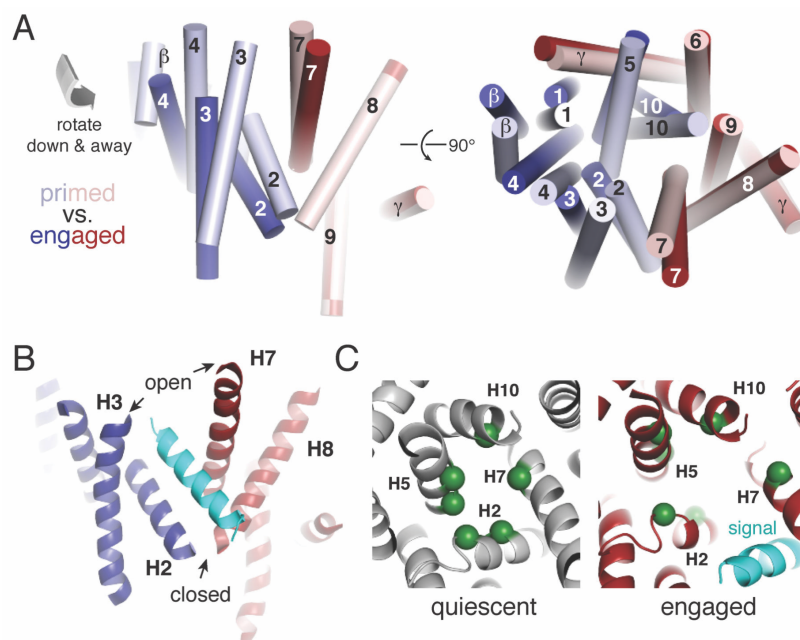


Figure 9: Sec61 changes its conformation upon binding of a signal peptide. (A) Helix movements in comparison of the ribosome-primed (PDB: 3J7Q) and engaged translocon. Blue helices are moved, while red helices remain comparably static. (B) The lateral gate opens asymmetrically at the luminal half, while the cytosolic half remains closed. Signal peptide in cyan. (C) Ring residues change their position upon signal engagement, together with the corresponding helices. Modified from Voorhees and Hegde (2016 I).

The further opening of the channel is coupled to the presence of a signal sequence. While the precise entry mechanism is yet unclear, Voorhees and Hegde (2016 I) could reconstitute the structure of a signal peptide intercalated between helices 2 and 7. In this observation, helices 2-5 and 10 were rotated in comparison to the idle state structure, distinct from helices still bound to the ribosome and resulting in a further opening of the lateral gate (asymmetrically towards the luminal part) (**Figure 10**).

Then, the signal sequence may easily avoid the hydrophilic surroundings of the pore's interior and reach the energetically more favorable position at the interface between lateral gate and membrane through the hydrophobic constriction ring, which is displaced from its idle planar conformation. It is important to keep in mind when evaluating the integration of hydrophobic segments based on lipid partitioning into the membrane, that, instead of polar surroundings, the hydrophobic constriction ring acts as one compartment besides the lipid environment.

The rearrangements of the channel's helices and the subsequent widening of both the lateral gate and the constriction ring also affects the plug domain, which is moved slightly, resulting in the "open" state of the translocon. The authors observe that the incorporation of the signal sequence at the lateral gate (leading eventually to exit into the membrane) essentially replaces the former idle position of helix 2, widening the lateral gate and the constriction ring, destabilizing the plug and facilitating (and maintaining) the active state of the translocon. This would suggest a possible role for helix 2 in the evaluation of possible signal and TM sequences.

Besides the ribosomal interaction, bacterial SecA is also known to bind to SecY involving both the N- and the C-terminal half of the channel via the loops between TM8 and TM9 and between TM2 and TM3. Since both halves of the translocon are affected, the opening of the lateral gate is observed to be much larger (Zimmer et al., 2008).

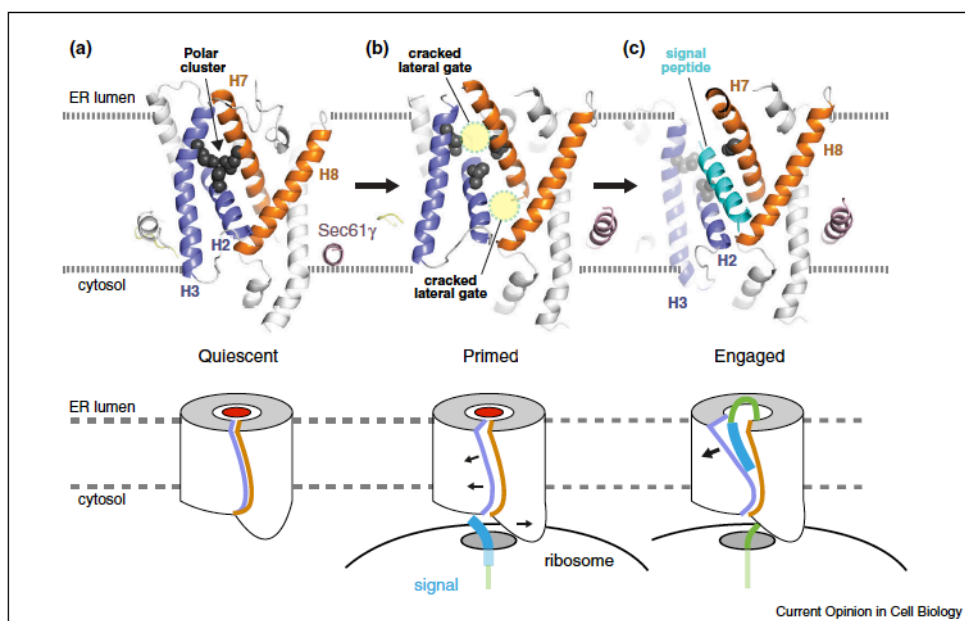


Figure 10: Model of Sec61 opening. (A) Quiescent state with a closed lateral gate and the plug domain (red). The closed lateral gate is stabilized by hydrogen bindings of polar residues (“polar cluster”). (B) Upon ribosome binding and priming of the translocon, conformational changes disrupt the polar cluster and the lateral gate is “cracked” into a semi-open state. (C) The interaction of the signal peptide (cyan) displaces helix 2 and induces a conformational change in the translocon, opening the lateral gate in an asymmetric fashion towards the luminal half and engaging the complex. Voorhees and Hegde, 2016 (II).

1.1.5 Membrane Insertion at the Sec61 translocon

1.1.5.1 The Topology of Transmembrane Segments is Determined by Several Factors

Once the RNC has been directed to Sec61 complex at the ER membrane and translocation has been initiated, it is decided whether proteins will be fully translocated into the ER lumen and follow the secretory pathway, or are integrated into the membrane. Single-spanning proteins may be further categorized into three groups: proteins with a cleavable signal that additionally contain a stop-transfer segment, exhibiting a $N_{\text{exo}}/C_{\text{cyt}}$ orientation (type I); proteins with a non-cleaved signal-anchor that are oriented $N_{\text{cyt}}/C_{\text{exo}}$ (type II); and proteins with a reverse signal-anchor, showing $N_{\text{exo}}/C_{\text{cyt}}$ topology (type III). Examples are shown in **Figure 11** (Higy et al., 2004).

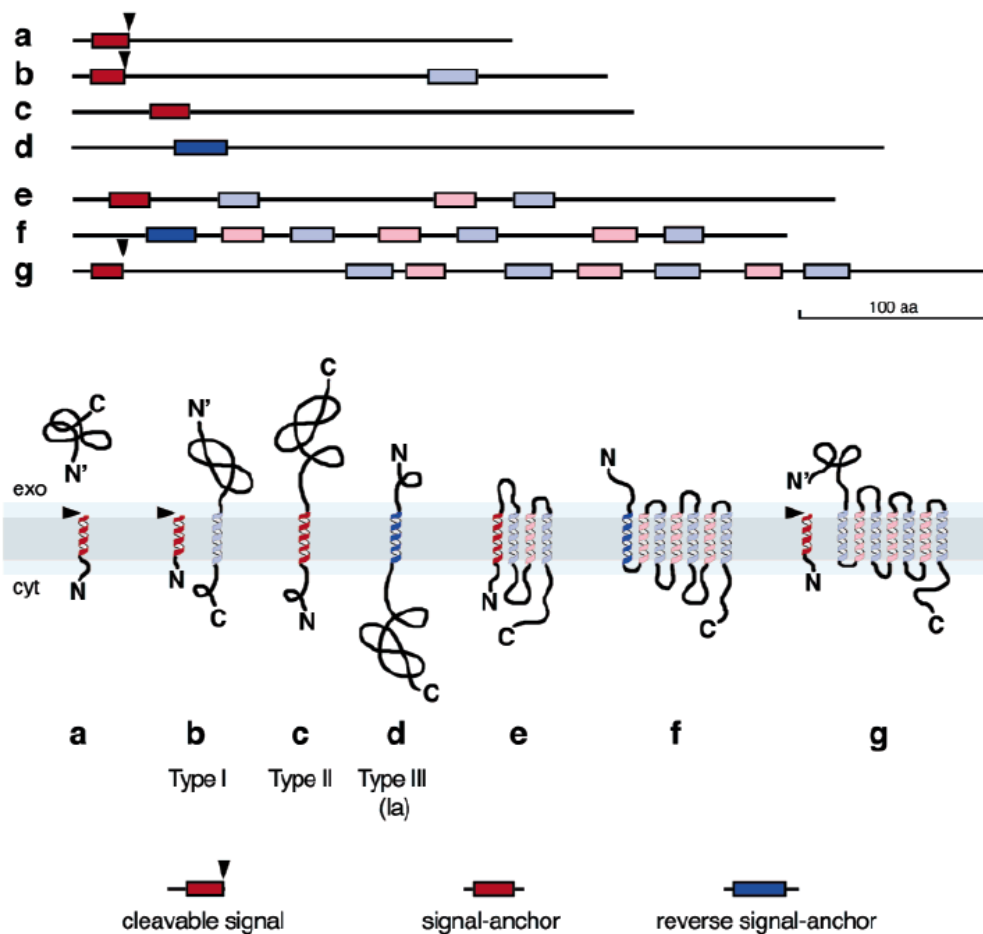


Figure 11: Signal sequences can be classified into three groups. (A) the signal peptide is cleaved and the protein is translocated into the lumen, as observed for secretory proteins. (B) Type I transmembrane protein with a cleaved signal and a stop transfer-signal that translocates the N-terminus into the lumen. (C) Type II transmembrane protein, where the signal sequence is not cleaved and serves as a signal anchor. The C-terminus is translocated. (D) Type III (IIa) transmembrane sequences that contain an uncleaved reverse signal-anchor. The N-terminus is translocated. (E) (F) (G) Multispanning proteins insert their transmembrane domains in alternating orientations. Higy et al. (2004).

It is known that the orientation of the first signal-anchor sequence in transmembrane proteins is dependent on the charges preceding and following it, resulting in the more positively charged region facing the cytosol. This phenomenon is referred to as the “positive-inside rule” and was first described in a statistical study of bacterial inner membrane proteins (von Heijne, 1986) and verified further in eukaryotes (Sipos and von Heijne, 1993). It is noteworthy that not positive charges alone mediate the orientation, but the charge differences between N- and C-terminal flanking regions have to be regarded (Hartmann et al., 1989). The major component of the translocon, Sec61p, was identified to contribute to the final topology with conserved charged residues, in accordance to the positive-inside rule (Goder et al., 2004). In bacteria,

the proton-motive force across the plasma membrane contributes to the preferred localization of positive charges on cytosol-facing parts (Cao et al., 1995).

However, charged flanking regions alone are not the only factor determining the topology. The folding states of the regions that precede a signal may prevent N-terminal translocation, if the structure leads to a steric hindrance that may overrule flanking charges (Denzer et al., 1995). Goder and Spiess (2003) confirmed that, while flanking charges are still a main factor determining the inversion rate of the N-terminal signal anchor, its hydrophobicity and the overall translation time, coupled to the length of the following C-terminal domain, also influence the amount of inversion. This is reasoned to be the result of a stabilized initial head-on insertion of the membrane sequence at the lateral gate of the translocon, with increasing hydrophobicity making it less favorable to disrupt the interactions of lipid and signal and prohibiting a change of orientation. A further probing of the environment that signal-anchor sequences encounter during topogenesis was conducted with the introduction of bulky hydrophobic amino acids into an oligoleucine signal sequence (Higy et al., 2005). The symmetric placement of these residues at either terminal region of the signal favored N-terminal translocation, whereas placement in a position corresponding to the position of acyl side chains resulted in more $N_{\text{cyt}}/C_{\text{exo}}$ orientation. According to the authors, this reflects the interaction of the signal sequence with the lipid environment and the symmetry of the lipid bilayer. Bulky residues are more easily accommodated in the central region of a membrane, where order and density is less strong than in the acyl side chain regions. When placed at the terminal regions of the signal, spacious amino acids interact with the interface between the apolar core and the head groups in a more favorable fashion, hence preventing inversion and subsequent C-terminal translocation. It was later shown that the signal sequence indeed interacts with the lipid environment through occupying the lateral gate, which is part of the translocon priming process (Voorhees and Hegde, 2016).

With these experiments, Goder and Spiess (2003) showed that the cytosolic orientation of the positive N-terminal charges is established after a head-on insertion into the translocon and a following inversion of its orientation, opposing to different

models of topogenesis that proposed a) retention of the positive N-terminal charges at the cytosolic side of the translocon or b) initial C-terminal transfer of the signal and loop formation of the nascent chain in the translocon channel. Both notions were found to be incompatible with the observed correlation of signal inversion and protein length. This was later confirmed *in vitro* by Devaraneni et al. (2011). These findings argue against the hypothesis that the final topology is assumed early after insertion of the nascent chain into the translocon, but may instead slowly change from $N_{\text{exo}}/C_{\text{cyt}}$ to $N_{\text{cyt}}/N_{\text{exo}}$ during a fixed time window.

1.1.5.2 Transmembrane Segments of Multispanning Proteins Show Cooperativity

Multispanning membrane proteins add a layer of complexity when investigating topogenesis of transmembrane segments. In the simplest notion, the “linear insertion model”, each hydrophobic transmembrane domain is regarded sequentially as a start- and stop-transfer sequence, resulting in an alternating orientation that is defined by the integration of the first segment (Blobel, 1980; Sabatini et al., 1982; Wessels and Spiess, 1988). However, besides the aforementioned factors that contribute to the topogenesis of single-spanning proteins (i.e. flanking charges, length of N- and C-terminal domains, folding states of N-terminal regions, hydrophobicity of the signal-anchor sequence), the transmembrane domains of multispanning proteins display another extrinsic factor influencing their membrane integration: the presence of neighboring transmembrane helices.

The observation that a moderately hydrophobic transmembrane sequence may depend on its predecessor for membrane integration gave rise to a second model of topogenesis. The “bundling model” pictures a transmembrane domain remaining in the vicinity of the translocon until the protein has fully been synthesized, allowing downstream transmembrane segments to interact with it (Borel and Simon, 1996). There is evidence that some transmembrane domains may depend on synergistic effects with other transmembrane domains to integrate (Enquist et al., 2009; Lin and Addison, 1995), even specifically over the interaction of charged residues inside the helices (Buck et al., 2007; Fagerberg et al., 2010). TRAM has also been suggested

as a possible interacting partner (Do et al., 1996). Earlier on, Ota et al. (1998) found that a strong orientational preference of a transmembrane helix can facilitate membrane insertion of a hydrophilic segment located upstream. Through the usage of model proteins based on bacterial leader peptidase with various lengths and transmembrane segments of different compositions, Heinrich and Rapoport (2003) investigated further and crosslinked nascent chains to the translocon, creating snapshots of possible transmembrane helix cooperation modes. Wild-type leader peptidase contains two transmembrane helices, of which the second one is less hydrophobic than the first, and its integration is dependent on the interaction and coiled-coil formation between both (Whitley et al., 1993). While keeping the first transmembrane segment unchanged, modifications of the second allowed for a characterization of these processes. This led to a multistep model in which the first transmembrane domain partitions into the membrane with a N_{lum} orientation, but stays in proximity of the translocon up to a specific chain length. Meanwhile, the second transmembrane segment emerges from the ribosome and enters the channel head-on, inverts and interacts with the first transmembrane segment, until both diffuse into the lipid before the translation is terminated.

As mentioned earlier, the topology of signal-anchor sequences is defined by flanking charges according to the positive-inside rule and hydrophobicity (Goder and Spiess, 2003). Öjemalm et al. (2013) utilized these factors to modify the orientation of a transmembrane helix and assess its influence on a moderately hydrophobic segment upstream, using leader peptidase with its natural TM helix 1 and three artificial hydrophobic segments (H1, H2 and H3), of which the latter two were outfitted with varying hydrophobicity and flanking charges. While the orientation of the N-terminus is defined and luminal, H3 was forced into N_{lum} or N_{cyt} orientations, resulting in either N_{lum}/C_{cyt} or N_{lum}/C_{lum} of the total protein. The first state reflects non-insertion of H2, the second state insertion, which was tracked by glycosylation patterns. The results proved that the orientation of H3 determined the threshold for integration of the mildly hydrophobic H2 located upstream via the aforementioned factors: hydrophobicity and flanking charges.

The “positive-inside” rule also applies for multispanning proteins in this context. The cytoplasmic loops between transmembrane segments are found to be enriched in residues displaying positive charges, but are not common in luminal regions (von Heijne, 1989). Positive charges can significantly increase membrane re-insertion of a mildly hydrophobic (potential) transmembrane segment when placed near its cytosolic end (Lerch-Bader et al., 2008). This extends to a situation where a single positive charge may influence overall protein topology even when placed at the very C-terminus, implying that the final topology is undecided until the whole protein has been synthesized (Seppälä et al., 2010).

While transmembrane helices of single-spanning membrane proteins are strongly hydrophobic in order to deliver efficient membrane integration, this is not always the case for transmembrane domains of multispanning transmembrane proteins. With prediction tools that assess hydrophobicity alone, about 25% of the transmembrane helices of proteins with known structure are not prognosed to act as such, and even when flanking charges are taken into consideration, the prediction is still not completely accurate. Of 16 transmembrane helices that were selected (with a predicted ΔG_{app} larger than 1.4 kcal/mol) and analyzed in more detail by Hedin et al. (2010), 11 of these “marginally hydrophobic transmembrane helices” were not able to be recognized as transmembrane helices when observed in an isolated context, but the number increased when the surrounding sequences were included into the experimental setup - that included both flanking charges as well as flanking transmembrane domains (Hessa et al., 2005; Hessa et al., 2007; Hedin et al., 2010). These findings regarding the topogenesis of multispanning transmembrane proteins suggest a level of plasticity that provides a challenge in the prediction of their topology.

1.1.5.3 Hydrophobicity Scales Characterize Contributions of Amino Acids to Membrane Insertion

Each amino acid has unique features and chemical properties. In the context that is relevant for this work, the varying degrees of hydrophobicity are of further interest, especially when evaluating their ability to integrate into the ER membrane during translation. Membrane insertion can most easily be analyzed in a model protein containing a signal anchor and a variable stop-transfer sequence. This has been introduced by Hessa et al. (2005), subsequently utilized (Junne et al., 2006; Junne et al., 2010) and in this work.

It is well known that the hydrophobicity of a protein segment is the main factor determining whether a stretch is inserted into the membrane, besides other factors also contributing to the integration process like the positive-inside rule (von Heijne, 1986) or repositioning events of the transmembrane helix (Kauko et al., 2010). Therefore, the prediction of possible transmembrane sequences in a protein's primary sequence is a field of ongoing interest, which requires a classification of amino acids regarding their contribution in free energy during membrane insertion. Depending on the experimental setup, many different hydrophobicity scales have been created, for example by observations from partitioning studies of varying conditions and complexity (e.g. Engelman et al., 1986; Guy, 1985; Radzicka et al., 1988; Wilce et al., 1995; Wimley and White, 1996), molecular dynamics simulations (MacCallum et al., 2008) or evaluations of literature data (Kyte and Doolittle, 1982).

Through studies involving the Sec61 translocon, the contribution of single amino acids within a pre-defined, mildly hydrophobic protein subsequence (H segment) was analyzed, also in regard to the precise positioning within the H segment. This was unique in that it emerged from a biological system analyzing membrane insertion during translocation and thus gave rise to a "biological hydrophobicity scale" (Hessa et al., 2005; Hessa et al., 2007) (**Figure 12**).

Hessa et al. (2005) stated that direct interactions with the surrounding lipid bilayer of a nascent peptide sequence in the process of Sec61 mediated translocation is crucial for their potential membrane insertion. In their experimental setup, rough microsomes derived from dog pancreas were used to explore the integration efficiency of a model protein containing a stretch of 19 alanines as the H segment. The alanines were replaced with differing amino acids at varying positions.

With an increasing amount of hydrophobic leucines that were placed in the middle of the H segment, it was found that the transition point towards a negative ΔG_{app} value was reached with three to four leucines introduced into the H segment, meaning that around 50% membrane insertion is observed. A linear correlation between the number of leucines and ΔG_{app} points to an additive effect of energies. Through symmetrical replacement of residues with the remaining amino acids, again in the middle of the H segment, a full ΔG_{app} scale was determined.

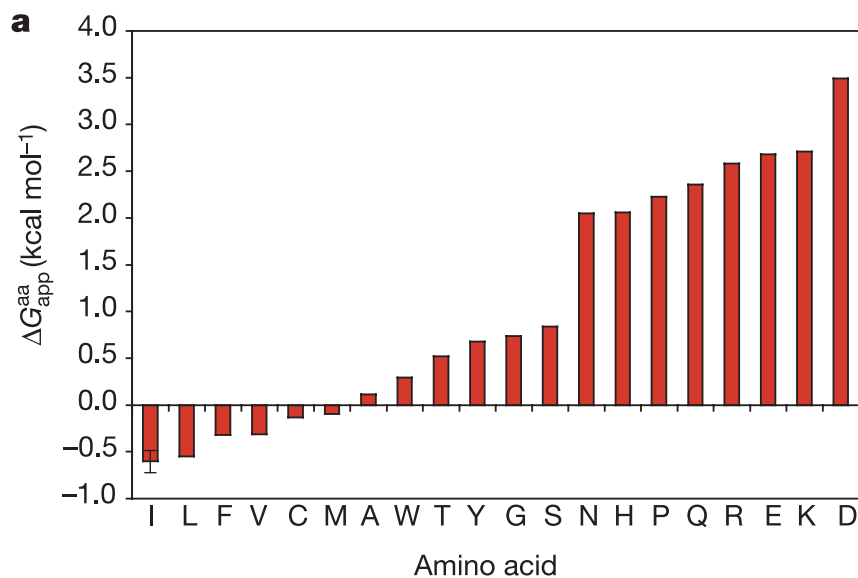


Figure 12: Biological hydrophobicity scale. Experimentally derived apparent ΔG values are indicated for each amino acid. The scale is derived from H segments with the indicated amino acid placed in the middle of the 19-residue hydrophobic stretch and does not consider further positioning effects. Hessa et al., 2005.

The authors compared their observed hydrophobicity scale with one derived through the partitioning of amino acids in a peptide context from water to octanol (Wimley et al., 1996) and found it to correlate “surprisingly well”, mentioning the more complicated conditions of a biological system. They deduced that this might hint

towards a direct interaction of the potential transmembrane segment and the lipid surroundings. It is noted, however, that this scale is only valid for residues that are placed in the center of the H segment, since a positioning apart from the center, but still in a symmetrical manner, yielded a position dependence with higher integration probability observed, the more centered the tested pairs of Leu/Ser and Asn/Lys residues were placed (Hessa et al., 2007). Even more, when the two polar residues were placed in a distance of six residues apart from to each other, ΔG_{app} values were increased. This was explained by the formation of an α -helix inside the translocon pore and its orientation allowing the polar residues to make contact to the less hydrophobic translocon pore, with the hydrophobic parts of the helix exposed to the surrounding lipids. Most transmembrane segments of proteins are characterized by a helical conformation (Oberai et al., 2006) and the H segment with its 19 residues (excluding insulating sequences) concurs with the observation that most membrane-spanning proteins are composed of 18 to 24 residues, forming an α -helix (Eisenberg et al., 1984). The presence of a helical conformation during translocation was further supported through the usage of prolines that, when introduced in the center of the H segment, but not at the termini, lead to decreased membrane integration. Proline is known as a “helix breaker” (MacArthur & Thornton, 1991), but may be accommodated near terminal regions (Yohannan et al., 2004).

While this biological hydrophobicity scale correlates well with other known hydrophobicity scales, it displays compressed values for the apparent insertion free energy ΔG_{app} . It has been discussed whether this observation reflects the fact that membrane insertion does not occur from water to membrane, but from an environment less polar than pure water (i.e. the translocon pore) to a surrounding that is less hydrophobic than pure hydrocarbon components of a membrane (i.e. the protein-lipid-interface of the translocon) (Hou et al., 2013; Junne et al., 2010; MacCallum & Tieleman, 2011).

1.1.5.4 The Translocon Contributes to the Integration Threshold

During co-translational translocation, nascent chains may be inserted into the membrane. This occurs via a lateral exit site that is formed by segments of TM2 and TM3 as well as TM7 and TM8, with the nascent chain's hydrophobicity as the driving force of displacement into the membrane. It is assumed that the helical gate structure may be easily opened, as structural analyses in *Pyrococcus furiosus* have shown a partial unfastening (Egea and Strout, 2010) and a “pre-opened” state of SecYE in *Thermus thermophilus* (Tsukazaki et al., 2008). With recent advancements in cryo-electron microscopy, a nascent chain positioned in between the helical units of the lateral gate could be visualized (Gogala et al., 2014), along with the characterization of Sec61 engaged with a nascent chain's signal sequence (Voorhees and Hegde, 2016 I).

The ten transmembrane helices comprise a hydrophilic channel through the surrounding membrane (Simon and Blobel, 1991) and contain a constriction that gives the channel an overall hourglass-like shape. This hydrophobic ring is formed by apolar side chains of six amino acid residues placed in TM helices 2, 5, 7 and 10, with solely isoleucines as side chains in *E. coli* but differing ones in other species (V82, I86, I181, T185, M294, M450 in yeast; same residues, but different positions in *H. sapiens*). The nascent peptide was shown to pass through this apolar narrowing in the center of the pore (Bol et al., 2007; Cannon et al., 2005) and its role in membrane integration was thoroughly characterized via the mutagenesis of ring residues (Junne et al., 2010) (**Figure 13**). It was surprising to observe that *S. cerevisiae* tolerated mutations of the constriction ring residues to alanines, serines, glycines and even the introduction of charged side chains with lysines and aspartates. With the deployment of mildly hydrophobic 19-alanine segments in the exoplasmic domain of dipeptidyl aminopeptidase B (DPAPB) as a model protein and the gradual exchange of the alanines with more hydrophobic leucines, as introduced by Hessa et al. (2005), the threshold for 50% membrane integration was observed at three to four leucines in the environment of the wild-type constriction ring, but was drastically reduced with its residues mutated to hydrophilic ones. This phenomenon can be explained by regarding the process of membrane integration not as a partitioning process between

bulk water and lipid surroundings, with the pore acting as a catalyst, but instead between pore and lipid with the pore as one characterizing environmental factor. Thermodynamic equilibration between these two compartments can account for a decreased integration threshold as a mutated, more hydrophilic pore may no longer accommodate a hydrophobic peptide segment in a manner that minimizes free energy, as opposed to its membrane integration.

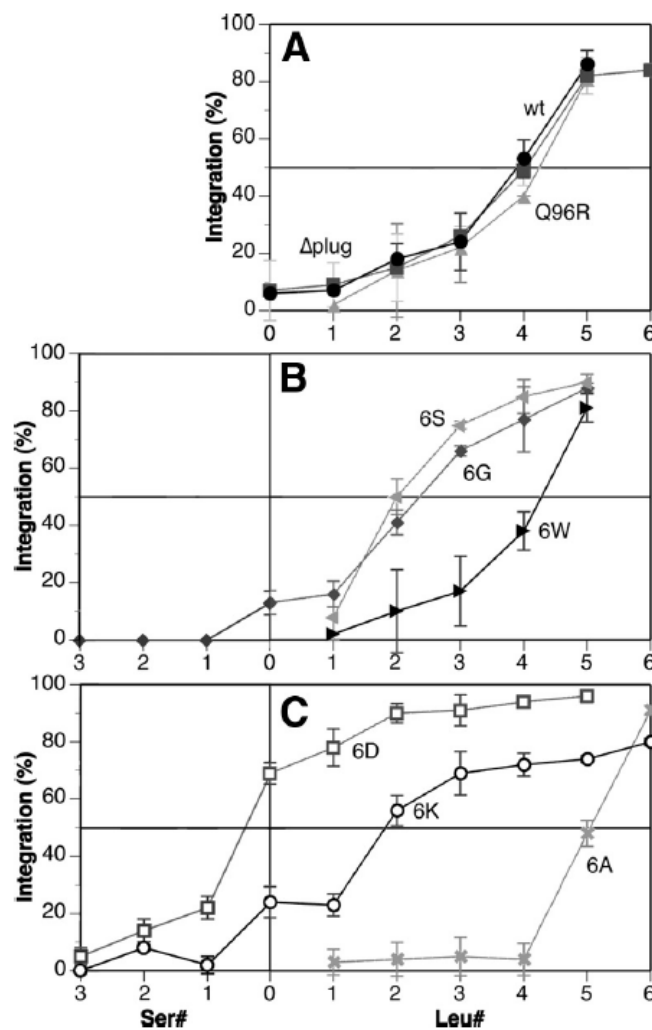


Figure 13: Membrane integration is altered in mutations of the Sec61 constriction ring. Into a segment of 19 alanines (H segment), one to six leucines were introduced that made the H segment more hydrophobic, or one to three serines that resulted in a more hydrophilic H segment. Substitution of the ring residues results in a lower (6 serines, 6 glycines) or a higher (6 tryptophanes, 6 alanines) integration threshold compared to the wild-type. (A-C) Integration values (y-axis) for an increasing number of leucines or serines in the H segment with an increasing number of leucines (x-axis). Junne et al. (2010).

Another physiological function of the constriction ring is the formation of a permeation barrier both in the idle state and during translocation with strong selectivity for protons (Dalal and Doung, 2009). This is further safeguarded by the plug domain, a hydrophobic helix located in the luminal cavity, that is stabilizing the closed state of the translocon. Both the plug and the constriction ring contribute to the permeation seal of the idle translocon, while during the active state the constriction ring forms a gasket-like structure around the nascent chain to hinder ion leakage. Translocation requires the plug domain to be shifted to allow the accommodation of the nascent chain, although less drastically than assumed (Gogala et al., 2014; Saparov et al., 2007; Park and Rapoport, 2011).

It has been shown, however, that many ring mutations were still viable (Junne et al., 2010). Furthermore, the plug domain is not essential for *S. cerevisiae*, as a deletion or mutations did not show effects towards viability or growth, but only mildly affected signal orientation or protein translocation. A plug deletion mutant appears to be able to assemble into stable and functional translocon complexes that are not degraded significantly faster than the wild-type, but show reduced steady-state levels, probably due to impaired folding or inefficient competition for the translocon subunits Sbh1p and Sss1p against the wild-type (Junne et al., 2006). In the absence of the plug domain, the translocon even appears to compensate for the deletion by rearranging itself to form a new plug, but since this makeshift solution cannot form interactions in the same manner as the wild-type plug, the closed state is no longer stabilized (Saparov et al., 2007) and signal orientation (Junne et al., 2006) as well as selection specificity for signal sequences in general is impaired (Maillard et al., 2007; Li et al., 2007).

1.2 Aim of Part I

The insertion of transmembrane segments cannot be described as partitioning from bulk water into bulk lipid, as the environment defined by the Sec61 pore influences membrane insertion. The apolar constriction ring has been recognized to define the hydrophobicity threshold in this context. Ring mutations consisting of less hydrophobic residues decreased the necessary hydrophobicity of a model protein for membrane integration (Junne et al., 2010). Altered conditions inside the pore therefore reflect the involvement of the translocon as a defining factor during thermodynamic equilibration.

In this work, we wish to further characterize the milieu inside the pore that defines one part of the thermodynamic equilibration process between pore and lipid. By this, we aim to enlarge our understanding of the mechanism for membrane integration.

Functional asymmetry within the Sec61p translocon

Erhan Demirci¹, Tina Junne¹, Sefer Baday, Simon Bernèche, and Martin Spiess²

Biozentrum, University of Basel, CH-4056 Basel, Switzerland

Edited by Tom A. Rapoport, Harvard Medical School/Howard Hughes Medical Institute, Boston, MA, and approved October 16, 2013 (received for review September 30, 2013)

The Sec61 translocon forms a pore to translocate polypeptide sequences across the membrane and offers a lateral gate for membrane integration of hydrophobic (H) segments. A central constriction of six apolar residues has been shown to form a seal, but also to determine the hydrophobicity threshold for membrane integration: Mutation of these residues in yeast Sec61p to glycines, serines, aspartates, or lysines lowered the hydrophobicity required for integration; mutation to alanines increased it. Whereas four leucines distributed in an oligo-alanine H segment were sufficient for 50% integration, we now find four leucines in the N-terminal half of the H segment to produce significantly more integration than in the C-terminal half, suggesting functional asymmetry within the translocon. Scanning a cluster of three leucines through an oligo-alanine H segment showed high integration levels, except around the position matching that of the hydrophobic constriction in the pore where integration was strongly reduced. Both asymmetry and the position effect of H-segment integration disappeared upon mutation of the constriction residues to glycines or serines, demonstrating that hydrophobicity at this position within the translocon is responsible for the phenomenon. Asymmetry was largely retained, however, when constriction residues were replaced by alanines. These results reflect on the integration mechanism of transmembrane domains and show that membrane insertion of H segments strongly depends not only on their intrinsic hydrophobicity but also on the local conditions in the translocon interior. Thus, the contribution of hydrophobic residues in the H segment is not simply additive and displays cooperativeness depending on their relative position.

protein translocation | transmembrane helix

The conserved Sec61/SecY translocon provides a passage for hydrophilic polypeptide sequences across the membrane of the endoplasmic reticulum (ER) or the bacterial plasma membrane (1). It consists of Sec61 α (Sec61p in yeast) with 10 transmembrane domains and the single spanning proteins Sec61 β (Sbh1p) and Sec61 γ (Sss1p), corresponding in bacteria to SecY/SecE/SecE. The translocon forms a compact helix bundle that can open a pore across the membrane with a lateral gate toward the lipid membrane. In the idle state, the central pore is closed by a constriction of six, almost invariably hydrophobic side chains and a luminal plug helix. The plug closes and stabilizes the inactive translocon and is displaced by translocating peptides, while the constriction residues form a gasket around them, keeping the translocon sealed to ions and small molecules (2–4).

The lateral gate allows transmembrane helices (TMs) to insert into the lipid phase. Systematic quantitative analyses of membrane integration of mildly hydrophobic sequences (H segments) defined the contribution of each amino acid to the probability of insertion into or transfer across the bilayer (5–9). These studies yielded “biological hydrophobicity scales,” similar to scales determined by physical partitioning, suggesting that membrane insertion may be a purely thermodynamic equilibration process. Particularly, it was observed that the contribution of residues is largely additive, with some position effect for certain residues (e.g., polar residues are less harmful, and tryptophan and tyrosine are more favorable at the ends of a TM than in its center; ref. 6). However, the apparent insertion-free-energy (ΔG_{app}) scale was found to be compressed in comparison with the biophysical

scales (10, 11), which rules out equilibration between free solution and the membrane catalyzed by the translocon. The choice is rather between the narrow translocation pore, where conditions differ from free solution, and the membrane environment close to the translocon, which may not be equivalent to bulk lipid (12–14). The most prominent feature within the pore is the constriction ring of apolar residues. Mutation of the constriction residues V82, I86, I181, T185, M294, and M450 in yeast Sec61p to more polar residues such as serines or glycines—or even aspartates or lysines—affected the integration process by lowering the threshold for membrane integration from four leucines in a 19-residue oligo-alanine H segment to two leucines or even fewer (15). Equilibration between the pore environment and the membrane can qualitatively account for these observations. Surprisingly, mutation to alanines increased the threshold to five leucines.

However, the overall process of translocation/insertion is a nonequilibrium process, because the substrate polypeptides are actively moved into the translocon and, unless anchored in the bilayer, pulled into the lumen by chaperone ratcheting in eukaryotes or pushed through by SecA in bacteria. In addition, the ribosome was implicated in influencing the translocon with respect to TM integration and pore sealing (e.g., refs. 16–18). Molecular dynamics (MD) analysis suggested that modulation of the channel’s gating kinetics is controlled by the TM’s hydrophobicity (19–21). Other computational studies support the notion that insertion kinetics underlie the experimentally observed thermodynamic partitioning (11) or even attempted to estimate the relevant energy states and barriers (22). The contribution of thermodynamics and kinetics and the detailed role of the translocon in the exit mechanism are not fully understood yet.

In the present study, we used model H segments of identical net composition, but with asymmetric distribution of hydrophobic

Significance

The Sec61/SecY translocon mediates translocation of hydrophilic amino acid sequences across the membrane and integration of hydrophobic segments as transmembrane helices into the lipid bilayer. The integration process is proposed to correspond to thermodynamic equilibration of the translocating sequence between the translocon and the membrane. Here we probed the conditions in the translocon interior in vivo by scanning a cluster of hydrophobic amino acids through the potential transmembrane segment, scoring for membrane insertion vs. translocation. The results reveal functional asymmetry within the translocon caused by the residues forming the central constriction in the translocation pore. Molecular dynamics simulations correlate the insertion behavior with the hydration profile through the pore.

Author contributions: E.D., T.J., S. Baday, S. Bernèche, and M.S. designed research; E.D., T.J., and S. Baday performed research; E.D., T.J., S. Baday, S. Bernèche, and M.S. analyzed data; and E.D., T.J., S. Bernèche, and M.S. wrote the paper.

The authors declare no conflict of interest.

This article is a PNAS Direct Submission.

¹E.D. and T.J. contributed equally to this work.

²To whom correspondence should be addressed. E-mail: martin.spie@unibas.ch.

This article contains supporting information online at www.pnas.org/lookup/suppl/doi:10.1073/pnas.1318432110/-DCSupplemental.

Molecular dynamics analysis was performed by Sefer Baday and Simon Bernèche. Preceding experiments (Figures 1 and 2), Sec61 ring mutations (published and previously unpublished) and supplementary experiments were made by Tina Junne.

1.3 Summary

The Sec61 translocon forms a pore to translocate polypeptide sequences across the membrane and offers a lateral gate for membrane integration of hydrophobic (H) segments. A central constriction of six apolar residues has been shown to form a seal, but also to determine the hydrophobicity threshold for membrane integration: Mutation of these residues in yeast Sec61p to glycines, serines, aspartates, or lysines lowered the hydrophobicity required for integration; mutation to alanines increased it. Whereas four leucines distributed in an oligo-alanine H segment were sufficient for 50% integration, we now find four leucines in the N-terminal half of the H segment to produce significantly more integration than in the C-terminal half, suggesting functional asymmetry within the translocon. Scanning a cluster of three leucines through an oligo-alanine H segment showed high integration levels, except around the position matching that of the hydrophobic constriction in the pore where integration was strongly reduced. Both asymmetry and the position effect of H segment integration disappeared upon mutation of the constriction residues to glycines or serines, demonstrating that hydrophobicity at this position within the translocon is responsible for the phenomenon. Asymmetry was largely retained, however, when constriction residues were replaced by alanines. These results reflect on the integration mechanism of transmembrane domains and show that membrane insertion of H segments strongly depends not only on their intrinsic hydrophobicity but also on the local conditions in the translocon interior. Thus, the contribution of hydrophobic residues in the H segment is not simply additive and displays cooperativeness depending on their relative position.

1.4 Introduction

The conserved Sec61/SecY translocon provides a passage for hydrophilic polypeptide sequences across the membrane of the endoplasmic reticulum (ER) or the bacterial plasma membrane (Park and Rapoport, 2012). It consists of Sec61 α (Sec61p in yeast) with 10 transmembrane domains and the single spanning proteins Sec61 β (Sbh1p) and Sec61 γ (Sss1p), corresponding in bacteria to SecY/SecE/SecZ. The translocon forms a compact helix bundle that can open a pore

across the membrane with a lateral gate toward the lipid membrane. In the idle state, the central pore is closed by a constriction of six, almost invariably hydrophobic side chains and a luminal plug helix. The plug closes and stabilizes the inactive translocon and is displaced by translocating peptides, while the constriction residues form a gasket around them, keeping the translocon sealed to ions and small molecules (Junne et al., 2006; Maillard et al., 2007; Park and Rapoport, 2011).

The lateral gate allows transmembrane helices (TMs) to insert into the lipid phase. Systematic quantitative analyses of membrane integration of mildly hydrophobic sequences (H segments) defined the contribution of each amino acid to the probability of insertion into or transfer across the bilayer (Hessa et al., 2005; Hessa et al., 2007; Hessa et al., 2009; Lundin et al., 2008; Xie et al., 2007). These studies yielded “biological hydrophobicity scales,” similar to scales determined by physical partitioning, suggesting that membrane insertion may be a purely thermodynamic equilibration process. Particularly, it was observed that the contribution of residues is largely additive, with some position effect for certain residues (e.g., polar residues are less harmful, and tryptophan and tyrosine are more favorable at the ends of a TM than in its center; Hessa et al., 2007). However, the apparent insertion-free-energy (ΔG_{app}) scale was found to be compressed in comparison with the biophysical scales (MacCallum and Tieleman, 2011; Gumbart et al., 2013), which rules out equilibration between free solution and the membrane catalyzed by the translocon. The choice is rather between the narrow translocation pore, where conditions differ from free solution, and the membrane environment close to the translocon, which may not be equivalent to bulk lipid (Hou et al., 2012; McCormick et al., 2003; Sadlish et al., 2005). The most prominent feature within the pore is the constriction ring of apolar residues. Mutation of the constriction residues V82, I86, I181, T185, M294, and M450 in yeast Sec61p to more polar residues such as serines or glycines - or even aspartates or lysines - affected the integration process by lowering the threshold for membrane integration from four leucines in a 19-residue oligo-alanine H segment to two leucines or even fewer (Junne et al., 2010). Equilibration between the pore environment and the membrane can qualitatively account for these observations. Surprisingly, mutation to alanines increased the threshold to five leucines.

However, the overall process of translocation/insertion is a nonequilibrium process, because the substrate polypeptides are actively moved into the translocon and, unless anchored in the bilayer, pulled into the lumen by chaperone ratcheting in eukaryotes or pushed through by SecA in bacteria. In addition, the ribosome was implicated in influencing the translocon with respect to TM integration and pore sealing (Lin et al., 2011 I; Lin et al., 2011 II; Pitonzo et al., 2009). Molecular dynamics (MD) analysis suggested that modulation of the channel's gating kinetics is controlled by the TM's hydrophobicity (Zhang and Miller, 2010; Zhang and Miller, 2012 I; Zhang and Miller, 2012 II). Other computational studies support the notion that insertion kinetics underlie the experimentally observed thermodynamic partitioning (Gumbart et al., 2013) or even attempted to estimate the relevant energy states and barriers (Rychokva and Warshel, 2013). The contribution of thermodynamics and kinetics and the detailed role of the translocon in the exit mechanism are not fully understood yet.

In the present study, we used model H segments of identical net composition, but with asymmetric distribution of hydrophobic residues, to analyze the insertion process by the yeast Sec61 translocon *in vivo*. Integration efficiency of these substrates may report on the conditions inside the translocation pore, particularly if insertion is dominated by thermodynamic effects. Indeed, we observed functional asymmetry within the translocon that is mainly mediated by the hydrophobic constriction ring, as could be demonstrated by mutation of the translocon's constriction residues. As a result, the contribution of hydrophobic residues in the H segment is not simply additive, but depends on their position and the internal structure of the translocation pore.

1.5 Results

1.5.1 Integration Efficiency Depends on the Distribution of Leucines in the H Segment

To explore the interior of the Sec61p translocon in yeast, we tested the integration efficiency of a variety of moderately hydrophobic H segments as introduced by Hessa et al. (2005; 2007). They were inserted into the exoplasmic domain of dipeptidyl aminopeptidase B (DPAPB), a type II single-spanning membrane protein with an uncleaved signal-anchor for cotranslational ER targeting and translocation of its downstream sequence. An H segment in DPAPB-H (as illustrated in **Figure 14A**) thus acts as a potential stop-transfer sequence. Integration of the H segment into the membrane results in modification of the four glycosylation sites in the translocated loop between the two TMs, whereas translocation into the lumen allows glycosylation of all seven sites. The H segments consist of a 19-residue oligo-alanine host sequence flanked by GGPG/GPGG hydrophilic helix-breaking insulators. To increase hydrophobicity, various residues were replaced by leucines, in a first series by introducing up to six leucines distributed throughout the H segment (**Figure 14B**). The fraction of translocated (T) and integrated (I) H segments was determined after pulse labeling, immunoprecipitation, gel electrophoresis, and autoradiography from the intensities of the fully and partially glycosylated forms (**Figure 14 C and D**). Slightly fewer than four leucines were required in this series to cause 50% integration.

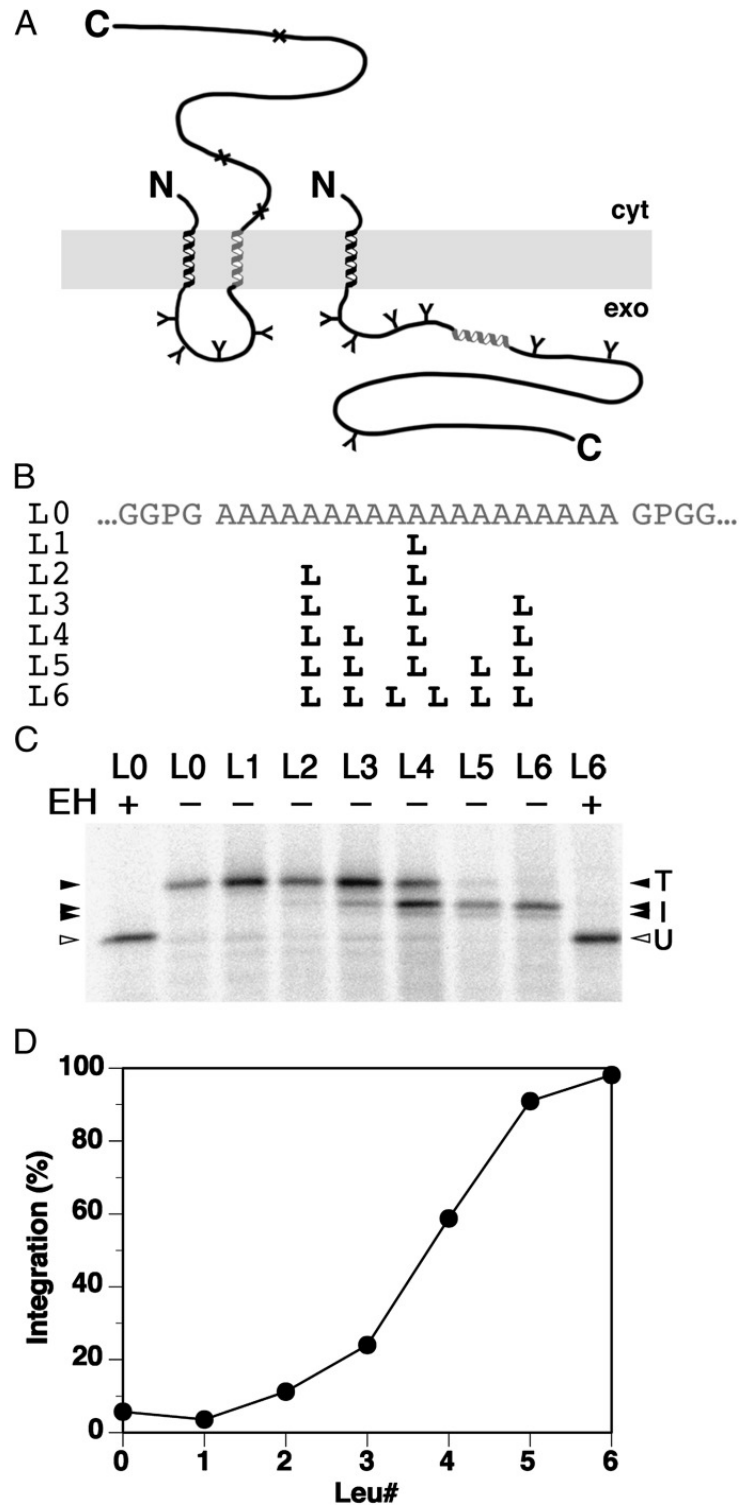


Figure 14: Membrane insertion assay. (A) Schematic presentation of the reporter construct DPAPB-H, composed of a signal-anchor sequence and containing an H segment of 19 alanines, of which an increasing number were replaced by leucines (as developed by Hessa et al., 2005). Glycosylations are indicated by Y, unused glycosylation sites by a cross. (B) H segment sequences with zero to six leucines distributed through the oligo-alanine host peptide. (C) Wild-type yeast cells expressing the indicated DPAPB-H constructs were pulse labeled with [35 S]-methionine for 5 min, and products were immunoprecipitated, separated by gel electrophoresis, and visualized by autoradiography. Translocated (T), integrated (I), and unglycosylated (U) forms could be distinguished. Glycosylation of the integrated form is somewhat incomplete, resulting in threefold or fourfold glycosylation. As controls, L0 and L6 products were also deglycosylated by endoglycosidase H digestion (EH). (D) Quantitation of the experiment shown in (C).

Surprisingly, when four leucines were placed asymmetrically into the H segment (**Figure 15**, wild-type translocon; wt), they caused significantly more membrane integration in the N-terminal half (L4N) than in the C-terminal half (L4C) or when distributed over the entire length (L4). Interestingly, threefold glycosylation was reduced for the H segment with the four leucines in the C-terminal half, suggesting a somewhat different position in the translocon or lipid bilayer and thus improved accessibility of the forth glycosylation site to oligosaccharyl transferase.

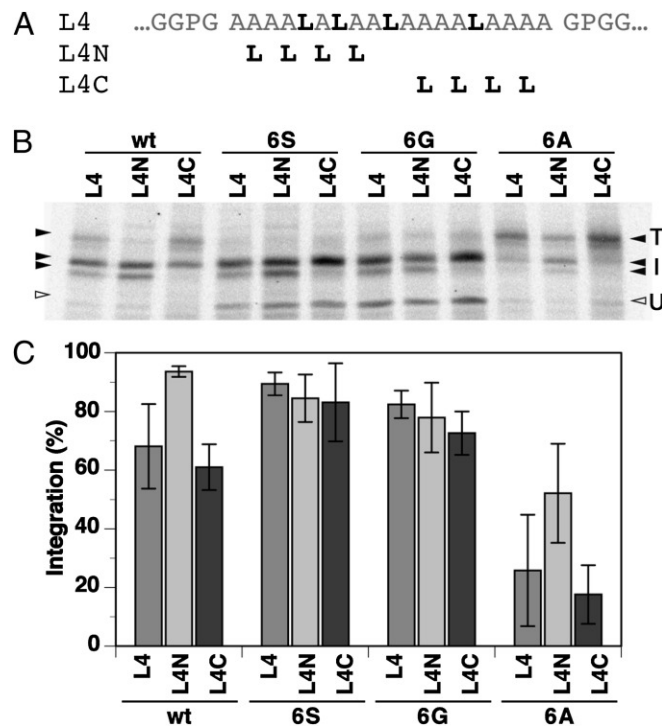


Figure 15: Asymmetric effects of leucines on membrane integration. (A) H segments containing four leucines positioned in the N- or C-terminal half in comparison with the original L4 construct. (B) and (C): DPAPB-H with these three H segments were expressed in cells with wild-type (wt) Sec61p or mutant translocons in which the six constriction residues were replaced by serines (6S), glycines (6G), or alanines (6A) and analyzed as in Figure 14. The average and SD of three independent experiments are shown.

To explore this asymmetric effect of hydrophobicity on membrane integration with higher resolution, a cluster of four consecutive leucines was placed at five different positions throughout the H segment (**Figure 16A**). Unexpectedly, the clustered leucines produced nearly complete integration at almost every position (**Figure 16B** and **C**). Integration was always higher than with four distributed leucines, suggesting that clustering of the hydrophobic residues within the H segment gives rise to an apparent cooperativeness that further promotes membrane insertion.

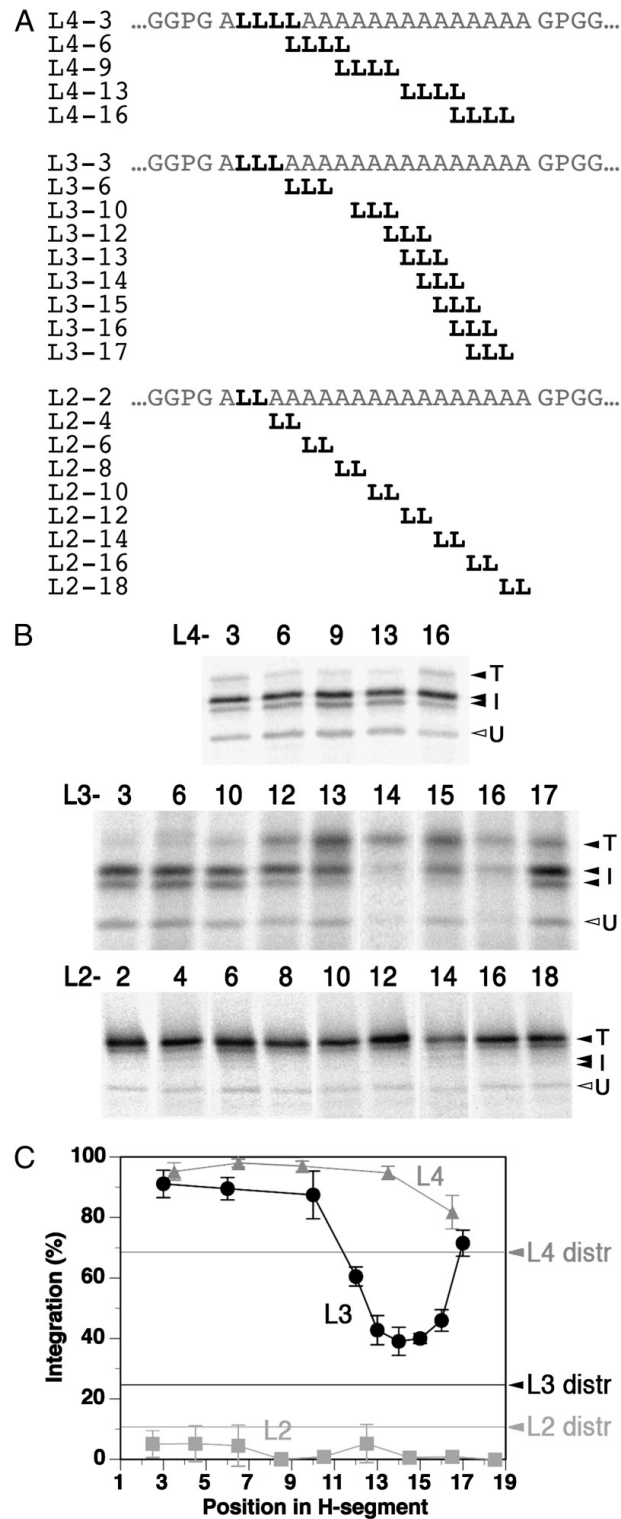


Figure 16: Scanning clustered leucines through the H segment. (A) H segments with four, three, or two consecutive leucine residues positioned throughout the sequence. The end number indicates the position of the second, central, or first L in the cluster, respectively. (B) and (C) DPAPB-H with these H segments were expressed in cells with wild-type Sec61p and analyzed as in Figure 14. Average and SD of at least four independent experiments are shown. The horizontal lines indicate the integration levels of distributed leucines as in Figure 14B.

1.5.2 Hydrophobicity at the Apolar Constriction in Sec61p Lowers Membrane Integration

To bring insertion back into the diagnostic range, clusters of only three and two leucines were scanned through the H segment (**Figure 16**). Double leucines were insufficient to mediate significant membrane insertion at any position. However, whereas three distributed leucines resulted in ~25% integration, three clustered leucines again integrated more efficiently everywhere (~40–90%) and with a pronounced asymmetry. Almost complete integration was obtained by triple leucines in the N-terminal half of the H segment or in the center, whereas only ~40% was observed for triple leucines centered at positions 13-16 in the C-terminal half. This location is exactly the position of the constriction ring in the translocon, as illustrated in **Figure 17**. The translocon is embedded in the lipid bilayer, protruding into the cytosol with its ribosome-binding loops. The N-terminal amphipathic helix of the γ subunit Sss1p lies flat on the cytoplasmic surface. The hydrophobic constriction is situated at the level of the cytoplasmic lipid monolayer. The pore environment may be more favorable for H segments with leucines that can interact with the apolar constriction residues than with leucines more N-terminal in the H segment at the level of the plug cavity or at the very C terminus above the ring.

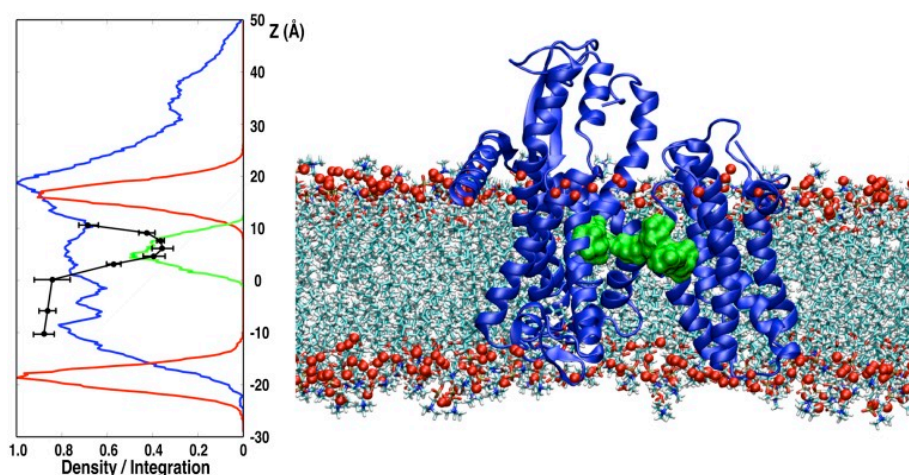


Figure 17: Minimal membrane integration of three-leucine cluster coincides with the position of the hydrophobic constriction ring in the cytoplasmic half of the membrane. The molecular system shows *Methanococcus jannaschii* SecYE β (blue) in a dimyristoylphosphatidylcholine lipid bilayer, with the phosphorus atom of each lipid rendered as a red sphere. The cytoplasm is shown above and the ER lumen below the membrane. The lateral gate of the translocon is open and facing the viewer. The hydrophobic residues forming the constriction ring are in green. The graph presents density profiles (arbitrary units) extracted from an MD simulation: protein is in blue, ring amino acids are in green, and lipid headgroup phosphates are in red. The integration efficiency of the Leu3 scan of Figure 16C is also shown.

To test whether the hydrophobic constriction is responsible for the observed asymmetry and position dependence of leucine residues, the various constructs were expressed in yeast cells with mutant Sec61p translocons. Asymmetry of insertion of L4N vs. L4C was lost with mutant translocons in which the six ring residues were mutated to serines (6S) or glycines (6G), but was retained in the alanine mutant (6A; **Figure 15**). 6S and 6G showed generally increased and 6A reduced integration levels compared with wild-type, consistent with the reduced and increased hydrophobicity threshold of the respective mutants (Junne et al., 2010). Scanning a triple-leucine cluster through the H segment revealed that the position effect was largely lost in translocons with 6S or 6G mutations (**Figure 18A**). This result confirms that the constriction ring is responsible for the position effects observed with the wild-type translocon. Disruption of the minor, nonessential Sec61 homolog Ssh1p did not significantly affect the insertion pattern of the triple-leucine H segments with wild-type and 6S Sec61p, confirming that the results reflect the properties of the Sec61 translocon.

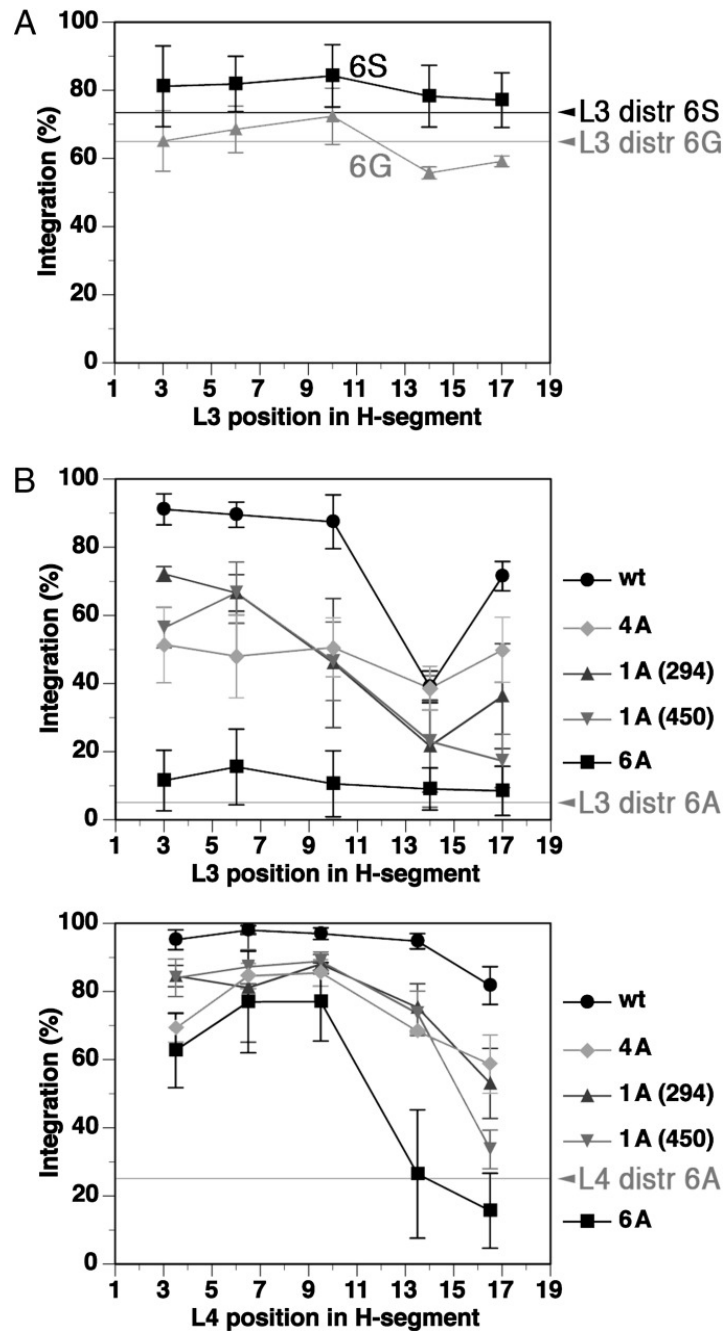


Figure 18: Mutation of the ring residues to serines or glycines, but not to alanines, eliminates the position effect of leucine clusters. (A) DPAPB-H with triple-leucine H segments were expressed in cells with Sec61p translocons in which the six constriction residues were replaced by serines (6S) or glycines (6G) and analyzed as in Figure 14. (B) DPAPB-H with H segments containing clusters of three (L3; B, Upper) or four leucines (L4; B, Lower) were expressed in cells with mutant Sec61p in which constriction residues were replaced by alanines. Residues M294 [1A (294)], M450 [1A (450)], the other four residues V82, I86, I181, and T185 (4A), or all six (6A) were mutated. Average and SD of at least three independent experiments are shown. The horizontal lines indicate the integration levels of distributed leucines (as in Figure 14B).

1.5.3 The 6A Translocon Mutant Retains Asymmetry of Integration

In agreement with its increased hydrophobicity threshold, the 6A mutant translocon produced very low integration levels for the triple-leucine H segments - too low to reveal any asymmetry (**Figure 18B, Upper**). For this reason, the constructs with four clustered leucines were analyzed (**Figure 18B, Lower**). Four-leucine clusters in the N-terminal half of the H segments or at the center produced ~60-70% integration - much more than four distributed leucines did - whereas in the C-terminal half they led to very low integration. It thus appears that leucine clusters in the 6A translocon pore are similarly favorable on the cytoplasmic side and unfavorable on the luminal side, as in the wild-type channel. This asymmetry was not abolished upon elimination of Ssh1p.

We also analyzed the behavior of construction intermediates in which only one residue of the constriction ring (M294 or M450) or four residues (V82, I86, I181, and T185) were exchanged for alanines. These partial mutants showed an intermediate level of integration for tri- and tetra-leucine clusters, generally consistent with the transition to an increased hydrophobicity threshold. The effects of the single mutants were similar in extent to those of the four-residue mutant, indicating that not all constriction residues contribute equally.

1.5.4 Hydration Profile of Wild-type and Mutant Translocons

The reduction in membrane integration of triple-leucine clusters located around position 14 in the H segment is likely to arise because the environment at the constriction is more hydrophobic than elsewhere in the translocation pore. Peptides with leucines at the level of the pore ring would be energetically more favorable and thus more stable in the pore and result in reduced membrane integration than with leucines at other positions, where the channel is potentially more polar and more hydrated.

To characterize the hydration profile of the translocon pore, we performed MD simulations of wild-type and mutant translocons [based on the *M. jannaschii* SecYE β structure] embedded in a lipid bilayer and containing an H segment (L3-14). The water densities in the respective pores are illustrated in **Figure 19**. In all cases, the water molecules form an hourglass shape and the peptide finds an equilibrium position at the interface between the water in the pore and the membrane lipid. The water density is interrupted at the level of the pore ring in the wild-type translocon and is minimal in the 6A mutant compared with the 6S and 6G mutants. The extent of hydration thus mirrors the observed asymmetry of insertion in the wild-type and 6A mutant translocon.

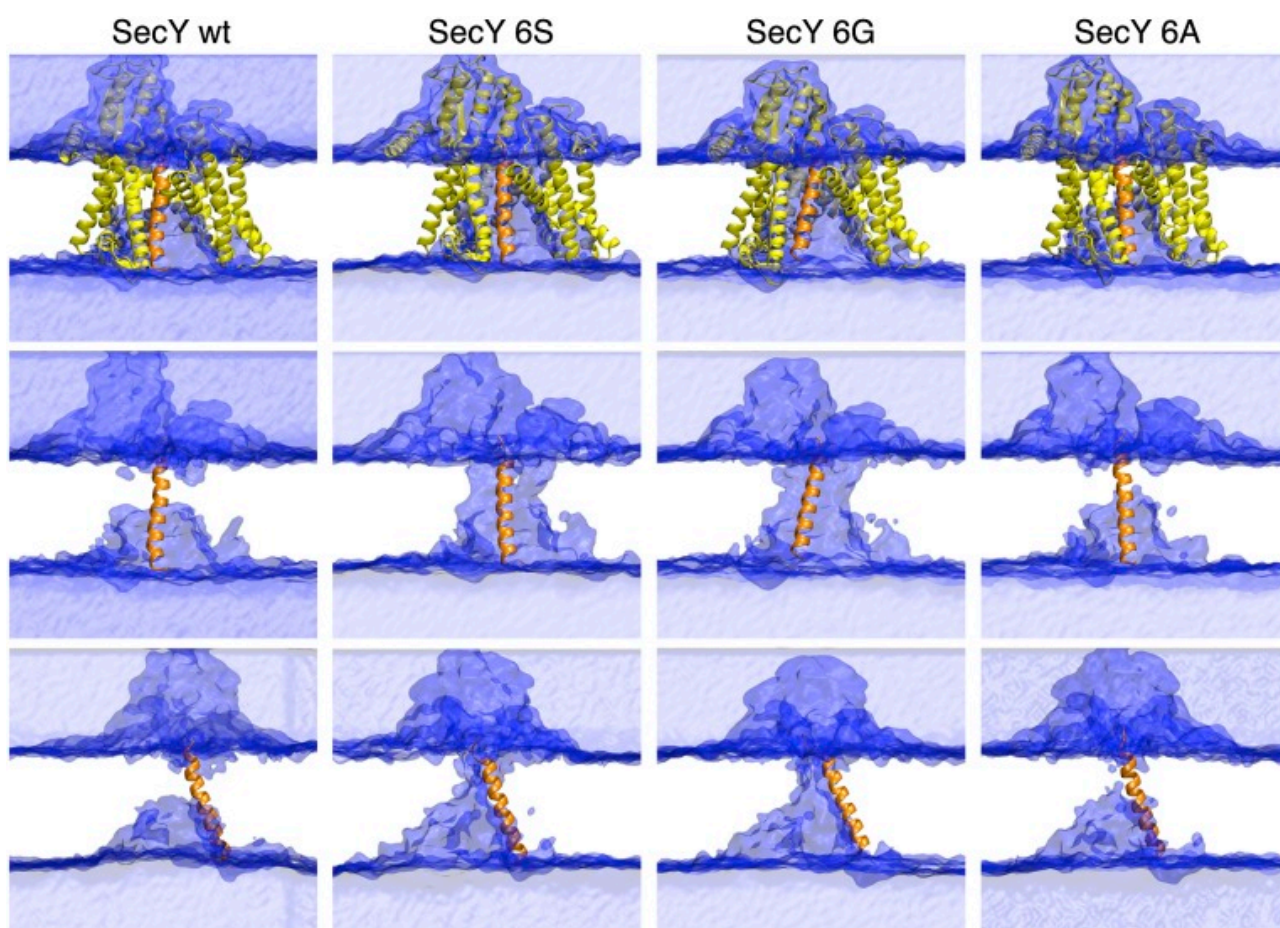


Figure 19: Hydration inside wild-type and mutant translocons. The averaged water density as observed in MD simulations was iso-contoured at 0.016 molecule per \AA^3 (i.e., half of bulk density) for the SecYE β translocon and the 6S, 6G, and 6A ring mutants containing the L3-14 H segment. Translocon polypeptides are shown in yellow and the H segments in orange. (Top and Middle) Front view facing the lateral gate. (Bottom) Side view with the lateral gate facing to the right. The constriction residues reside at the level of the upper, cytoplasmic half of the membrane.

1.6 Discussion

Thermodynamic equilibration of a translocating peptide segment between the translocon and the lipid membrane is an attractive mechanism of membrane integration of TMs. In its simplest form, the polypeptide passes through the pore as it is synthesized by the ribosome and, when in register with the lipid bilayer, is free to exit the pore and to return, thus sampling the environments inside and outside the translocon. This process is stopped when the peptide has moved out of register. If the transport rate is limited by the rate of translation, which is in the range of 3-10 residues per second in yeast (Siwiak and Zielenkiewicz, 2010), equilibration would occur in a time window in the order of ~ 1 s.

Because the lipid phase can be considered symmetrical, any asymmetry of integration found for H segments of identical composition, but unequal distribution of residues, reflects an asymmetry within the translocon. If the most hydrophobic residues of an H segment match the most apolar environment within the translocon, one would predict reduced membrane integration, whereas in the opposite case, increased stop-transfer activity would be expected. Such uneven insertion behavior was observed for H segments with leucine clusters placed throughout an oligo-alanine host sequence. Asymmetric efficiency of membrane insertion was found with a minimum for leucine triplets in the cytoplasmic half centered at position 14. This location corresponds to the apolar region at the level of the constriction ring, which forms a gasket around the translocating peptide. The translocon with a height of $\sim 65\text{\AA}$ is asymmetrically embedded in the membrane extending $\sim 25\text{\AA}$ into the cytoplasm. The central constriction ring is situated at the level of the cytoplasmic half of the lipid bilayer (as illustrated in **Figure 17**), with the plug cavity matching up with the luminal half. The observed insertion pattern thus highlights that the environment within the translocation pore is not homogeneously aqueous, but structured, and that hydration is limited by the spatial confinement of the passage.

Mutation of the apolar ring residues to serines - which provide hydrogen-bond partners - or to glycines - which provide space and access to the polar peptide backbone to water molecules - eliminates the hydrophobic belt in the pore and is

reflected in a loss of integration asymmetry. In contrast, mutation to alanines retained asymmetry, suggesting lower polarity in the cytoplasmic half of that portion of the translocon that is embedded in the lipid bilayer. This finding is qualitatively supported by the MD simulations that show low hydration of a model H segment in this portion of the 6A mutant translocon.

Previous MD simulations (Zhang and Miller, 2010) and cryo-electron microscopy structures (Frauenfeld et al., 2011; Hizlan et al., 2012) suggested that the plug might not completely leave its cavity in the translocon, but only move sideways to accommodate the translocating peptide. Indeed, immobilization of the plug inside bacterial SecYEG did not impair functionality of the translocon (Lycklama et al., 2011). Fluorescence lifetime analysis of N-((2-(iodoacetoxy)ethyl)-N-methyl)amino-7-nitrobenz-2-oxa-1,3-diazole (NBD)-modified plugs showed an increase in solvent exposure with a translocation intermediate, but clearly less than expected for full solvent exposure (Lycklama et al., 2011). With the plug domain largely remaining in the channel, the water content in the luminal cavity and the polarity difference to the cytoplasmic half of the pore is thus most likely less pronounced than suggested in **Figure 19** in the absence of the plug. By its surface properties and narrowness, the translocon also facilitates the folding of the H segment into an α -helical state matching the dimensions of the hydrophobic lipid core, as suggested by simulations (Gumbart et al., 2011).

Insertion of the polypeptide into the pore already causes partial opening of the gate and allows H segments to contact lipids, as is apparent from the structure of *Pyrococcus furiosus* SecYE β (where the C-terminal helix of one SecY in the crystal is partially inserted in the other; Egea and Strout, 2010) and from MD simulations (Gumbart et al., 2013; Zhang et al., 2010; Zhang and Miller, 2012). It is thus likely that the H segment orients itself in the pore and the gate to maximize contact of hydrophobic residues with the lipid. This behavior might in part explain why three or four consecutive leucines generally yield more membrane integration in the wild-type translocon than dispersed ones, because more leucines will have to face the interior of the pore. It has previously been observed that the helical hydrophobic moment of leucine-containing oligo-alanine H segments correlates with varying integration

efficiency (Hessa et al., 2005). Furthermore, dispersed leucines may be more easily accommodated within an oligo-alanine sequence than clustered ones, which are sterically unfavorable within a narrow pore.

Surprisingly, Hessa et al. (2007) only observed minimal position effects for similar triple-leucine clusters in the mammalian *in vitro* system. Whether this discrepancy is due to the reduced translation rates or BiP binding efficiencies in the *in vitro* system or to other differences to the yeast situation remains to be analyzed.

In the yeast system, we find that the contribution of amino acids to membrane integration is not strictly additive. This finding does not detract from the generality and the predictive power of the von Heijne rules and does not argue against the influence of the ribosome on translocon function (Lin et al., 2011), but highlights how the detailed environment within the translocon channel affects the thermodynamics of the integration process, causing striking asymmetry of membrane insertion for the leucine/alanine model sequences.

1.7 Materials and Methods

Yeast Strains

Yeast strains expressing wild-type and mutant Sec61p with and without SSH1 were described in Junne et al. (15). They are based on RSY1293 (mata, ura3-1, leu2-3,-112, his3-11,15, trp1-1, ade2-1, can1-100, sec61::HIS3, [pDQ1]) (Pilon et al., 1997), in which pDQ1 [i.e., YCplac111 (LEU2 CEN) containing SEC61 with codons 2–6 replaced by codons for H6RS and with its own promoter] was exchanged for YCPlac33 (URA3 CEN) with the same SEC61 gene. Mutant sec61 in YCplac111 (LEU2 CEN) was introduced by plasmid shuffling using 5-fluoro-orotic acid.

Model Proteins

To analyze membrane integration, potential transmembrane segments were inserted into the translocated domain of DPAPB replacing codons 170–378 by PCR mutagenesis (Junne et al., 2010), resulting in model proteins as illustrated in **Figure 14A** with H segment sequences shown in **Figures 14B, 15A and 16A**. They were cloned into the expression plasmid pRS426 (URA3 2μ) with a glyceraldehyde-3-phosphate dehydrogenase promoter and a C-terminal triple-HA tag.

Labeling and Immunoprecipitation

Yeast cells were *in vivo* pulse-labeled for 5 min with 150 $\mu\text{Ci/mL}$ [^{35}S] methionine/cysteine (PerkinElmer). Cells were lysed with glass beads, heated at 95 °C for 5 min with 1% SDS, cleared by centrifugation, subjected to immunoprecipitation, and analyzed by SDS-gel electrophoresis and autoradiography as described (Junne et al., 2006). Signals were quantified by phosphorimager. For deglycosylation, the immune complexes were released from protein A-Sepharose by boiling in 50 mM Na citrate, pH 6, and 1% SDS, and incubated with 1 mU endo- β -d-N-acetyl glucosaminidase H for 2 h at 37 °C.

MD Simulations

The simulation systems were prepared by using the crystal structure of the SecY translocon from *M. jannaschii* (Protein Data Bank ID code 1RHZ) in which the lateral gate is in a closed state (van den Berg et al., 2004). Because plug-deleted mutants were shown to be viable (Junne et al., 2006), the plug domain was removed to simplify the placement of a peptide into the pore of SecY. Residues 46–67 forming the plug domain were replaced by a single glycine.

By using the CHARMM-GUI web server (Jo et al., 2008), the protein was assembled into a bilayer composed of 389 dimyristoylphosphatidylcholine lipids and solvated with 29,000 water molecules and 0.15 M KCl. The system containing 142,352 atoms was placed in an orthogonal box of $116 \times 125 \times 96 \text{ \AA}^3$. All simulations were

performed with the NAMD (Philips et al., 2005) simulation package by using the CHARMM 27 force field (MacKerell et al., 1998). The cutoff for van der Waals interactions was taken at 12Å with a switching function used after 10Å. The calculation of electrostatic interactions was performed by using the Particle-Mesh Ewald algorithm. The integration time step was 1 fs. Short-range nonbonded interactions were calculated every two steps and long-range interactions every four steps. Simulations were performed in an isothermal-isobaric ensemble with a pressure of 1 atm and a temperature of 315 K.

The lateral gate of SecY was opened by steered MD using the ABF and COLVARS modules of NAMD (Philips et al., 2005). The gate opening was of 16Å, wide enough to fit an α -helical peptide inside the pore of SecY. After 5 ns of equilibration of the structure with the lateral gate opened, the L3-14 helical peptide was placed into the pore of SecY. The center of mass of the L3-14 peptide was aligned with the center of the bilayer. The systems for the different SecY mutants were prepared by mutating the pore-ring residues in the equilibrated system of the plug-deleted SecY with its lateral gate open. Simulations were performed for 70 ns. Water densities shown in **Figure 19** were calculated by using the last 50 ns of the simulation trajectories.

1.8 Concluding remarks

Our data show, together with the findings by Junne et al. (2010), that the constriction ring is important in the assessment of hydrophobicity and presents a key factor in the recognition of transmembrane segments within the context of our model proteins.

As the gasket surrounding the translocating polypeptide and sealing the pore, the constriction ring constitutes a major part of the pore and thus greatly influences the equilibration between pore and membrane. Our results show that the constriction ring is positioned asymmetrically relative to the lipid. Natural sequences may take advantage of this and may have co-evolved to enhance or reduce membrane integration via an asymmetric distribution of their hydrophobic residues. However, no general hydrophobic gradients have been detected statistically in natural transmembrane sequences. Viability of ring mutants (Junné et al., 2010) suggests that most membrane proteins are not affected by a shift in the hydrophobic threshold,

as the main function of the constriction ring is to create a seal and not to reflect asymmetry in signal sequences. In addition, signal anchors and stop-transfer sequences in biological systems seldom display “moderate” hydrophobicity (with the exception of some transmembrane segments of multispinning proteins). Even when this is the case, failsafe implementations presumably would have co-evolved to ensure membrane integration and prevent mislocalization or nonfunctional topologies, which could have disastrous effects for the organism. Our experimental setting therefore does not necessarily reflect physiological relevance in transmembrane segment recognition, but is an abstraction that allows the characterization and portrayal of its mechanisms.

We also observed the phenomenon that clustered hydrophobicity within an H segment promoted integration more than when distributed. This effect of “local hydrophobicity” has further been acknowledged by Stone et al. (2015; 2016). With H segments consisting of serines and leucines, the effect of concentrating the hydrophobic residues versus a dispersed distribution was drastic. The same number of leucines was predicted to show identical ΔG_{app} , regardless of distribution or position. However, the experimental outcome reflected a decrease into negative kcal/mol values when the leucines were placed at the N-terminus of the H segment, or when grouped to a block. This confirms our observation that a hydrophobic cluster facing the constriction ring inserts less efficiently into the membrane, while N-terminal leucines lead to membrane integration even in the context of otherwise polar residues in the H segment.

In the introduction, several factors that contribute to topogenesis were presented, and recently extrinsic factors that control membrane integration have been identified. Junne and Spiess (2017) recognized the influence of downstream sequences on integration efficiency. While the precise underlying mechanism remains to be characterized, the conformation of the downstream segment may loosen or tighten the tether between the translocon and the RNC, either allowing it to diffuse into the lipid and be removed from the thermodynamic equilibration process, or fixing its position in the proximity of the lateral gate, possibly anticipating further transmembrane segments that are not yet synthesized. This argues against bulk

substrate hydrophobicity as the only factor for determining the fate of possible transmembrane sequences, since the hydrophobic constriction ring and the arrangement of hydrophobic residues have been proven to participate in this process. Due to this, the prediction of transmembrane segments is furthermore complicated.

Overall, our findings and the subsequent studies are consistent with thermodynamic equilibration as the driving force for membrane insertion, where transmembrane segments aim to minimize their free energy in different environments, including components of the Sec61 translocon: the hydrophobic constriction ring and the lateral gate as the interface between pore and lipid.

Addendum

2. Disulfide Loops of Peptide Hormones as a Motif for Protein Aggregation

2.1 General Introduction

2.1.1 ER Quality Control Ensures Correct Folding

Newly synthesized proteins entering the ER encounter an environment that is different from the cytosol in many aspects. Ca^{2+} concentration and oxidizing conditions as well as the repertoire of chaperones and enzymes allow for distinct processing steps. Here, the signal sequence is cleaved, if applicable, and the proteins may undergo a series of covalent modifications. Proteins whose destination is beyond the ER are retained until they have acquired their native conformation, which represents a state of minimized free energy, or are ultimately degraded, if they fail to do so. The recognition of non-natively or unfolded proteins is not dependent on intrinsic qualities like specific signal sequences, but applies to all proteins, with misfolded ones displaying general biophysical characteristics like the exposure of hydrophobic regions, free cysteine residues, or aggregate formation. Chaperones belong to the families of heat shock proteins (Hsp40s, Hsp90s and Hsp70s with BiP as the most prominent member; Hellman et al., 1999), lectins (calnexin and calreticulin; Helenius et al., 1997) or oxidoreductases, such as PDI (protein disulfide isomerase) or ERp57 (Fra et al., 1993).

One well-studied mechanism in the recognition and retention misfolded glycoproteins is the calnexin-calreticulin cycle (Hammond et al., 1994) (**Figure 20**). The nascent chain receives the initial N-linked glycosylation by OST, consisting of the addition of the oligosaccharide $\text{Glc}_3\text{Man}_9\text{GlcNAc}_2$. Subsequently, glucosidases I and II remove two glucose units, resulting in a monoglucosylated glycan structure. This is recognized and bound by calnexin and calreticulin, preventing premature ER exit (Rutkevich et al., 2011). The complex in turn recruits ERp57 (Oliver et al., 1997), a thiol-disulfide oxidoreductase that forms disulfide bonds of free cysteines. The last of the three glucose molecules is then cleaved by glucosidase II. Proteins that have not reached their native conformation are targeted by UDP-glucose:glycoprotein glucosyltransferase, which re-initiates the cycle by adding one molecule of glucose back. If the protein fails to assume its conformation, ER α 1,2-mannosidase I removes one mannose. Additional mannose trimming initiates contact with ER degradation-

enhancing α -mannosidase like proteins (EDEM; Ninagawa et al., 2014). EDEM1 doubles as a mediator and delivers the misfolded protein to ER-associated degradation complexes (ERAD).

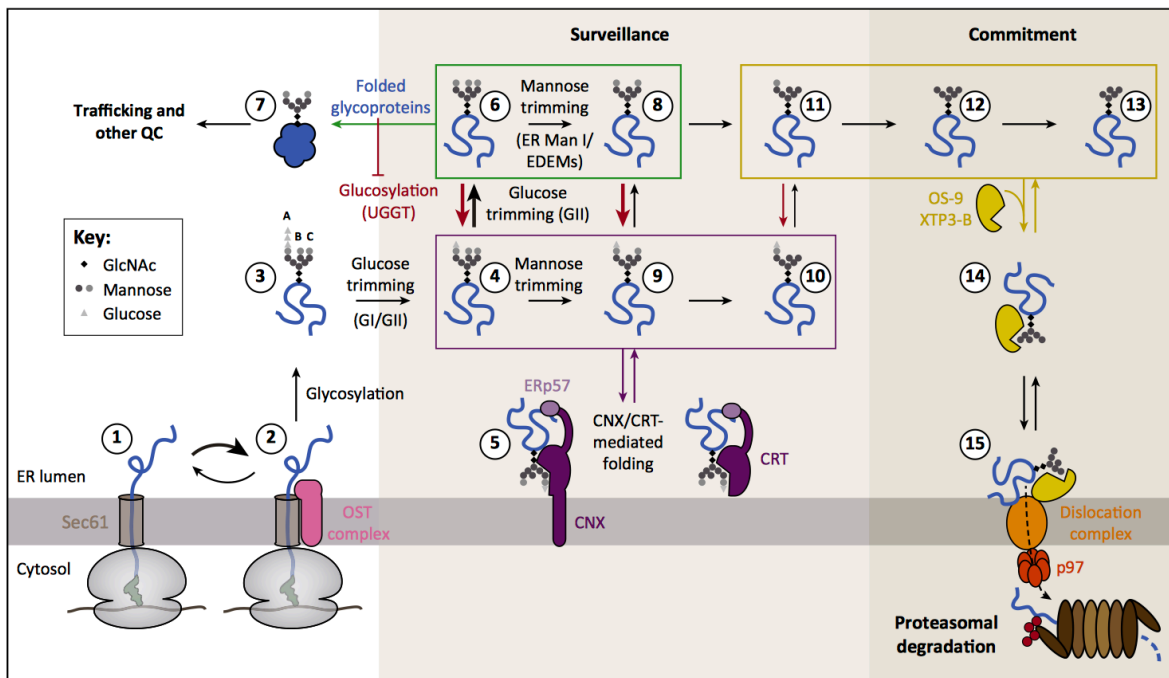


Figure 20: Quality control of glycoproteins. (1 and 2) The OST complex is associated with the translocon and glycosylates the substrate at defined asparagine residues. (3) The core glycan is trimmed by glucosidases I and II (GI, GII), resulting in a monoglycosylated product (4). The substrate can initiate folding cycles with calnexin and calreticulin (CNX, CRT, 5). GII removes the last glucose molecule (6) and the correctly folded protein is able to exit the ER (7). Unfolded proteins are re-glycosylated by UDP-glucose-glycoprotein glucosyltransferase (UGGT) and the protein re-enters the calnexin/calreticulin cycle. Mannosidases like ER mannosidase I (ER Man I) or ER degradation-enhancing α -mannosidase like proteins (EDEMs) remove mannose from unglucosylated or monoglycosylated substrates (“mannose trimming”), granting them additional rounds of glycosylation cycles. Further mannose trimming (12, 13) removes them from the cycle and are recognized by OS-9 and XTP3-B lectins to be handed over to degradation (14, 15). Shao and Hegde (2016).

2.1.2 Misfolded Proteins are Degraded by the Ubiquitin/Proteasome System

Misfolded substrates show diverse features in their folding states, their repertoire of modifications or oligomerization. Nevertheless, the degradation machinery has to provide compatibility with numerous possible substrates. General means are the exposure of hydrophobic patches that are non-accessible in natively folded proteins, or in the case of glycosylated proteins, their specific pattern. Chaperones like BiP/Kar2 are known for binding exposed hydrophobic parts and delivering the protein

to ERAD complexes (Molinari and Helenius, 2000). In non-glycosylated substrates, the mechanisms involving recognition and degradation are less well described.

Targeting to ERAD pathways requires recognition of these substrates, retro-translocation into the cytosol, ubiquitination and degradation by the 26S proteasome. Proteins that are meant to be recycled are covalently linked to the C-terminus of ubiquitin, a strongly conserved protein that can be attached to lysine residues or, less frequently, to serine or threonine. Linkage to the N-terminus of a protein is also observed. Ubiquitin itself may serve as a substrate for further ubiquitination steps, resulting in either unbranched chains or branched chains. Each of these modifications has specific effects. Unbranched polyubiquitination over K48 is the most abundant signal for proteasomal degradation. Here, the addition of at least four ubiquitin molecules is required for targeting the substrate to the 26S proteasome (Thrower et al., 2000). The linkage reaction involves three sequential enzymatic reactions described by a ubiquitin-activating enzyme (E1), a ubiquitin-conjugating enzyme (E2) and a ubiquitin ligase (E3).

Since targeted proteins may display different topologies, the associated degradation pathways and the involved E3 ligase complexes may further be classified in regard to the affected misfolded part of the protein: ERAD-L for luminal segments, ERAD-M for transmembrane segments, ERAD-C for cytosol-exposed parts and ERAD-T for translocon-associated degradation (Stevenson et al., 2016).

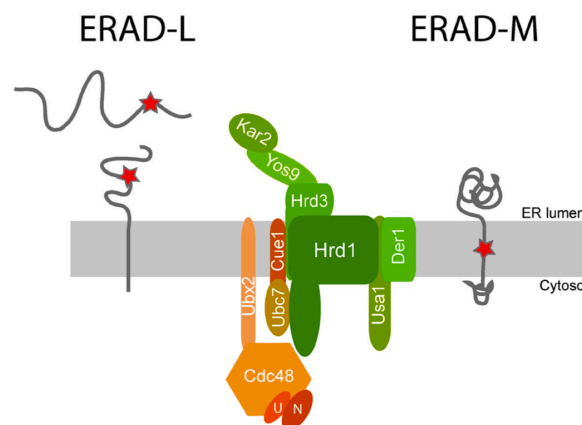


Figure 21: The degradation of proteins displaying misfolded luminal domains and transmembrane segments (red star) is mediated by the Hrd1 complex in the ERAD-L and ERAD-M pathway. For descriptions and abbreviations, see text. Ruggiano et al. (2014).

The best characterized E3 ligase complex is the Hrd1 complex which facilitates degradation of luminal and transmembrane proteins (**Figure 21**). For the recognition of substrates, the complex requires Hrd3 (SEL1L in mammals), which also ensures its overall stability. The lectin Yos9 (OS9, XTP3-B) is responsible for the binding of misfolded glycosylated proteins, while the chaperone Kar2 (BiP) binds exposed hydrophobic regions of the substrates to keep them in a soluble state. Once the substrate has been captured, proteins of the Derlin family transfer it to Hrd1. Both proteins are assumed to be the main factors in retrotranslocation (Carvalho et al., 2010; Lilley and Ploegh, 2004). For this, their oligomerization is required and initiated by Usa1 (HERP). The E2 ubiquitin-conjugating enzyme Ubc7 (UBE2G1, UBE2G2) is recruited and activated by Cue1. In its function as a E3 ligase, Hrd1 not only ubiquitinates substrates, but also requires auto-ubiquitination of its cytosolic RING finger domains, a zinc finger motif, to initiate retrotranslocation (Baldrige and Rapoport, 2016). The energy for protein dislocation and also for membrane extraction of misfolded membrane proteins is achieved by the ATPase activity of Cdc48 (p97/VCP in mammals) after its recruitment to ERAD complexes by Ubx2 (UBXD8), together with its cofactors Npl4 and Ufd1 (NPL4, UFD1). Its ATP hydrolysis triggers substrate clearance from the Hrd1 complex after retrotranslocation (Ruggiano et al., 2014).

2.1.3 ER Stress Triggers the Unfolded Protein Response

When the ER machinery is ultimately overloaded with folding-deficient proteins and when the burden of protein folding exceeds its capacity, intracellular signaling pathways are activated, which are referred to as the unfolded protein response (UPR). Two modes of action are employed to maintain homeostasis: the load of newly synthesized proteins entering the ER is decreased and the folding apparatus is upscaled. Cells that fail to reach a less severe state of stress are prone to apoptosis (Tabas and Ron, 2011).

In the signal transduction pathways that trigger UPR, three major pathways are well-defined, each described by a family of proteins involved in signaling: IRE1 (inositol requiring enzyme I), PERK (double stranded RNA-activated protein kinase-like

endoplasmic reticulum kinase) and ATF6 (activating transcription factor 6) (**Figure 22**). These branches are not excluding each other, show cell-type specific expression patterns and utilize unique toolsets to achieve the same goal: the production of transcription factors that activate UPR-related genes.

The transcription factor ATF6 in its inactive form is a transmembrane protein with a long luminal domain. It is restrained in the ER by interaction with BiP. Once the number of un- or misfolded proteins in the ER increases, BiP binding diminishes, ATF6 is sorted into COPII vesicles and transported to the Golgi apparatus, where it is processed by the proteases S1P and S2P (site-1 and site-2 protease) (Schindler and Schekman, 2009). With the sequential removal of the luminal domain and the transmembrane anchor, the cytosolic domain ATF6(N) is now free to move into the nucleus, where it acts on genes coding for BiP or PDI, increasing the level of proteins available for the heavy-loaded folding processes in the ER.

PERK is a transmembrane kinase that is monomeric in non-stressed conditions. When the UPR is activated, PERK oligomerizes via its N-terminal luminal domains and trans-phosphorylates itself at the C-terminal cytosolic domain. Now activated, PERK phosphorylates translation initiation factor 2 (eIF) (Cui et al., 2011), which is in turn inactivated and lowers mRNA synthesis, thus reducing the load of proteins entering the ER and potentially mitigating ER stress. However, an exception is formed by some mRNAs whose translation is enforced when eIF2 is inhibited: one example is the mRNA of another transcription factor ATF4. ATF4 in turn increases expression of genes that code for proteins involved in apoptosis.

IRE1 comprises two functions with a kinase and an endoribonuclease activity. Upon accumulation of unfolded proteins, IRE1 dimerizes and autophosphorylates. These dimers form oligomers with other dimers, which further promotes autophosphorylation and activates the nuclease capabilities. IRE1 now is able to cleave the mRNA of the transcription factor XBP1 (X-box binding protein), achieving an alternative splice variant that acts both on biolipid synthesis and components of ERAD (Lee et al., 2003).

The integration of multiple pathways allows a cell to carefully regulate its tools against ER stress, from conservative strategies like reducing the amount of expressed proteins up to severe means that lead to controlled cell death (Walter and Ron, 2011).

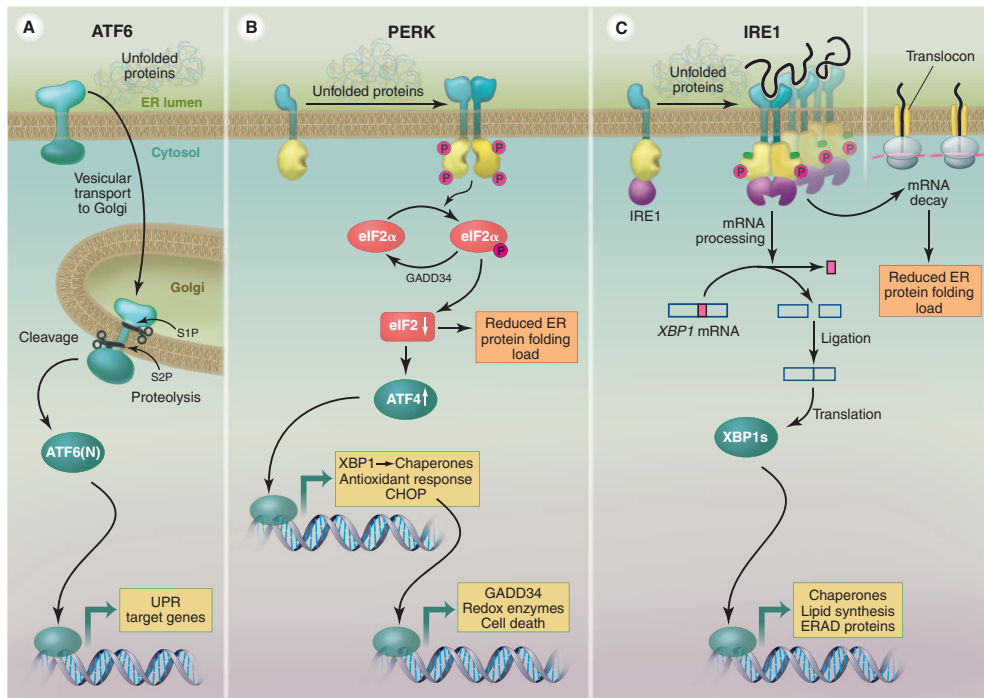


Figure 22: Three branches of the UPR are served by different signaling pathways. (A) ATF6 acts over proteolysis, (B) PERK over translational control and (C) IRE over mRNA splicing. PERK and IRE1 reduce the protein load in the ER by downregulating protein translation and mRNA decay. Walter and Ron (2011).

2.1.4 Transport between ER and Golgi is bidirectional

Secretory proteins leave the ER after translocation and processing towards the Golgi apparatus. Intracellular traffic between compartments is based on the formation and budding of transport vesicles that contain cargo proteins and their subsequent fusion with target membranes. A variety of vesicle types that differ in their origin and their destination is distinguished by the molecular composition of their coat assembly. These coat proteins mediate membrane bending, which is a decisive step in the biogenesis of vesicles.

The formation of vesicles that originate from the ER is characterized by the action of COPII proteins (**Figure 23A**). This machinery is made of the five cytosolic proteins Sar1, Sec13, Sec23, Sec24 and Sec31 (Barlowe et al., 1994). Sec23 and Sec24

form heterodimers and Sec13 forms heterotetramers with Sec31. Sar1, a small GTPase, initiates the recruitment cascade when activated by the guanine nucleotide exchange factor (GEF) Sec12 at the ER membrane. Once its GDP is exchanged for GTP, an amphipathic helix is revealed that associates with the membrane. Sar1 then recruits Sec23-Sec24 heterodimers, forming the “pre-budding complex” as cargo membrane proteins are recruited over the action of Sec24. The cargo displays specific export signals in their cytoplasmic domains that contain, among others, di-hydrophobic, di-acidic or C-terminal aromatic and hydrophobic sequences (Barlowe, 2003). A direct interaction is however not a prerequisite for ER export, as it can also occur via adaptor proteins or entirely passive diffusion into forming vesicles, a process named “bulk flow” (Thor et al., 2009). Cargo sorting is further facilitated by the arrival of Sec13-31. The heterotetramer bends the membrane and polymerizes to complete the formation of the coat, until the vesicle buds off. COPII coat proteins alone are sufficient to pinch the vesicle off the ER membrane and do not require additional factors (Matsuoka et al., 1998). Coat disassembly is linked to the GTPase activity of Sar1. While the intrinsic activity is rather low, Sec23 serves as a GTPase-activating protein (GAP), which itself is enhanced by Sec13-Sec31. This ensures that the coat is removed prior to fusion with the target membrane, similar to a timed mechanism (Antonny et al., 2003; Lee and Miller, 2007).

In higher eukaryotes, vesicles arrive and fuse at the ER-Golgi intermediate compartment (ERGIC), a tubular vesicular cluster that serves as a first sorting station. The lectin ERGIC-53 was described as a marker protein by Schweizer et al. (1998) and subsequent studies revealed the ERGIC structure to be independent of both the ER and the Golgi (Sesso et al., 1994). From here, or in yeast directly from the Golgi, anterograde transport is initiated, or retrograde transport of ER-resident proteins that have escaped their milieu. The latter are recognized by a binding motif that interacts with a specific receptor: the sequence KDEL in soluble proteins, that is recognized by the KDEL receptor, and KKXX in the cytosolic domain of ER membrane proteins, that directly interacts with COPI coat proteins (Pelham, 1996).

COPI vesicles mediate retrograde transport towards the ER and inter-Golgi transport (**Figure 23B**). They are formed in a similar fashion like COPII vesicles. Here, the

small cytosolic GTPase Arf1 (ADP ribosylation factor) is activated by the membrane-bound GEF GEA1 (guanine nucleotide exchange on ARF), upon which it associates with the membrane over an amphipathic helix. The pre-assembled heptameric COPI coatomer complex is recruited, which mediates cargo recognition, further polymerization and membrane curvature. Subsequently, ARF GAP stimulates GTP hydrolysis and the coat is dissolved (Lee et al., 2004).

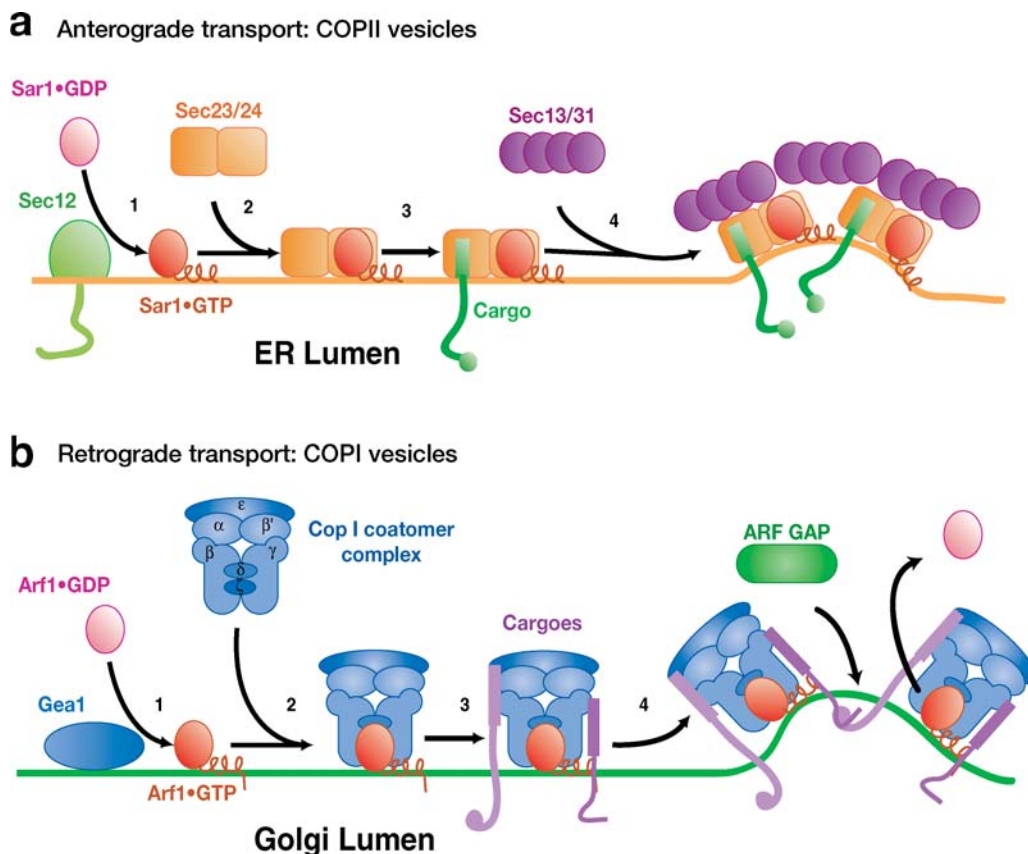


Figure 23: The assembly of coats and vesicle budding. (A) The formation of COPII coats is initiated by Sec12 as a GEF for Sar1. Its nucleotide exchange reveals an amphipathic helix that associates with the ER membrane (1). The Sec23/24 dimer is recruited (2) and the complex interacts with cargo proteins (3). Sec13/31 drives polymerization of the coat and membrane bending (4). (B) COPI coat formation is initiated by a similar mechanism with Gea1 acting as a GEF for Arf1. The amphipathic helix associates with the membrane (1), the pre-assembled coatomer complex is recruited (2) and mediates cargo binding (3). Polymerization and membrane binding occur through unknown mechanisms. Arf1 is activated by a GAP and the complex dissociates (4). Lee et al. (2004), modified.

2.1.5 Two Non-Exclusive Models Describe Transit through the Golgi Apparatus

The Golgi apparatus is the cell's central hub for transport and trafficking. Its structure resembles several stacked cisternae and can be described with a *cis* (cis-Golgi network, CGN), a *medial* and a *trans* (trans-Golgi network, TGN) side, where vesicles arrive from the ER (or leave towards it) and leave the Golgi to form secretory vesicles or fuse with endosomes (or arrive from there), respectively. As the proteins that arrive at the *cis*-Golgi traverse through the stacks, they are further post-translationally modified (e.g. glycosylation, sulfation or phosphorylation). The molecular inventory of each stack and sub-compartment may vary.

Two models have been described to illustrate the movement of proteins between the cisternae: the vesicular transport model and the cisternal maturation model (**Figure 24**). In the first view, Golgi structures are understood as stable entities with defined and maintained enzymatic setups that do not change as vesicles merge and leave. In contrast to this, the cisternal maturation model portrays the Golgi cisternae as dynamic structures that are derived from incoming vesicles and their subsequent maturation through the uptake and removal of specific Golgi-resident proteins. Here, the cisternae as a whole move through the Golgi stack towards the *trans* side, where vesicles bud off until they ultimately dissolve, while at the *cis* side new cisternae are formed from incoming vesicles. It is assumed that aspects of both models are applicable (Rothman and Wieland; 1996; Farquhar and Palade, 1998; Glick and Nakano, 2009; Emr et al., 2009). Transport of large cargo, such as procollagen fibers, is however most easily explained by cisternal maturation (Bonfanti et al., 1998).

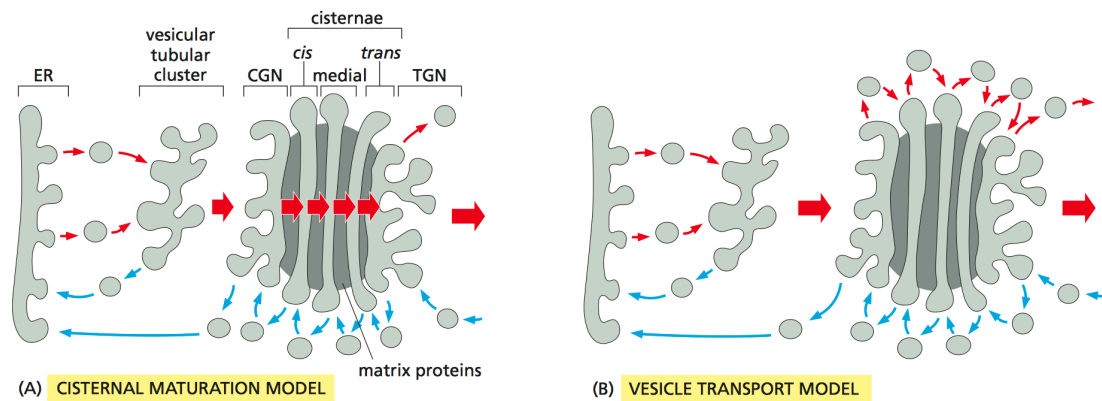


Figure 24: Trafficking through the Golgi is described by two non-exclusive models. (A) The cisternal maturation model describes Golgi cisternae as dynamic structures. Vesicles arriving from the ER and the ERGIC fuse and form the *cis* Golgi. The enzymatic setup is altered throughout the maturation into medial and *trans* structures, until the stack dissolves into target-specific vesicles. Retrograde transport accounts for retrieval of resident proteins into earlier stacks via COPI vesicles. (B) The vesicle transport model portrays Golgi stacks as static entities to which incoming vesicles fuse as they progress through the compartment. Each stack contains characteristic resident proteins. At the *trans* side, sorted vesicles bud off. Alberts (2016).

2.1.6 Secretory Granules Store their Cargo in the Regulated Secretion Pathway

In (neuro)endocrine cells, secretory granules are used for storage and regulated secretion of peptide hormones and neuropeptides. These specialized organelles have a densely packed core that is built by insoluble protein aggregations. Upon a stimulus, the granules fuse with the plasma membrane and release their cargo, which distinguishes this regulated form of secretion process from the always-active constitutive secretion (Burgess and Kelly, 1987). During their TGN exit and packaging, peptide hormones are present in the form of larger precursors. As the maturation of the secretory granules progresses, these prohormones are processed and cleaved by carboxypeptidases and prohormone convertases, which are activated by increasing acidification (Borgonovo et al., 2006).

The mechanisms of sorting into secretory granules have been proposed on the basis of two different models: “sorting for entry” and “sorting by retention”. “Sorting for entry” describes that elevated Ca^{2+} levels and a slightly acidic pH at specialized TGN regions favor aggregation of cargo molecules and their sorting by receptors over specialized signal sequences, with the mannose 6-phosphate receptor as a well-studied example for the sorting of lysosomal hydrolases (Kornfeld and Mellman,

1989). “Sorting by retention” implies the maturation of secretory granules through further concentration of the eventual cargo, which is facilitated by sustained removal of captured non-cargo molecules and their re-routing to the constitutive pathway. For the formation of the retrograde transport vesicles, clathrin and the adaptor protein AP-1 are required and frequently found on immature secretory granules (Dittie et al., 1996). Only the cargo is retained in the vesicles (Kuliawat and Arvan, 1992). These two models may complement each other and are not exclusive. Beuret et al. (2004) revealed that misexpressed proteins of the regulated secretion pathway are able to sort into granule-like structures in cell lines that lack regulated secretion. The expression of several peptide hormones and granins in COS cells was sufficient to segregate these proteins from co-expressed constitutively secreted proteins and to form dense aggregates, suggesting that aggregation does not necessarily rely on additional extrinsic factors like specific receptors, but can be achieved by the cargo itself.

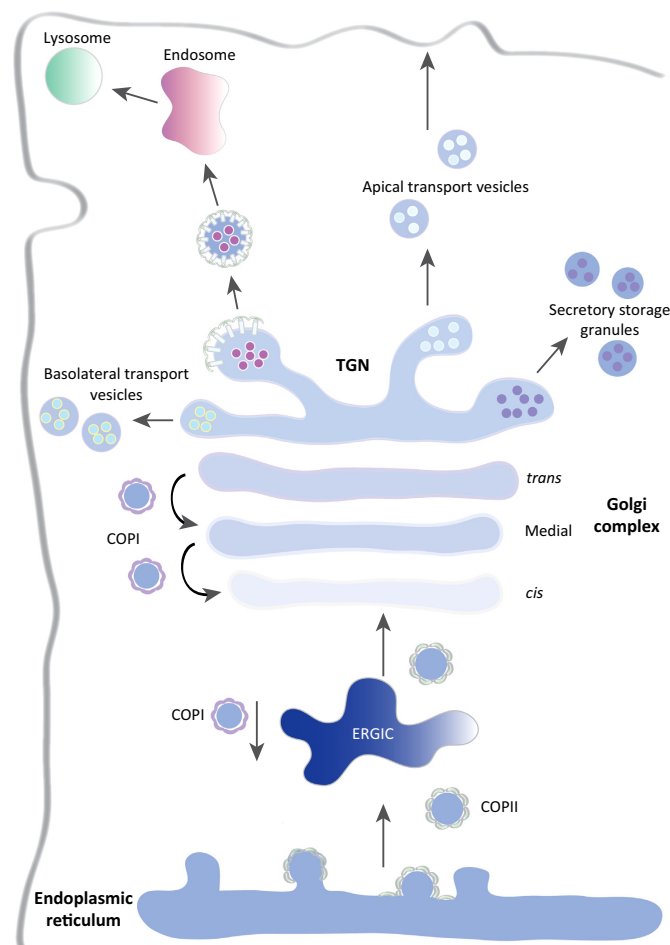


Figure 25: Overview over protein trafficking. COPII coated vesicles derived from the ER are transported to the Golgi apparatus over the ER-Golgi intermediate compartment (ERGIC). The vesicles then traverse the Golgi towards the TGN, from where multiple vesicle types originate, including secretory granules. Kienzle and von Blume (2014).

2.2 Diabetes Insipidus

2.2.1 Vasopressin Regulates Water Homeostasis

Kidneys are responsible for maintaining many homeostatic functions in the body, such as the regulation of electrolyte concentrations, the overall volume of body fluids and clearance of metabolic waste and other substances from the blood stream. This occurs through capillary filtration in the functional units of the kidney, the nephronic glomeruli. In a healthy organism, the resulting primary urine is free of proteins, but the large volume of approximately 180 liters per day requires further concentration through re-absorption of water and ions in a strictly regulated manner. The water permeability of distal renal tubules accounts for the re-uptake of 90% of the glomerular filtrate and enables urine concentration through the action of the antidiuretic hormone ADH, or vasopressin. Vasopressin is synthesized as a prohormone in magnocellular neurons of the paraventricular and supraoptic nucleus in the hypothalamus, from where it is transported into the posterior pituitary gland, or neurohypophysis, and stored in secretory granules (**Figure 26**). The nerve endings make contact with capillaries, allowing for release of vasopressin into the blood stream upon a stimulus. Osmoreceptors are modified neurons and register changes in extracellular fluid composition: when its concentration becomes too high in a state of dehydration, the osmoreceptors shrink and relay this information towards the vasopressinergic neurons, triggering the release of vasopressin into the blood.

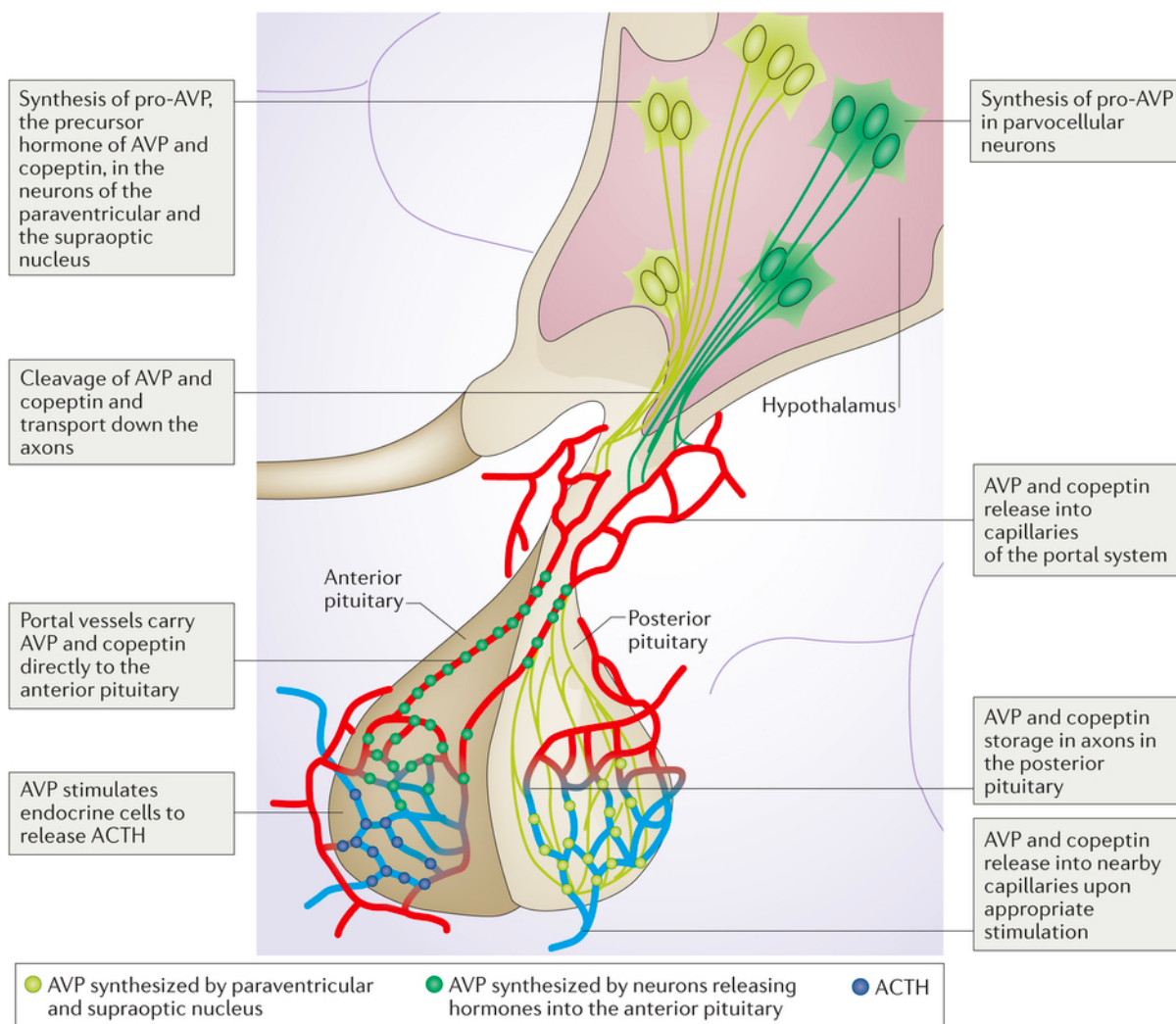


Figure 26: Synthesis of AVP and its glycopeptide copeptin. Synthesis occurs in magnocellular neurons at the paraventricular and supraoptic nucleus, from where the products are transported and stored at the pituitary gland until their release into the bloodstream upon a stimulus. Christ-Crain and Fenske (2016).

Vasopressin is humorally transported into the kidneys, where binds to its receptor V_2 on renal principal cells at the collecting duct. In its function as a G-protein coupled receptor, it facilitates nucleotide exchange at $G\alpha$, which in turn activates adenylate cyclase (AC) and gives rise to the cAMP-based cascade, protein kinase A (PKA) activity and phosphorylation of aquaporin 2 (AQP2). The subsequent incorporation into the membrane facing the tubular lumen increases water permeation and aquaporins 3 and 4 (AQP3, AQP4) on the basolateral side of the cell membrane allow the water to flow through the cell (Boone and Deen, 2008) (**Figure 27**).

The dysregulation of water re-uptake and the subsequent excretion of larger volumes of diluted urine (approximately 10-15 liters per day) is described as a condition called diabetes insipidus (DI). This disorder can be the result of different underlying causes, among others: the inability for ADH production or secretion in neurohypophyseal cells, described as neurohypophyseal diabetes insipidus or central diabetes insipidus, which may be acquired through head trauma, but is in most cases hereditary; or the inability of the kidneys to adequately respond to ADH in nephrogenic diabetes insipidus. This is observed as a side effect of certain drugs, like antibiotics or lithium-based treatments against manic-depressive disorders, but may also be caused by genetic aberrations, leading to impaired function of the vasopressin receptor (Guyton and Hall, 2015; Oiso et al., 2013). In the further context, the focus will be set on congenital neurohypophyseal diabetes insipidus.

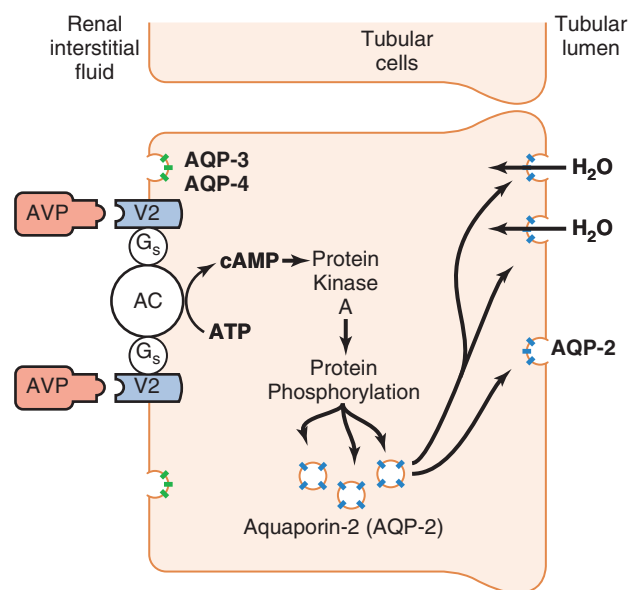


Figure 27: Arginine vasopressin (AVP) acts on epithelial cells in renal tubules and collecting ducts. It binds at its receptor (V2) which in turn activates a cAMP cascade. Subsequently, aquaporin-2 (AQP-2) is incorporated into the luminal membrane and allows re-absorption of water. AQP-3 and AQP-4 at the opposite side of the cell grant water flow. Guyton and Hall (2015).

2.2.2 Mutations in the Vasopressin Precursor cause Diabetes Insipidus

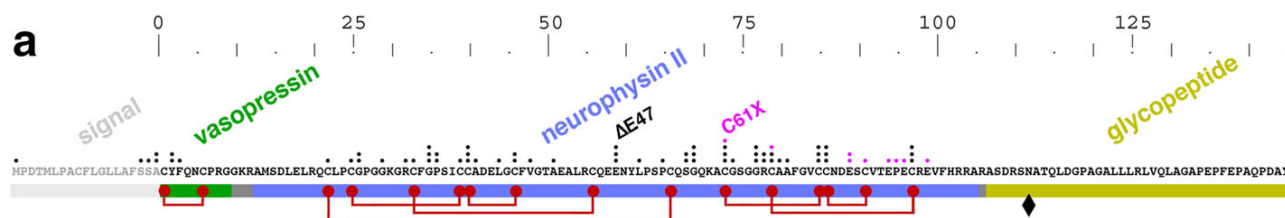


Figure 28: Domain organization of provasopressin with vasopressin in green, neurophysin II (NPII) in blue, the glycopeptide in yellow and the black diamond as its glycosylation site. Red circles indicate cysteines and the corresponding disulfide bridges. Each black dot represents a mutation that is known to cause ADNDI (black: missense, pink: nonsense). In this study, a truncated version NPII_{trunc} based on the C61X mutation and the Δ E47 mutant without the glycopeptide Δ GP will be used. Modified from Beuret et al. (2017).

Vasopressin is synthesized in a precursor form (**Figure 28**). The prohormone can be divided into its domains for the nonapeptide vasopressin (CYFQNCPRG), neurophysin II with 93 amino acids (NPII) and a 39 residue glycopeptide with one glycosylation site. The crystal structure of lysine vasopressin (K7 instead of R7) complexed with bovine NPII shows that vasopressin binds into a pocket formed by NPII, where the disulfide bond formed by C1-C6, and the residue Y2 are concealed. This pocket appears to be accessible without the presence of vasopressin, suggesting an early interaction site during prohormone folding. The α -amino group of vasopressin C1 forms a hydrogen bond as well as an electrostatic interaction with the carboxyl group of the NPII E47. Vasopressin Y2 interacts with several NPII backbone residues and side chains, among them E47 (Wu et al., 2001) (**Figure 29**). After traversing the ER and the Golgi apparatus, the prohormone is packed into secretory granules, where it is processed and cleaved by prohormone convertase 1. The C-terminus is amidated, resulting in the final vasopressin nonapeptide.

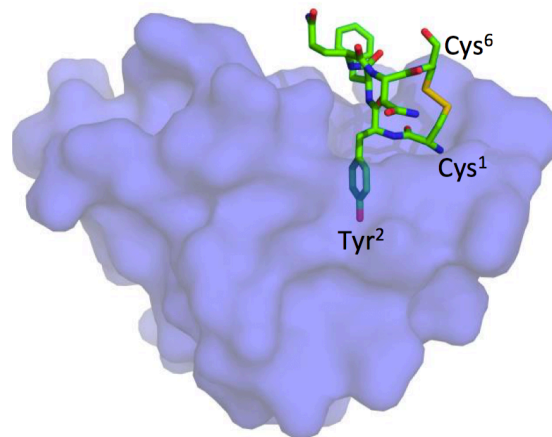


Figure 29: Illustration showing vasopressin (lysine variant) binding to the pocket provided by NPII. C1, C6 and Y2 are hidden inside the pocket and the interaction of Y2 is required for binding. PDB 1JK4, Wu et al. (2001). Image by Käser (2016, Master thesis).

More than 70 mutations throughout the prohormone, except the glycopeptide, are known to cause congenital autosomal dominant neurohypophyseal diabetes insipidus (ADNDI, Jendle et al., 2012). Patients suffer from a lack of functional vasopressin and are subject to DI shortly after birth, despite the presence of a functional allele. Autopsies revealed the degeneration of vasopressinergic neurons and instead showed scar tissue in their place (Bergeron et al., 1991). This represents the dominant phenotype of ADNDI, in that mutant vasopressin leads to cell death and functional vasopressin can no longer be produced. The neurodegenerative character was confirmed in a murine knock-in model, where heterozygous mice expressed the ADNDI mutant C67X (where X means a mutation to a stop codon) and displayed characteristic symptoms of DI as well as the progressive loss of vasopressin-producing neurons in the paraventricular and supraoptic nucleus (Russell et al., 2003). The involvement of autophagy was suggested (Hagiwara et al., 2014).

In cell culture experiments, ER retention of mutant provasopressin was described as a general observation in ADNDI mutants, as to be expected for misfolded proteins (Jameson and Ito, 1997; Nijenhuis et al., 1999). Retrotranslocation and proteasomal degradation was observed over the ERAD machinery (Friberg et al., 2004). However, a significant amount of misfolded precursor proteins was shown to accumulate in the ER over the formation of degradation-resistant aggregates (Beuret et al., 1999).

Aggregate formation of several ADNDI mutants were later on characterized as homo-oligomers with fibrillar ultrastructure that could be reconstituted *in vitro* (**Figure 30**). Disulfide bonds proved to be required for both mutant-derived oligomer formation as well as for correct folding of provasopressin. Upon mutation of groups of cysteines, folding was found to be impaired and oligomers were formed, which were eliminated when no cysteines were present (Birk et al., 2009; Käser, 2016, Master thesis).

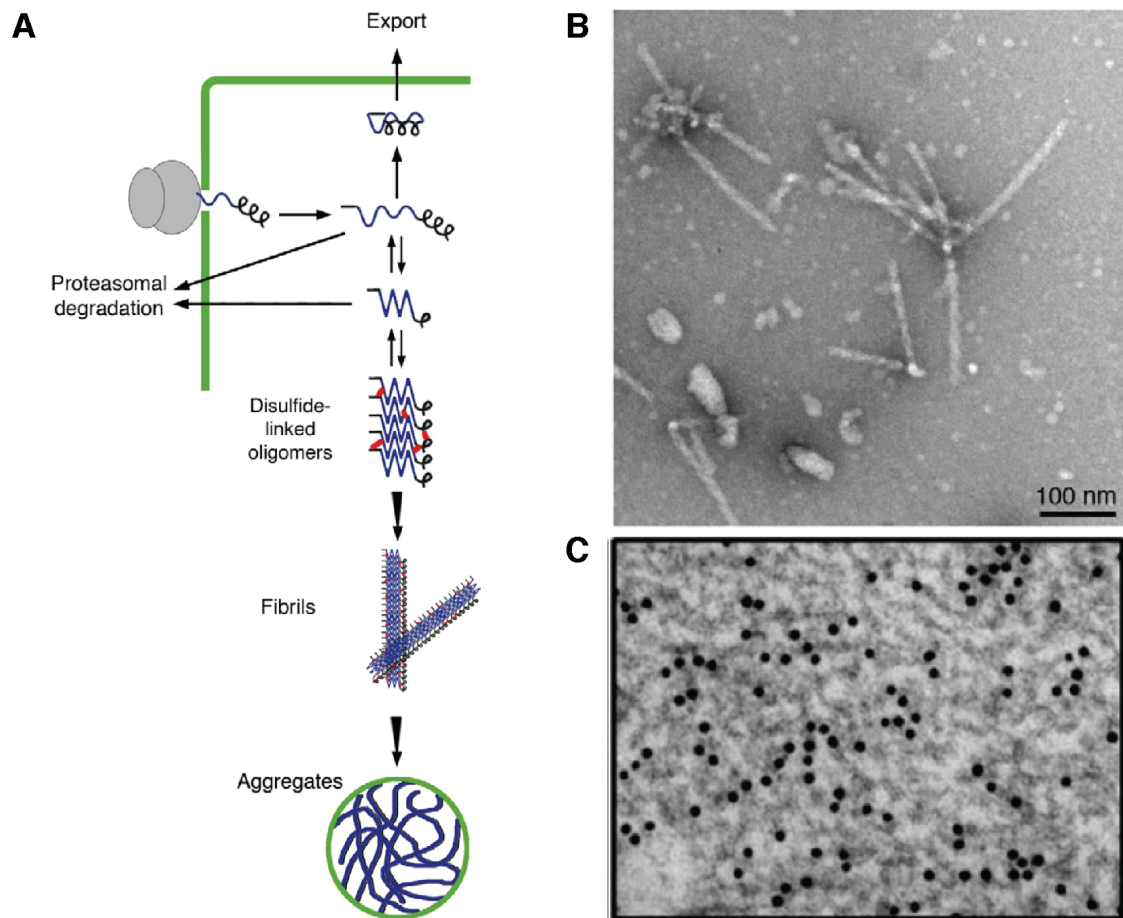


Figure 30: Fibrillar aggregation in the ER by provasopressin. (A) Natively folded proteins pass ER quality control and leave the ER to be sorted into secretory granules at the TGN. Misfolded variants are degraded, but may also form disulfide-linked oligomers (red). (B) EM picture of fibril formation by the ADNDI mutant $\Delta E47$ *in vitro*. (C) EM picture with 10nm immunogold staining of the ADNDI mutant C61X. The folding-deficient mutant is ER retained and forms a fibrillar network of aggregates. (A), (B) Birk et al. (2009); (C) Beuret et al. (2017).

Beuret et al. (2017) have further investigated the prerequisites for the aggregation of folding-deficient and ER-retained precursors, based on the natural mutants $\Delta E47$ and C61X. Scans with a ten-residue proline/glycine segment, truncation experiments and fusion constructs of reporter proteins with N-terminal portions of provasopressin were conducted. These experiments identified the glycopeptide and vasopressin as

independent motifs for pathogenic fibrillar ER aggregation in folding-deficient mutants, but also as sufficient to mediate granule sorting of the folding competent prohormone. It is proposed that the vasopressin nonapeptide is not accessible under ER conditions, where it is hidden in the binding pocket offered by NPII (De Bree et al., 2003). The milieu provided at the TGN is then likely to promote vasopressin-mediated aggregation in concert with the glycopeptide and subsequent sorting into the emerging immature granules. Folding-deficient and ER-retained mutants however may not display the binding pocket, leaving vasopressin accessible for oligomerization.

These findings place ADNDI in the group of neurodegenerative diseases that show fibrillar protein aggregation, as observed in diseases linked to amyloid formation.

2.2.3 Amyloids as a Storage Mechanism in Secretory Granules

The observed aggregation of provasopressin can be interpreted within both pathological (in the ER) and physiological (during granule formation) content. The latter notion was fueled by Maji et al. (2009), where it was proposed that the same aggregation mechanisms may serve as a natural storage for secretory granules into the pituitary gland in the form of functional amyloids. Amyloid fibrils consist of intermolecular cross- β -sheet structures in a strictly arranged pattern that renders proteins resistant to degradation. This insolubility, a hallmark of amyloids, is reflected in their resistance to DTT and SDS. Histologically they may be identified by staining with the dyes Congo Red and Thioflavin S that empirically bind amyloids (Ramabaran and Serpell, 2008).

Amyloids were mainly associated with diseases like Alzheimer's, spongiform encephalopathies or some cases of type II diabetes. Recently, functional amyloids have been characterized in melanosomes formed by the protein Pmel17, in the biofilm component curli of *E. coli*, and others (Chiti and Dobson, 2006; Fowler et al., 2007). Maji et al. (2009) showed that amyloids are commonly encountered in secretory granules containing pituitary gland peptide hormones. This was demonstrated with immunohistological stainings of mouse pituitary glands, where the

peptide hormones prolactin, adrenocorticotrophic hormone (ACTH), growth hormone, oxytocin and vasopressin co-localized with the amyloid-specific dye Thioflavin S. Furthermore, X-ray fiber diffraction of purified secretory granules from AtT20 cells expressing ACTH showed characteristics typical for amyloid fibrils. The formation of amyloid fibers was confirmed *in vitro* for several hormones, similar to Birk et al. (2009). With these findings, the authors argued that the formation of amyloid structures may occur with a physiological function.

In this context, it is eye-catching that deposits of amyloids are frequently found in the pituitary, both in aging and in the occurrence of pituitary adenomas. Their morphology, size and localization varies in these forms, but a specific correlation of deposit types and these features has not been successful. The involvement of at least prolactin, ACTH and growth hormone has been shown by immunohistochemistry (Westermarck, 2005). Since the physiological appearance of pituitary hormones in secretory granules was suggested to present a natural storage mechanism by Maji et al. (2009), the formation of pathological amyloids may be attributed to the same underlying mechanism. As Beuret et al. (2017) demonstrated, the nonapeptide vasopressin is necessary for both ER aggregation of folding-deficient provasopressin mutants and sorting of correctly folded wild-type provasopressin into secretory granules. Cargo aggregation is believed to contribute to granule formation at the TGN in the regulated secretory pathway. Depending on the context, it appears therefore likely that the same mechanism applies for aggregation of misfolded proteins in the ER.

2.2.4 Several Peptide Hormones Share a Structural Similarity

It is not surprising that both oxytocin- and vasopressin- containing granules stain positive for Thioflavin S, given the similarity of their sequence differing in only two residues (CYFQNCPRG in vasopressin, CYIQNCPLG in oxytocin). In previous experiments, it was shown that replacing vasopressin with oxytocin in the folding deficient $\Delta E47$ mutant without the glycopeptide (thus containing no other sequence that can mediate aggregation or granule sorting; Beuret et al., 2017) was able to achieve ER aggregation, implying that oxytocin, like vasopressin, mediates amyloid-

like aggregation (Janoschke, personal communication). The peptide hormones that were proposed to be stored as amyloids by Maji et al. (2009), including vasopressin and oxytocin, display one structural similarity: a short disulfide loop that is not obscured or buried, but localized either at the termini or at the surface and easily accessible.

In this context, the N-terminal disulfide loop displayed by amylin (islet amyloid polypeptide, IAPP, produced in pancreatic β -cells) has been shown to mediate fibril formation *in vitro*. In contrast to the full-length protein, which is aggregation-prone and involves the formation of β -sheets, fibrils formed by the N-terminal part containing the disulfide loop are non-amyloid in nature and characterized by a β -turn. A contribution of the N-terminal disulfide loop to the pathological aggregation of IAPP has been proposed (Cope et al., 2013).

The aggregate formation of somatostatin was further characterized by Anoop et al. (2014) (**Figure 31**). The 14-residue peptide hormone with its disulfide bond was shown to form aggregates *in vitro* earlier (Maji et al., 2009), and subsequent immunohistochemical experiments suggested that somatostatin is stored in secretory granules in the form of amyloids. To shed light on the role of the disulfide bond, comparisons with a reduced form of somatostatin lacking the disulfide bond were conducted in several experimental setups. If amyloid formation acts as a natural storage mechanism in secretory granules, the problem arises that these amyloids must be able to readily dissolve upon secretion and release functional monomers. Amyloids in turn are known for their insolubility and stability, which would render hormones stored in this form useless for the organism. Interestingly, it was described that the disulfide loop regulates amyloid formation *in vitro*: the non-reduced form aggregated slower than the reduced form without the disulfide loop, and fibrils formed by them dissolved faster. The disulfide loop therefore appears to regulate aggregation in a physiological useful manner, viz. a readily-dissolvable yet dense storage form. This further advocates the theory of short disulfide loops in granule biogenesis and storage of peptide hormones.

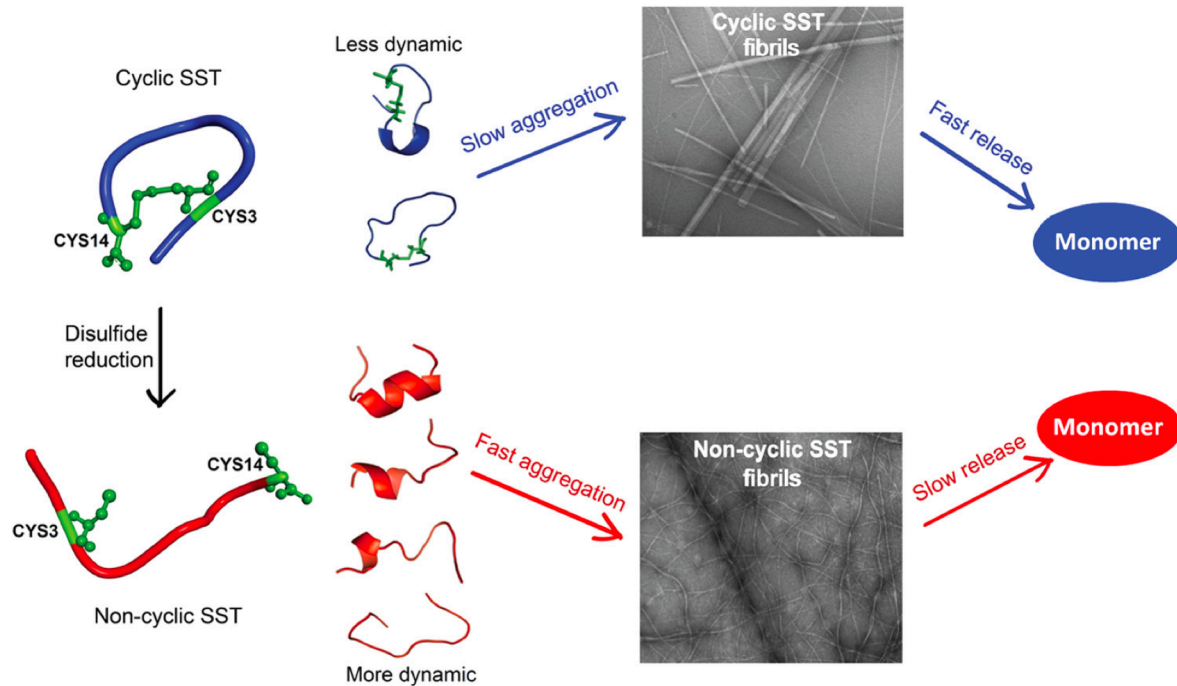


Figure 31: Somatostatin aggregate formation is controlled by the disulfide loop. With the loop, cyclic somatostatin (blue) shows slow aggregation kinetics leading to fibril formation. Dissociation and monomer release is fast when compared to the behaviour of non-cyclic somatostatin without the disulfide loop (red). Here, aggregation is faster and the fibrils are more stable, leading to slow release of monomers. This suggests a regulatory function of the disulfide loop to ensure feasible dissociation of aggregated and stored hormones upon a stimulus. Anoop et al. (2014).

Interestingly, a disulfide loop was also shown to be sufficient for granule sorting of chromogranin B, although the loop is much larger with 22 residues (Glombik et al., 1999). Likewise, vasopressin with its 6-residue disulfide loop is sufficient to mediate ER aggregation of the folding-deficient prohormone mutant (Beuret et al., 2017). Further extending the view onto other peptide hormones that present a disulfide loop in a comparable fashion may help to answer the question whether disulfide loops act as a common aggregation motif not only in pathology, but also in physiologic and functional granule sorting.

2.3 Aim of Part II

The finding that the vasopressin nonapeptide contains an aggregation motif, both in amyloid-like pathological fibril formation and in physiological granule sorting (Beuret et al., 2017), is in accordance to the suggested role of amyloids as a storage mechanism in regulated secretion (Maji et al., 2009). A short and terminal disulfide loop as a structural similarity to other peptide hormones, which are also characterized by amyloid-like granule formation and, in some cases, pathological aggregation, is eye-striking.

Ultimately, we wish to test if these disulfide loops act as a general motif in the biogenesis of secretory granules. In the present work, we approach this question by investigating disulfide loop-mediated aggregation in the ER, as observed for ADNDI-causing provasopressin mutants. ER aggregation is easy to test for and the possibility that disulfide loops could facilitate aggregation in the ER may hint towards a general mechanism of aggregation that provides the same functionality at the TGN. We therefore aim to answer the question whether disulfide loops are able to significantly increase ER aggregation of folding-deficient neurophysin II and replace the vasopressin nonapeptide in this context.

2.4 Summary

A role of amyloid formation in the regulated secretory pathway has been proposed for several peptide hormones during their granule biogenesis and the formation of fibrillar aggregates *in vitro*. Some notable examples, including vasopressin, contain solvent-exposed small disulfide loops at their N- or C-termini, which have been shown to initiate aggregation, or regulate this process in order to enable faster dissolution of the stored hormones when necessary. In this context, our work focuses on the question whether disulfide loops may serve as a general motif in granule biogenesis at the TGN through an aggregation-promoting mechanism. We challenged disulfide loops of the peptide hormones prolactin, prorenin, amylin, growth hormone and calcitonin for their aggregation ability of a misfolded and ER-retained protein. By fusing these loop-containing regions to folding-deficient variants of neurophysin II, we found that all tested loops are able to mediate aggregation in the ER. Electron microscopy revealed densely packed structures with sizes ranging between 100 and 300nm. Our results suggest that the tested disulfide loops contain intrinsic information that allows aggregation in the context of folding-deficient NPII, which by itself is not sufficient to mediate significant aggregation. In order to extend this observation towards granule biogenesis, further experiments with adequate reporter proteins will be necessary.

2.5 Introduction

Diabetes insipidus is a dominant disease that is linked to mutations in the vasopressin precursor, leading to its ER retention (Jameson and Ito, 1997), fibrillar aggregation (Birk et al., 2009) and degeneration of vasopressinergic neurons (Bergeron et al., 1991). Both the vasopressin nonapeptide and the glycopeptide have been identified as necessary and independent motifs to mediate ER aggregation of a folding deficient precursor, or sorting into secretory granules of the functional wild-type protein, respectively (Beuret et al., 2017).

In the context of a proposed physiological function of amyloid formation, the vasopressin-linked aggregation of its misfolded precursor may be derived from the very same properties that normally mediate aggregation into secretory granules, as it likely has evolved to employ this mechanism solely as a natural storage mechanism post-TGN. To prevent ER aggregation as seen in the pathological scenario, vasopressin is normally concealed in a binding pocket provided by neurophysin II. Once this protection is no longer available due to misfolding, vasopressin is free to oligomerize in an organelle where it has disastrous effects, ultimately submitting the cell to apoptosis.

The vasopressin nonapeptide is sufficient to initiate ER aggregation of an unrelated reporter protein, as shown by Beuret et al. (2017). In its native context within provasopressin, its presence enables the precursor to be sorted into secretory granules. Oxytocin, differing from vasopressin by only two residues, can replace vasopressin within this experimental setup (Janoschke, personal communication).

Other peptide hormones have been suggested to form amyloids as a storage mechanism in secretory granule biogenesis, including provasopressin. Several of the proteins analyzed by Maji et al. (2009) display a common feature: a short and exposed disulfide loop at either terminus or at the protein surface. The disulfide loop of chromogranin B has been characterized to mediate sorting into secretory granules (Glombik et al., 1999). Likewise, *in vitro* experiments suggested that the disulfide-loop of amylin may be involved in the formation of aggregates (Cope et al., 2013). A regulatory effect has been proposed for the disulfide loop of somatostatin (Anoop et al., 2014). These findings may hint towards a general involvement of disulfide loops during granule biogenesis. To test this, we focused on several peptide hormones that are known to form pathogenic amyloid deposits (Westermarck, 2005), of which all show a disulfide loop at their surface that is potentially free to engage in interactions (**Table I**). We isolated these loops and fused them to a folding-deficient variant of provasopressin, exchanging the vasopressin nonapeptide with the disulfide loop of other hormones (**Figure 32**). ER aggregation mediated by these loops may strengthen the argument that aggregate formation is supported by disulfide loops.

Table I: The disulfide loops of several peptide hormones. The cysteines forming the disulfide bridge are highlighted in red. Blue: N-terminal loops. Yellow: loops that are not terminal, but are exposed and accessible. Green: C-terminal loops. These loops have been used in further experiments with the indicated abbreviations. The loops of pro-oxytocin and chromogranin B (grey) are referred to in the introduction. The control sequence does not contain a disulfide loop and the sequence is composed of glycines and prolines.

(Pro)hormone	Sequence
Provasopressin (Vaso)	NH ₂ -CYFQNCPRG...
Amylin (Amy)	NH ₂ -KCNTATCATQ...
Calcitonin (Calc)	NH ₂ -RCGNLSTCMLGT...
Prolactin N (PLN)	NH ₂ -TPVCPNGPGNCQVSLR...
Renin (REN)	...-SSKCSRLYTACVYHK...
Prolactin C (PLC)	...LLNCRIIYNNNC-COOH
Growth hormone (GH)	...VMKRRFAESSCAF-COOH
Pro-oxytocin	NH ₂ -CYIQNCPLG...
Chromogranin B	...VTYRCIIEVLSNALSKSSAPTITPECRQVLR...
Control sequence (ProGly)	NH ₂ -GPPGPGTPGP...

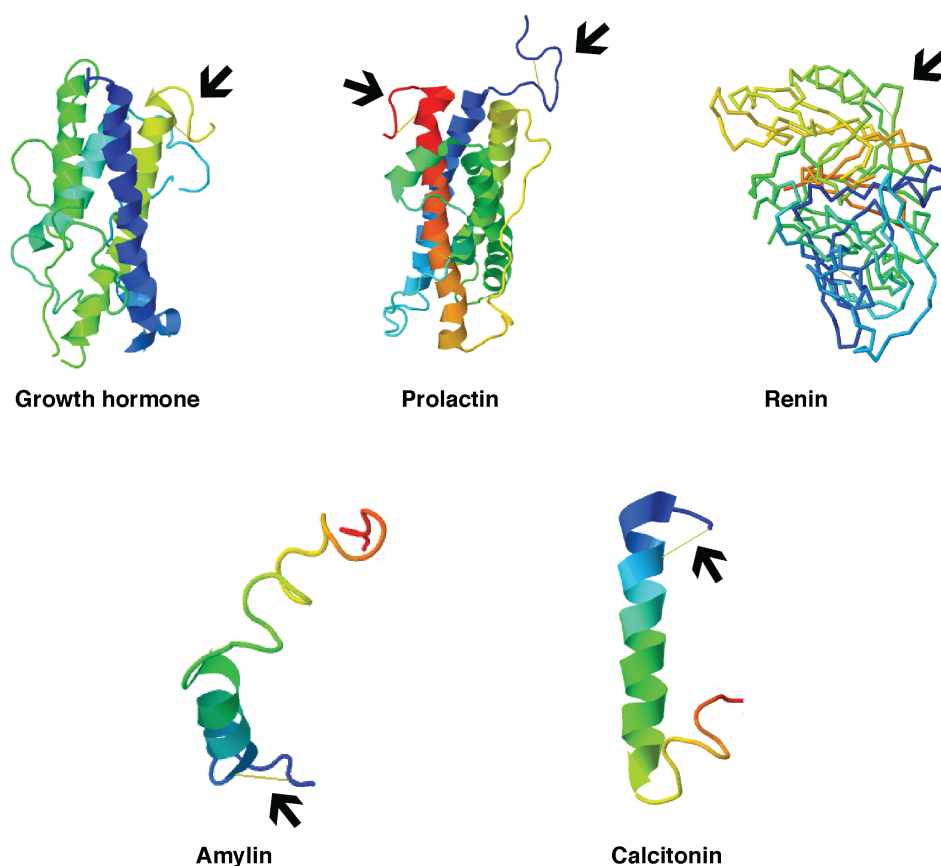


Figure 32: Structural visualization of five peptide hormones, from N (blue) to C-terminus (red). The secondary structure of renin is omitted for clarity. Each hormone displays a disulfide loop (yellow line, marked by arrow) at exposed positions. Growth hormone: Chantalat et al. (1995), PDB 1HGU. Prolactin: Teilum et al. (2005), PDB 1RW5. Renin: Morales et al. (2012), PDB 3VCM. Amylin: Rodriguez Camaro et al. (2017), PDB 5MGQ. Calcitonin: Andreotti et al. (2006), PDB 2GLH.

2.6 Results

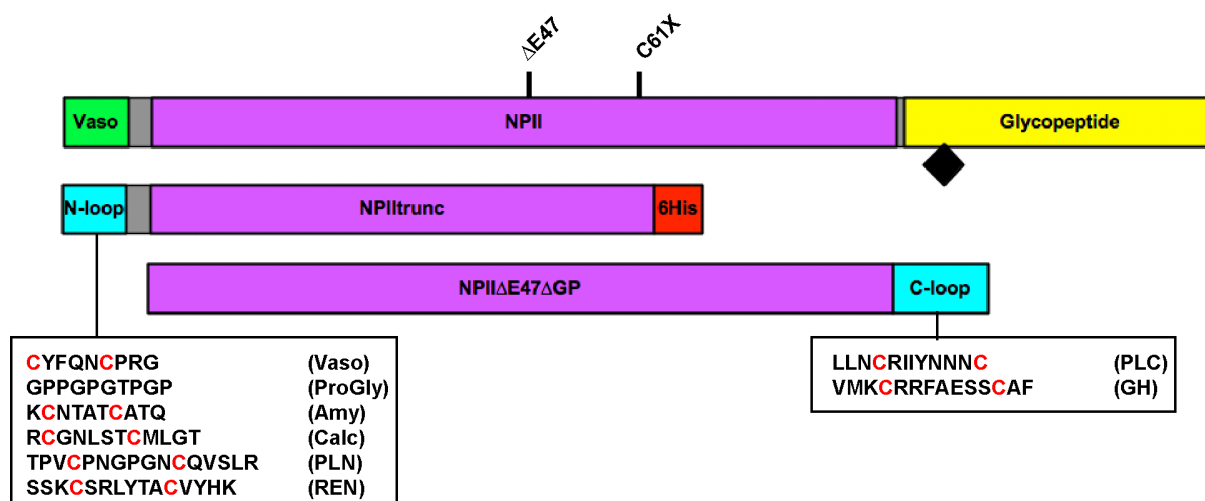


Figure 33: Overview of the disulfide loop-containing constructs used, from top to bottom: wild-type provasopressin, folding-deficient mutants NPII_{trunc} and $\Delta E47\Delta GP$. These mutants are based on naturally occurring mutations leading to ADNDI and are indicated (C61X for NPII_{trunc}, $\Delta E47$ for $\Delta E47\Delta GP$). The black diamond is the position of N-linked glycosylation. The glycopeptide contains an aggregation motif on its own and was therefore removed. For N-terminal disulfide loops originating from the indicated proteins (abbreviations see Table I), NPII_{trunc} with a His-tag was used. N-terminal loops were also combined with $\Delta E47\Delta GP$. For C-terminal disulfide loops, $\Delta E47\Delta GP$ has been used to ensure recognition by the antibody against NPII and to avoid interference through C-terminal tags in the proximity. The cysteines contained in the short disulfide loops are highlighted in red. ProGly as a negative control does not display disulfide loops.

Two provasopressin mutants leading to ADNDI were selected to act as a carrier: C61X, which is truncated (X for stop codon), and $\Delta E47\Delta GP$, which contains the full NPII domain with an ADNDI point mutation. The glycopeptide was deleted, as it contains an aggregation motif on its own (Beuret et al., 2017). The sequences shown in Table I were fused to either the N-terminus (in the case of the N-terminal loop of prolactin, amylin, calcitonin and a loop-containing region from the middle of the prorenin sequence), or the C-terminus (prolactin, growth hormone). A His-tag was added to C61X-based constructs to ensure detection. The constructs were transiently expressed in the neuroblastoma cell line Neuro 2a, pituitary corticotroph tumor cells AtT20, and fibroblastoma-like COS-1 originating from the kidney. The constructs are displayed in **Figure 33**.

2.6.1 Disulfide Loops Mediate Aggregation of a Misfolded Provasopressin Carrier in Neuronal Cell Lines

The neuronal cell lines Neuro 2a (N2a) and AtT20 are capable of regulated secretion and have been used to investigate granule sorting in previous studies. While wild-type provasopressin is sorted into the cell tips where it colocalizes with a granule marker, the ADNDI mutants C61X and Δ E47 are retained in the ER. The vasopressin nonapeptide was shown before as necessary for aggregation of ER-retained NPII, which is abolished when replaced with prolines and glycines (Beuret et al., 2017).

In the context of transient transfection, NPII mutants with short disulfide loops of other peptide hormones were expressed in N2a and AtT20 cells and analyzed with immunofluorescence. Vasopressin fused to NPII mutants was used as a positive control for aggregation, whereas the proline and glycine-containing construct served as a negative control. Aggregates manifest themselves as sharp and dense structures that are easily distinguished from cellular background. Aggregate formation in at least 100 expressing cells was quantified, which was regarded as positive when showing more than three visible aggregates in the cell body.

All tested disulfide loops were able to replace the vasopressin nonapeptide in NPII mutants to mediate ER aggregation (**Figure 34**), with aggregates formed in more than 70% of expressing cells (**Figure 35**) each. Colocalization with the ER-resident KDEL receptor is shown exemplary for the construct Amy-NPII_{trunc} in (**Figure 36**). While morphological variances were distinguishable (i.e. size or shape), none could be attributed to a specific disulfide loop. These findings in N2a cells were also applicable for AtT20 cells (data not shown).

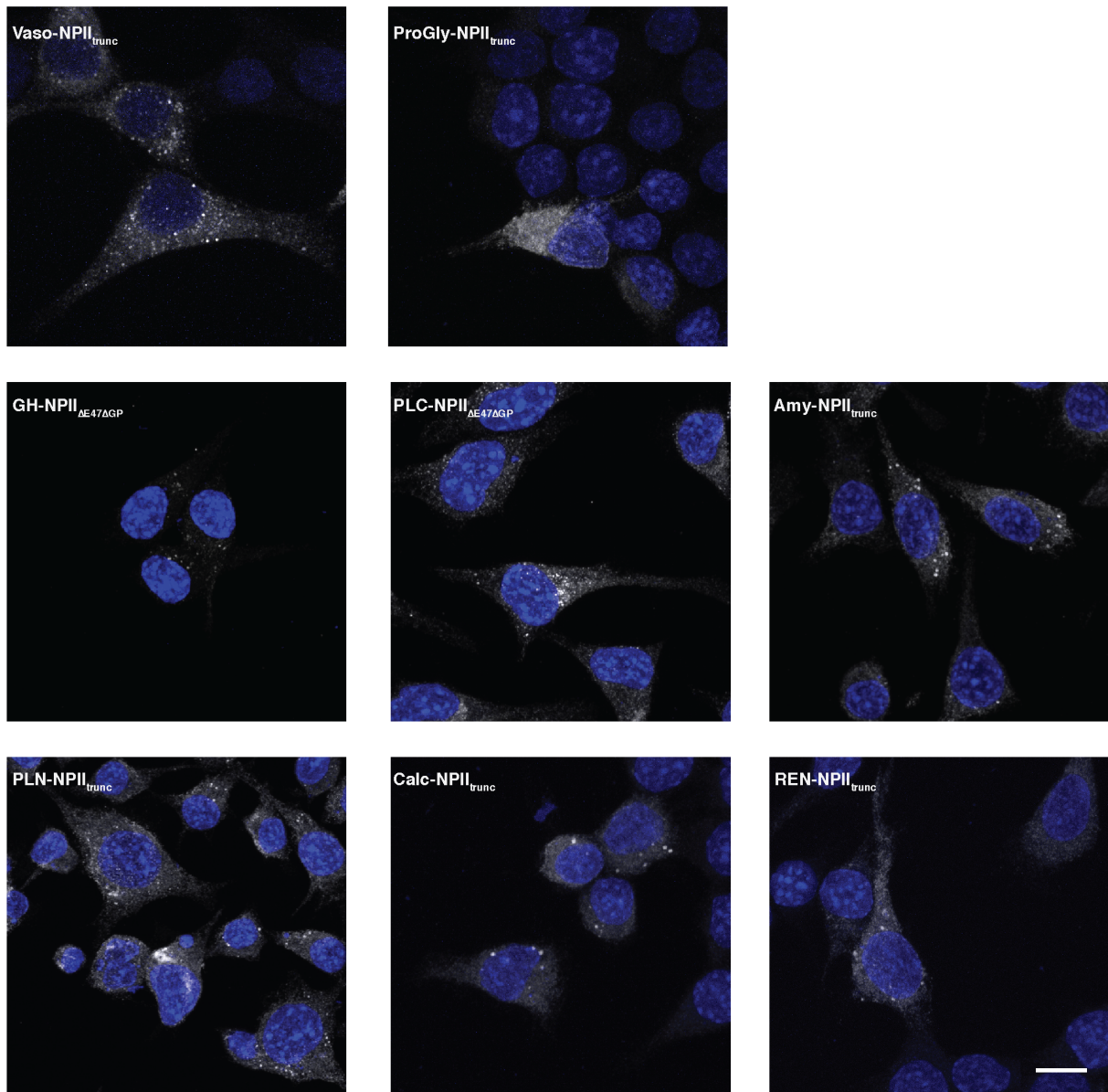


Figure 34: In the tested neuronal cell lines (N2a shown), the presence of all tested disulfide loops with folding-deficient NPII domains lead to significant aggregation that resembled vasopressin-mediated aggregation. Vaso-NPII_{trunc} was used as a positive control. Aggregates were no longer formed when vasopressin was replaced with prolines and glycines in the construct ProGly-NPII_{trunc}. Size bar 10 μ m.

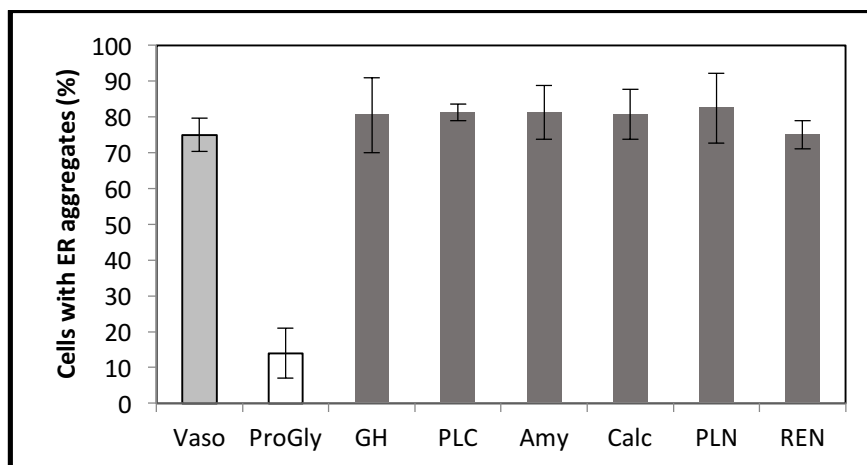


Figure 35: For all introduced disulfide loops, aggregation is drastically increased and on comparable to the action of vasopressin. Quantification was conducted in N2a cells with ER aggregates, counting at least 100 expressing cells. A cell that shows at least three dense dot-like structures and not localized at the cell tips are regarded as positive. In contrast, the negative control ProGly does not form ER aggregates to a significant amount. Error bars represent SD from at least three independent experiments.

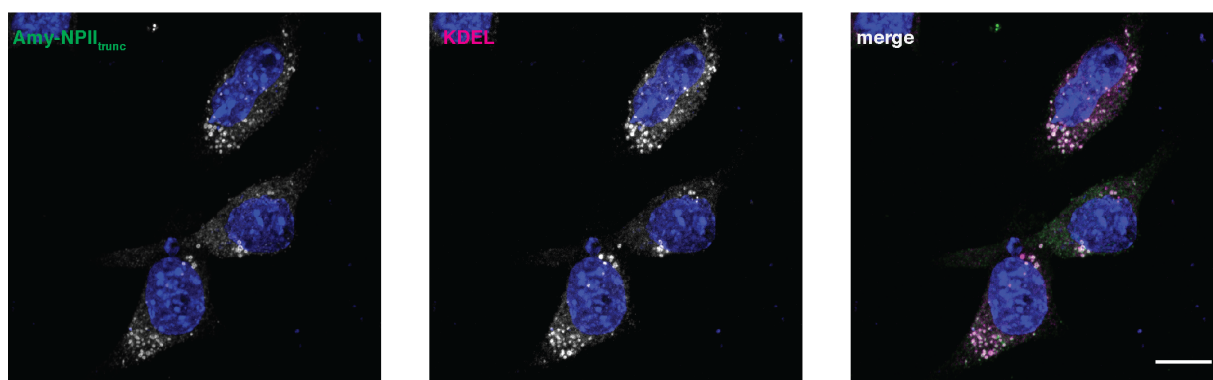


Figure 36: Colocalization of Amy-NP11_{trunc} with the KDEL receptor shows their ER localization. This was applicable for all tested constructs in all cell lines (N2a shown above). Size bar 10 μ m.

2.6.2 Disulfide Loops are Sufficient to Drive Protein Aggregation in Constitutively Secreting Cells

In contrast to the tested endocrine cell lines, Cos-1 cells do not utilize the pathway for regulated secretion. We analyzed ER aggregation of disulfide loops with folding-deficient NP11 mutants in this cell line to exclude a possible contribution of mechanisms specific to endocrine cell lines.

It was demonstrated beforehand that the expression of regulatively secreted proteins in a cell line that is only capable of constitutive secretion is sufficient to separate this cargo from co-expressed constitutively secreted proteins (Beuret et al., 2004), suggesting that no endocrine-specific machinery is involved in this process. Likewise, ADND1 provasopressin mutants were shown to form ER-retained aggregates in COS-1 cells (Birk et al., 2009).

We found that replacing vasopressin with the aforementioned disulfide loops showed protein aggregation in similar quantities of NP11 mutants (**Figure 37**). The presence of any tested disulfide loop was able to strongly increase aggregation to a comparable extend as in N2a and AtT20 cells (**Figure 38**). Likewise, aggregate formation was abolished in the proline-glycine control. We therefore conclude that the observed aggregation is not the result of specific endocrine cell functions, but cell type independent.

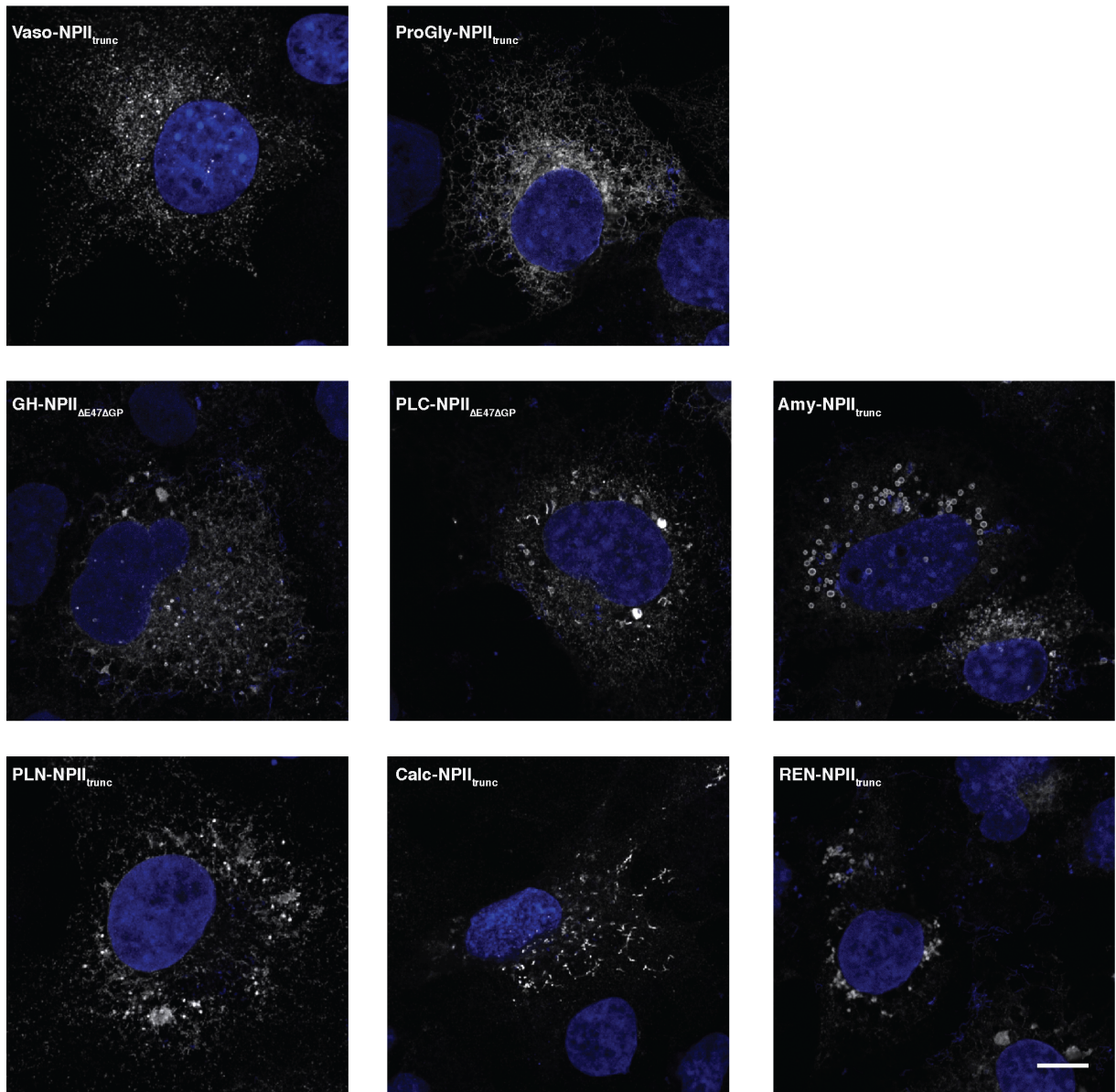


Figure 37: All tested disulfide loops mediate aggregation of the folding-deficient and ER-retained NPII domains in COS-1 cells. The presence of the vasopressin nonapeptide is necessary for aggregation. In contrast, the negative control ProGly-NPII_{trunc}, where the vasopressin nonapeptide is replaced with glycines and prolines, does not contain a sequence for aggregation and is localized uniformly throughout the tubular network. Size bar 10 μ m.

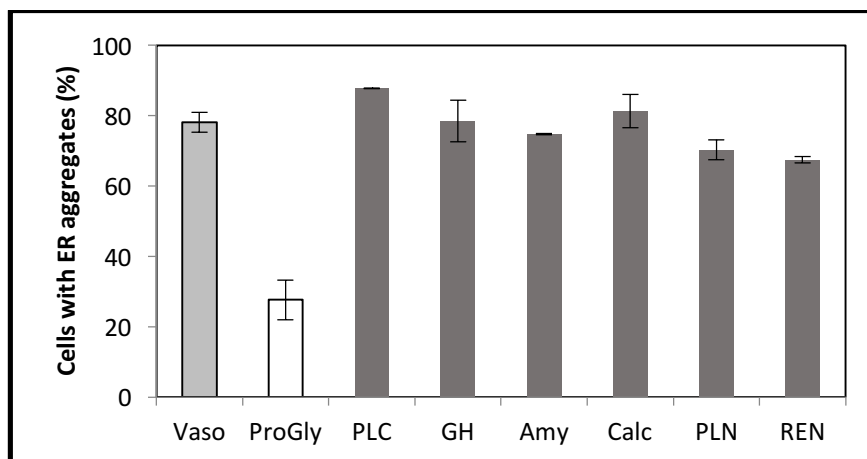


Figure 38: Quantification of COS-1 cells with ER aggregates. Cells are regarded as positive that show at least 3 dot-like aggregates. Cells with granule-like structures or strong Golgi localization were not regarded. The number of cells with aggregates is comparable to N2a cells. Error bars represent SD from at least three independent experiments.

COS-1 cells expressing disulfide loops with folding-deficient $\Delta E47$ NP11 mutants were analyzed with electron microscopy. Immunogold labelling with 10 nm gold particles against the NP11 domain revealed the presence of disulfide loop constructs packed in electron dense structures with 100 to 300 nm diameter size (**Figure 39**). Membrane enclosure and ribosomal presence reflect a localization in the rough ER. The aggregates appeared nearly homogenous, which is inconsistent with the ultrastructure of vasopressin-mediated aggregates and their organization in a fibrillar network (Beuret et al., 2017). This observation might hint towards geometrical differences of aggregates mediated by different disulfide loop structures.

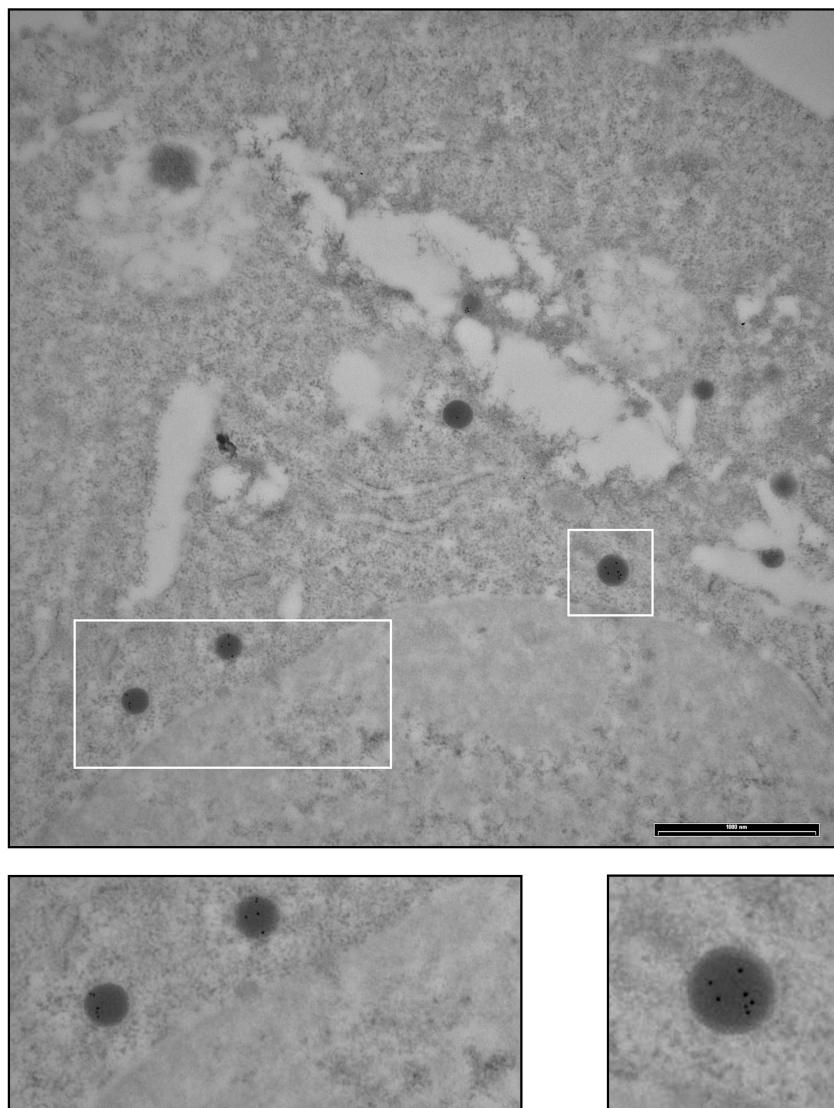


Figure 39: Electron micrographs of COS-1 cells expressing $\Delta E47\Delta GP$ -GH reveal a dense arrangement marked with 10nm gold particles that stain positive for NP11. Membrane enclosure and partial visibility of membranes and attached ribosomes suggest ER localization. The aggregates are up to 300 nm in diameter. Size bar 1000nm, rectangles are enlarged. Image by Cristina Baschong.

2.6.3 Constructs Containing the N-Terminal Disulfide Loop of Prolactin Exit Frequently Exit the ER

In endocrine cells, wild-type provasopressin is sorted into secretory granules, where it colocalizes with chromogranin A as a granule marker. The NP11 mutants that we utilized in our analyses are folding-deficient and therefore ER retained. However, some leakage out of the ER and sorting into secretory granules at the cell tips could be observed for all constructs (**Figure 40**). This was especially apparent for the prolactin-derived disulfide loop constructs, where this localization was displayed by approximately 50% of the expressing cells. Both the ADND1 point mutation $\Delta E47$,

where the NPII domain is present in its full length, and the truncated version derived from the C61X mutant displayed this behaviour when fused to the disulfide loop. This was no longer observed for the proline-glycine control.

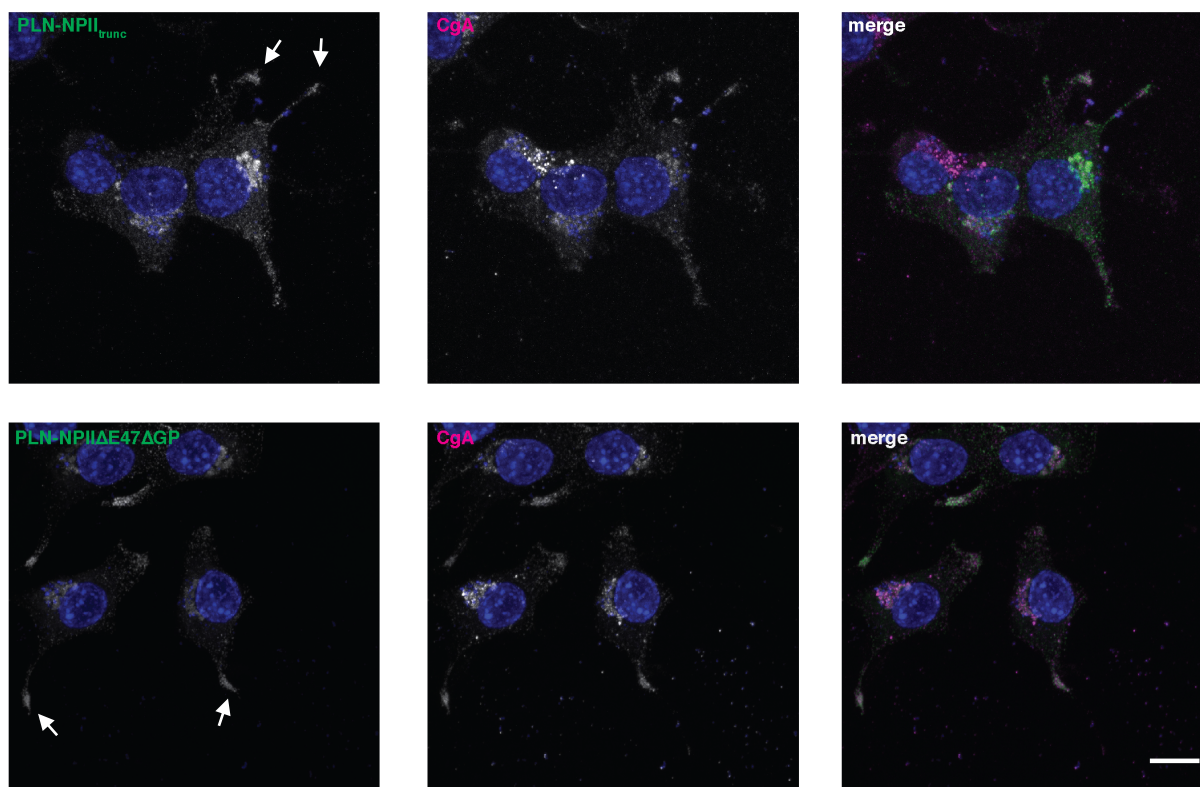


Figure 40: In N2a cells, a significant population of PLN-NP11_{trunc} expressing cells show localization at the cellular tips (indicated by arrows), where it colocalizes with chromogranin A as a granule marker. The same pattern is observed for PLN-NP11ΔE47ΔGP. Size bar 10μm.

2.7 Discussion

It has long been recognized that self-aggregation at the TGN is a contributing mechanism to the biogenesis of secretory granules. Maji et al. (2009) now suggested this aggregation to be amyloid in nature. This proposal placed the finding that mutant provasopressin produces fibrillar, amyloid-like aggregates in the ER, causing eventual cell death, into a different light. It implied that provasopressin evolved the ability to aggregate in the TGN, which expressed itself in the context of folding mutations with the formation of fibrillar aggregates occurring in the wrong compartment with toxic consequences. Consistent with this notion, the same sequences were found to be responsible for granule formation in the TGN and for ER aggregation. One of the aggregating sequences, the nonapeptide hormone itself,

forms a short disulfide loop. Disulfide loops with similarities regarding their length and position are also present in other peptide hormones. We here present the aggregation capabilities of several disulfide loop-containing peptide hormones in the ER. In the context of folding-deficient NPII, they display identical properties of aggregation like the vasopressin nonapeptide. The observed ER aggregation therefore supports the hypothesis of a general role of disulfide loops at granule biogenesis, for which self-aggregation at the TGN is a prerequisite.

To further investigate this, several additional experiments are required. Since the aggregation of mutant provasopressin depends on the presence of further disulfide bonds in the NPII domain, synergistic effects acting on the analyzed disulfide loops cannot be excluded in the presence of NPII. This may be represented in such a way that only a small contribution to oligomerization may be amplified to significant aggregation, which could explain the strong and equal aggregation score for all tested loops. To increase the stringency of our analyses, it is therefore required to introduce the disulfide loops into a context that does not resemble any similarities to provasopressin-related aggregation. During this work, several reporters have been examined, but none fulfilled the requirement of showing no significant self-aggregation. The identification of suitable candidates is still ongoing.

Furthermore, the caveat of transient expression has to be regarded. High expression levels and protein loads inevitably lead to ER stress responses, especially when misfolded mutants are expressed. Proteins that are prone to aggregation, as demonstrated for several disulfide loop-containing peptide hormones (Cope et al., 2013; Westermarck, 2005), may show amplified aggregate formation under conditions of macromolecular crowding (Munishkina et al., 2004). While a high cargo concentration is a requirement for physiological aggregation during granule biogenesis, these effects may be masked by artificial overexpression. It is therefore crucial to investigate the aggregation potential of disulfide loops under physiological expression levels. Stable cell lines generally show moderated expression levels and inarguably provide a more convincing experimental setup.

The observed TGN exit and granule sorting of constructs containing the N-terminal prolactin disulfide loop is presumably the consequence of decreased functionality in both ER retention and quality control, as these mechanisms are challenged with an overload of misfolded proteins, which is probably intensified in transient overexpression. ER leakage is likely to be observed in this scenario, while subsequent localization at the TGN might then be sufficient to sort into granules via aggregation. Although this would further acknowledge self-aggregation as a general device in granule formation, our experimental setup does not provide the requirements to conclude a causality linked to disulfide loops as a motif for granule sorting. To address the question whether the prolactin loop sequence contributes to this, its capabilities have to be analyzed in the context of a reporter that is not folding-deficient. This again highlights the necessity of a more stringent reporter that is not related to the provasopressin prohormone and NPII. If disulfide loop-reporter constructs are permitted ER exit and mediate similar granule sorting properties under these conditions, a more general assessment will be possible.

Despite of this, the N-terminal disulfide loop of prolactin appears as a promising candidate to broaden the understanding of disulfide-mediated aggregation and granule sorting. So far, experiments with provasopressin have revealed that mutation of the residues C1, C6 or Y2 (involved in the interaction of vasopressin with the NPII binding pocket) to alanines leads to folding defects and ER retention, implying that either amino acid is necessary for correct folding (Käser, 2016, Master thesis). However, for ER aggregation of a folding-deficient precursor, none of the vasopressin residues is individually necessary, including C1 and C6. This means that the formation of an intramolecular disulfide loop originating from one of the cysteines in the vasopressin sequence is not required for aggregation. In this notion, somatostatin was shown to regulate its aggregation during granule biogenesis over its disulfide loop (Anoop et al., 2014). Under this context it seems possible that the disulfide bridge in general is not required for aggregation, but may fulfil other physiological functions. A similar mutation analysis under more stringent conditions appears promising for gaining knowledge about the precise role of disulfide loops in aggregation.

With this study, we showed that disulfide loops are necessary for ER aggregation of a folding-deficient NP11 domain. Aggregation capabilities are an acknowledged mechanism in cargo concentration of secretory granules. For our future perspective, we wish to extend our view to evaluate a general role of disulfide loops during granule biogenesis.

2.8 Materials and Methods

Cloning

Both N- and C-terminal loop fragments were introduced as complementary oligonucleotides that were annealed at 95°C with equimolar concentrations for five minutes and slowly cooled to room temperature. The target vectors for cloning contained Vasopressin-NP11-75X and Vasopressin- Δ E47 Δ GP. With PCR, ClaI was introduced in front of NP11 for N-terminal loop constructs and ClaI-XbaI behind NP11 for C-terminal loop constructs. The loops were cloned into the vectors using the corresponding restriction sites (BsrGI and ClaI for N-terminal loops; ClaI and XbaI for C-terminal loops) and the sequence was verified by sequencing (Microsynth).

Cell culturing, transfection and immunofluorescence

COS-1 cells were cultivated in high glucose DMEM (6g/L glucose, Sigma) supplemented with 10% FCS, 100 units/mL Pen-Strep and 2mM L-Gln at 7.5% CO₂. Cells were passaged every 72 h to a maximum of 10 repetitions.

Neuro 2a cells were cultivated in low Glucose DMEM (4.5g/L glucose, Sigma), and AtT20 cells in high glucose DMEM, with 10% FCS, 100 units/ml Pen-Strep and 2mM L-Gln at 5% CO₂. Cells were passaged every 48 hours to a maximum of 10 repetitions.

4.5×10^4 COS-1 cells and 6×10^4 Neuro 2a cells were grown on coverslips for 24 h. For transfection, 0.2 μ g of plasmid DNA was used with 2 μ L Fugene HD (Promega). The medium was replaced 24 h after transfection. Differentiation of Neuro 2a cells was induced with the addition of DMEM containing no FCS and 1mM valproic acid. 48 h after transfection, the cells were prepared for immunofluorescence. For this, the cells were washed with PBS and

fixed with 3% PFA for 30 min. The reaction was quenched with 50mM NH₄Cl-PBS for 5 min. After repeated washing with PBS, cells were permeabilized with 0.1% Triton X-100 in PBS for 10 min, washed and blocked in 1% BSA-PBS for 15 min. Primary antibody staining was applied for 2 h at room temperature. After washing with BSA-PBS, secondary antibody staining followed for 30 min at room temperature. The coverslips were washed, rinsed with ddH₂O and mounted with Fluoromount-G by Hoechst premixed with 0.5µg/mL DAPI.

Image visualization was accomplished with the Axioplan 2 Microscope System and Point Scanning Confocal LSM700 by Zeiss. For image processing, Zen, Fiji and Huygens Suite was used. Figures were created with IBS (Lio et al., 2015) and MolView, images were arranged with Adobe Illustrator.

Aggregates were counted in at least 100 cells of each preparation. Cells that showed a localization of the expressed constructs in the cell tips were disregarded for the quantification of ER aggregates.

Oligonucleotides

TGTACAGGCAAAATGCAACACTGCCACATGTGCAACGCAAATCGAT	Amylin-BC1
ATCGATTTGCGTTGCACATGTGGCAGTGTTGCATTTTGCCTGTACA	Amylin-BC2
TGTACAGGCACGGTGCGGTAATCTGAGTACTTGCATGCTGGGCACAATCGAT	Calc-BC1
ATCGATTGTGCCAGCATGCAAGTACTCAGATTACCGCACCGTGCCTGTACA	Calc-BC2
TGTACAGGCATCCTCCAAGTGCAGCCGTCTCTACACTGCCTGTGTGTATCACAAAATCGAT	Renin-BC1
ATCGATTTTGTGATACACACAGGCAGTGTAGAGACGGCTGCACTTGGAGGATGCCTGTACA	Renin-BC2
TGTACAGGCAACCCCGTCTGTCCCAATGGGCCTGGCAACTGCCAGGTATCCCTTCGAATCGAT	ProlacN-BC1
ATCGATTGGAAGGATACCTGGCAGTTGCCAGGCCATTGGGACAGACGGGGTTGCCTGTACA	ProlacN-BC2
ATCGATTTGCTGAATTGCAGAATCATCTACAACAACAAGTCTAATCTAGA	Prolac-CX1
TCTAGATTAGCAGTTGTTGTTGTAGATGATTCTGCAATTCAGCAAATCGAT	Prolac-CX2
ATCGATGTCATGAAGTGTGCGCCGCTTTGCGGAAAGCAGCTGTGCTTTCTAGTCTAGA	GrowthH-CX1
TCTAGACTAGAAAGCACAGCTGCTTTCCGCAAAGCGGCGACACTTCATGACATCGAT	GrowthH-CX2

Antibodies

Designation	Host	Dilution	Provider
α CgA	polyclonal, goat	1:100	Santa Cruz
α HIS	monoclonal, mouse	1:1000	Millipore
α KDEL	monoclonal, mouse	1:100	MBL
α myc 9E10	monoclonal, mouse	1:50	Hybridoma
α NPII	polyclonal, rabbit	1:200	self
α mouse Alexa 488	donkey	1:400	ThermoFisher
α mouse Alexa 568	donkey	1:400	ThermoFisher
α rabbit Alexa 488	donkey	1:400	ThermoFisher
α rabbit Alexa 568	donkey	1:400	ThermoFisher
α goat Alexa 568	donkey	1:400	ThermoFisher
DAPI		1:10000	Sigma

3. References

- Abell BM, Rabu C, Leznicki P, Young JC, High S. Post-translational integration of tail-anchored proteins is facilitated by defined molecular chaperones, *J Cell Sci* 120 (2007) 1743–1751
- Akopian D, Shen K, Zhang X, Shan S. Signal Recognition Particle: An Essential Protein-Targeting Machine. *Annu Rev Biochem* 82 (2013) 693-721
- Alder NN, Shen Y, Brodsky JL, Hendershot LM, Johnson AE. The molecular mechanisms underlying BiP-mediated gating of the Sec61 translocon of the endoplasmic reticulum. *J Cell Biol* 168 (2005) 389–399
- Andreotti G, Mendez BL, Amodeo P, Morelli MA, Nakamuta H, Motta A. Structural determinants of salmon calcitonin bioactivity: the role of the Leu-based amphipathic alpha-helix. *J Biol Chem* 281 (2006) 24193-24203
- Anoop A, Ranganathan S, Das Dhaked B, Jha NN, Pratihari S, Ghosh S, Sahay S, Kumar S, Das S, Kombrabail M, Agarwal K, Jacob RS, Singru P, Bhaumik P, Padinhateeri R, Kumar A, Maji SK. Elucidating the role of disulfide bond on amyloid formation and fibril reversibility of somatostatin-14: relevance to its storage and secretion. *J Biol Chem* 289 (2014) 16884-16903
- Antony B, Gounon P, Schekman R, Orci L. Self-assembly of minimal COPII cages. *EMBO Rep* 4 (2003) 419–424
- Ast T, Cohen G, Schuldiner M. A network of cytosolic factors targets SRP-independent proteins to the endoplasmic reticulum. *Cell* 152 (2013) 1134-45
- Auclair SM, Bhanu MK, Kendall DA. Signal peptidase I: Cleaving the way to mature proteins. *Protein Sci* 21 (2012) 13–25
- Aviram N, Ast T, Costa EA, Arakel EC, Chuartzmann SG, Jan CH, Haßdenteufel S, Dudek J, Jung M, Schorr S, Zimmermann R, Schwappach B, Weissman JS, Schuldiner M. The SND proteins constitute an alternative targeting route to the endoplasmic reticulum. *Nature* 540 (2016) 134-138
- Baldrige RD and Rapoport TA. Autoubiquitination of the Hrd1 ligase triggers protein retrotranslocation in ERAD. *Cell* 166 (2016), 394-407
- Barlowe, C, Orci L, Yeung T, Hosobuchi M, Hamamoto S, Salama N, Rexach MF, Ravazzola M, Amherdt M, Schekman, R. COPII: A membrane coat formed by sec proteins that drive vesicle budding from the endoplasmic reticulum. *Cell* 77 (1994) 895-907
- Barlowe, C. Signals for COPII-dependent export from the ER: What's the ticket out? *Trends Cell Biol* 13 (2003) 295-300
- Bauer BW, Rapoport TA. Mapping polypeptide interactions of the SecA ATPase during translocation. *Proc Natl Acad Sci USA* 106 (2009) 20800–5
- Beck K, Wu LF, Brunner J, Muller M. Discrimination between SRP- and SecA/SecB dependent substrates involves selective recognition of nascent chains by SRP and trigger factor *EMBO J* 19 (2000) 134–43
- Becker T, Bhushan S, Jarasch A, Armache JP, Funes S, Jossinet F, Gumbart J, Mielke T, Berninghausen O, Schulten K, Westhof E, Gilmore R, Mandon EC, Beckmann R. Structure of monomeric yeast and mammalian Sec61 complexes interacting with the translating ribosome. *Science* 326 (2009) 1369–73

- Beckmann R, Spahn CM, Eswar N, Helmers J, Penczek PA, Sali A, Frank J, Blobel G. Architecture of the protein-conducting channel associated with the translating 80S ribosome, *Cell* 107 (2001) 361–372
- Benyair R, Ron E, Lederkremer GZ. Protein quality control, retention, and degradation at the endoplasmic reticulum". *Int Rev Cell Mol Biol* 292 (2011) 197–28
- Bergeron C, Kovacs K, Ezrin C, Mizzen C. Hereditary diabetes insipidus: an immunohistochemical study of the hypothalamus and pituitary gland. *Acta Neuropathol* 81 (1991) 345-348
- Bernasconi R, Galli C, Calanca V, Nakajima T, Molinari M. Stringent requirement for HRD1, SEL1L, and OS-9/XTP3-B for disposal of ERAD-L S substrates. *J Cell Biol* 188 (2010) 223–35
- Bernstein HD, Poritz MA, Strub K, Hoben PJ, Brenner S, Walter P. Model for signal sequence recognition from amino-acid sequence of 54K subunit of signal recognition particle. *Nature* 340 (1989) 482–6
- Beuret N, Rutishauser J, Bider MD, Spiess M. Mechanism of endoplasmic reticulum retention of mutant vasopressin precursor caused by a signal peptide truncation associated with diabetes insipidus. *J Biol Chem* 274 (1999) 18965–18972.
- Beuret N, Stettler H, Renold A, Rutishauser J, Spiess M. Expression of regulated secretory proteins is sufficient to generate granule-like structures in constitutively secreting cells. *J Biol Chem* 279 (2004) 20242–20249
- Beuret N, Hasler F, Prescianotto-Baschong C, Birk J, Rutishauser J, Spiess M. Amyloid-like aggregation of provasopressin in diabetes insipidus and secretory granule sorting. *BMC biology* 15 (2017) 5
- Birk J, Friberg MA, Prescianotto-Baschong C, Spiess M, Rutishauser J. Dominant pro-vasopressin mutants that cause diabetes insipidus form disulfide-linked fibrillar aggregates in the endoplasmic reticulum. *J Cell Sci* 122 (2009) 3994–4002
- Blank B, von Blume J. Cab45-Unraveling key features of a novel secretory cargo sorter at the trans-Golgi network. *Eur J Cell Biol* (2017) Mar 18
- Blobel G, Sabatini DD. Ribosome-membrane interaction in eukaryotic cells. *Biomembranes* 2 (1971) 193–195
- Blobel G. Intracellular protein topogenesis. *Proc. Natl Acad. Sci. USA* 77 (1980) 1496
- Bol R, de Wit JG, Driessen AJ. The active protein-conducting channel of *Escherichia coli* contains an apolar patch. *J. Biol. Chem.* 282 (2007) 29785–29793
- Bonfanti L, Mironov AA Jr, Martinez-Menarguez JA, Martella O, Fusella A, Baldassarre M, Buccione R, Geuze HJ, Mironov AA, Luini A. Procollagen traverses the Golgi stack without leaving the lumen of cisternae: evidence for cisternal maturation. *Cell* 95 (1998), 993-1003
- Boone M, Deen PMT. Physiology and pathophysiology of the vasopressin-regulated renal water reabsorption. *Pflugers Archiv* , 456 (2008), 1005–1024
- Borel AC, Simon, SM. Biogenesis of polytopic membrane proteins: membrane segments assemble within translocation channels prior to membrane integration. *Cell* 85 (1996) 379-389
- Borgese N, Colombo S, Pedrazzini E. The tale of tail-anchored proteins: coming from the cytosol and looking for a membrane, *J Cell Biol* 161 (2003) 1013–1019
- Borgonovo B, Ouwendijk J, Solimena, M. Biogenesis of secretory granules. *Curr Opin Cell Biol* 18 (2006), 365–370

- Bozkurt G, Stjepanovic G, Vilardi F, Amlacher S, Wild K, Bange G, Favaloro V, Rippe K, Hurt E, Dobberstein B, Sinning I. Structural insights into tail-anchored protein binding and membrane insertion by Get3. *Proc Natl Acad Sci USA* 106 (2009) 21131–36
- Bradshaw N, Neher SB, Booth DS, Walter P. Signal sequences activate the catalytic switch of SRP RNA. *Science* 323 (2009) 127-30
- Burgess TL, Kelly RB. Constitutive and regulated secretion of proteins. *Annu Rev Cell Biol* 3 (1987) 243-93
- Cannon KS, Or E, Clemons WM Jr, Shibata Y, Rapoport TA. Disulfide bridge formation between SecY and a translocating polypeptide localizes the translocation pore to the center of SecY. *J Cell Bio*. 169 (2005) 219–225
- Cao G, Kuhn A, Dalbey R. The translocation of negatively charged residues across the membrane is driven by the electrochemical potential: evidence for an electrophoresis-like membrane transfer mechanism. *EMBO J* 14 (1995) 866–75
- Carvalho P, Stanley AM, Rapoport TA. Retrotranslocation of a misfolded luminal ER protein by the ubiquitin-ligase Hrd1p. *Cell* 143 (2010) 579–9
- Chantalat L, Jones ND, Korber F, Navaza J, Pavlovsky AG. (1995) The crystal-structure of wild-type growth hormone at 2.5 Angstrom resolution. *Protein Pept Lett* 2 (1999) 333-340
- Cheng Z, Jiang Y, Mandon EC, Gilmore R. Identification of cytoplasmic residues of Sec61p involved in ribosome binding and cotranslational translocation. *J Cell Biol* 168 (2005) 67–77
- Chiti F, Dobson CM. Protein misfolding, functional amyloid, and human disease. *Annu Rev Biochem* 75 (2006) 333–366
- Christ-Crain M, Fenske W. Copeptin in the diagnosis of vasopressin-dependent disorders of fluid homeostasis. *Nat Rev Endocrinol* 12 (2016) 168-76
- Conti BJ, Devaraneni PK, Yang Z, David LL, Skach WR. Cotranslational Stabilization of Sec62/63 within the ER Sec61 Translocon is Controlled by Distinct Substrate-Driven Translocation Events. *Molecular Cell*, 58 (2015), 269-283
- Cope SM, Shinde S, Best RB, Ghirlanda G, Vaiana SM. Cyclic N-Terminal Loop of Amylin Forms Non Amyloid Fibers. *Biophys J* 105 (2013) 1661–1669
- Cui W, Li J, Ron D, Sha B. 2011. The structure of the PERK kinase domain suggests the mechanism for its activation. *Acta Cryst D*67 (2011), 423-428
- De Bree FM, Van der Kleij AAM, Nijenhuis M, Zalm R, Murphy D, Burbach JPH. The hormone domain of the vasopressin prohormone is required for the correct prohormone trafficking through the secretory pathway. *J Neuroendocrinol* 15 (2003), 1156-1163
- Dalal K, Duong F. The SecY complex forms a channel capable of ionic discrimination. *EMBO Rep*. 10 (2009), 762–768
- Deshaies RJ, Sanders SL, Feldheim DA, Schekman R. Assembly of yeast Sec proteins involved in translocation into the endoplasmic reticulum into a membrane-bound multisubunit complex. *Nature* 349 (1991) 806-8
- Denzer AJ, Nabholz CE, Spiess M. Transmembrane orientation of signal-anchor proteins is affected by the folding state but not the size of the aminoterminal domain. *EMBO J* 14 (1995), 6311-6317

- Devaraneni PK, Conti B, Matsumura Y, Yang Z, Johnson AE, Skach WR. Stepwise insertion and inversion of a type II signal anchor sequence in the ribosome-Sec61 translocon complex. *Cell* 146 (2011), 134-147
- Deville K, Gold VA, Robson A, Whitehouse S, Sessions RB, Baldwin SA, Radford SE, Collinson I. The oligomeric state and arrangement of the active bacterial translocon. *J Biol Chem* 286 (2011) 4659–69
- Denks K, Vogt A, Sachelaru I, Petriman NA, Kudva R, Koch HG. The Sec translocon mediated protein transport in prokaryotes and eukaryotes. *Molec Membrane Biol* 31 (2014) 58-84
- Dittie AS, Hajibagheri N, Tooze SA. The AP-1 adaptor complex binds to immature secretory granules from PC12 cells, and is regulated by ADP-ribosylation factor. *J Cell Biol* 132 (1996) 523-36
- Do H, Falcone D, Lin J, Andrews DW, Johnson AE. The cotranslational integration of membrane proteins into the phospholipid bilayer is a multistep process. *Cell* 85 (1996) 369–78
- Driessen AJ, Nouwen N. Protein translocation across the bacterial cytoplasmic membrane. *Annu Rev Biochem* 77 (2008) 643-67
- Egea PF, Stroud RM. Lateral opening of a translocon upon entry of protein suggests the mechanism of insertion into membranes. *Proc Natl Acad Sci USA* 107 (2010) 17182–17187
- Eisenberg D, Schwarz E, Komaromy M, Wall R. Analysis of membrane and surface protein sequences with the hydrophobic moment plot. *J Mol Biol* 179 (1984) 125-142
- Emr S, Glick BS, Linstedt AD, Lippincott-Schwartz J, Luini A, Malhotra V, Marsh BJ, Nakano A, Pfeffer SR, Rabouille C, Rothman JE, Warren G, Wieland FT. Journeys through the Golgi - Taking stock in a new era. *J Cell Biol* 187 (2009) 449–453
- Engelman DM, Steitz TA, Goldman A. Identifying nonpolar transbilayer helices in amino acid sequences of membrane proteins. *Annu Rev Biophys Chem* 15 (1986) 321–353
- Enquist K, Fransson M, Boekel C, Bengtsson I, Geiger K, Lang L, Pettersson A, Johansson S, von Heijne G, Nilsson I. Membrane-integration characteristics of two ABC transporters, CFTR and P-glycoprotein. *J Mol Biol* 387 (2009) 1153–64
- Erdmann F, Schäuble N, Lang S, Jung M, Honigmann A, Ahmad M, Dudek J, Benedix J, Harsman A, Kopp A, Helms V, Cavalie A, Wagner R, Zimmermann R. Interaction of calmodulin with Sec61a limits Ca^{2+} leakage from the endoplasmic reticulum. *EMBO J* 30 (2011) 17–31
- Erlanson KJ, Miller SB, Nam Y, Osborne AR, Zimmer J, Rapoport TA. A role for the two-helix finger of the SecA ATPase in protein translocation. *Nature* 455 (2008) 984–87
- Farquhar MG, Palade GE. The Golgis apparatus: 100 years of progress and controversy. *Trends Cell Biol* 8 (1998) 2–10
- Flanagan JJ, Chen JC, Miao Y, Shao Y, Lin J, Bock PE, Johnson AE. Signal recognition particle binds to ribosome-bound signal sequences with fluorescence-detected subnanomolar affinity that does not diminish as the nascent chain lengthens. *J Biol Chem* 278 (2003) 18628–37
- Fra AM, Fagioli C, Finazzi D, Sitia R, Alberini CM. Quality control of ER synthesized proteins: an exposed thiol group as a three-way switch mediating assembly, retention and degradation. *EMBO J* 12 (1993) 4755–4761
- Fowler DM, Koulov AV, Balch WE, Kelly JW. Functional amyloid – from bacteria to humans. *Trends BiochemSci* 32 (2007) 217–224

- Frauenfeld J, Guzmart J, van der Sluis EO, Funes S, Gartmann M, Beatrix B, Mielke T, Berninghausen O, Becker T, Schulten K, Beckmann R. Cryo-EM structure of the ribosome-SecYE complex in the membrane environment. *Nat Struct Mol Biol* 18 (2011) 614–621
- Friberg MA, Spiess M, Rutishauser J. Degradation of wild-type vasopressin precursor and pathogenic mutants by the proteasome. *J Biol Chem* 279 (2004) 19941-19947
- Fujita H, Yamagishi M, Kida Y, Sakaguchi M. Positive charges on the translocating polypeptide chain arrest movement through the translocon. *J Cell Sci* 124 (2012) 4184-4193
- Gierasch LM. Signal sequences *Biochem* 28 (1989) 923–930
- Ghaemmaghami S, Huh WK, Bower K, Howson RW, Belle A, Dephoure N, O’Shea EK, Weissman JS. Global analysis of protein expression in yeast. *Nature* 425 (2003), 737-741
- Glick, B. S. & Nakano, A. Membrane traffic within the Golgi apparatus. *Annu Rev Cell Dev Biol* 25 (2009) 113–132
- Glombik MM, Krömer A, Salm T, Huttner WB, Gerdes HH. The disulfide-bonded loop of chromogranin B mediates membrane binding and directs sorting from the trans-Golgi network to secretory granules. *EMBO J* 18 (1999), 1059-1070
- Goder V, Spiess M. Molecular mechanism of signal sequence orientation in the endoplasmic reticulum. *EMBO J* 22 (2003) 3645-3653
- Goder V, Crottet P, Spiess M. In vivo kinetics of protein targeting to the endoplasmic reticulum determined by site-specific phosphorylation. *EMBO J* 19 (2000) 6704-6712
- Goder V, Junne T, Spiess M. Sec61p contributes to signal sequence orientation according to the positive-inside rule. *Mol Biol Cell* 15 (2004) 1470–1478
- Gogala M, Becker T, Beatrix B, Armache JP, Barrio-Garcia C, Berninghausen O, Beckmann R. Structures of the Sec61 complex engaged in nascent peptide translocation or membrane insertion. *Nature* 506 (2014) 107-110
- Gumbart J, Chipot C, Schulten K. Free energy of nascent-chain folding in the translocon. *J Am Chem Soc* 133 (2011) 7602–7607
- Gumbart JC, Teo I, Roux B, Schulten K. Reconciling the roles of kinetic and thermodynamic factors in membrane-protein insertion. *J Am Chem Soc* 135 (2013) 2291–2297
- Guy HR. Amino acid side-chain partition energies and distribution of residues in soluble proteins. *Biophys Jour* 47 (1985) 61-70
- Guyton and Hall Textbook of medical physiology, 13th edition, Elsevier Ltd. ISBN 1455770051
- Hagiwara D, Arima H, Morishita Y, Wenjun L, Azuma Y, Ito Y, Suga H, Goto M, Banno R, Sugimura Y, Shiota A, Asai N, Takahasi M, Oiso Y. Arginine vasopressin neuronal loss results from autophagy-associated cell death in a mouse model for familial neurohypophysial diabetes insipidus. *Cell Death Dis* 5 (2014) 1148
- Hainzl T, Huang S, Merilainen G, Brannstrom K, Sauer-Eriksson AE. Structural basis of signal sequence recognition by the signal recognition particle. *Nature Struct Molec Biol.* 18 (2011) 389–91
- Halic M, Becker T, Pool MR, Spahn CMT, Grassucci RA, Fank J, Beckmann R. Structure of the signal recognition particle interacting with the elongation-arrested ribosome. *Nature* 427 (2004) 808–14
- Halic M, Beckmann R. The signal recognition particle and its interactions during protein targeting. *Curr Opin Struct Biol* 15 (2005) 116-125

- Hammond C, Braakman I, Helenius A. Role of N-linked oligosaccharide recognition, glucose trimming, and calnexin in glycoprotein folding and quality control. *Proc Natl Acad Sci USA* 91 (1994) 913–917
- Harada Y, Li H, Lennarz WJ. Oligosaccharyltransferase directly binds to ribosome at a location near the translocon-binding site. *Proc Natl Acad Sci USA* 106 (2009) 6945–6949
- Hartmann E, Rapoport TA, Lodish HF. Predicting the orientation of eukaryotic membrane-spanning proteins. *Proc Natl Acad Sci USA* 86 (1989) 5786–5790
- Hartmann E, Görlich D, Kostka S, Otto A, Kraft R, Knespel S, Bürger E, Rapoport TA, Prehn S. A tetrameric complex of membrane proteins in the endoplasmic reticulum. *Eur J Biochem* 214 (1993) 375–381
- Hedin LE, Öjemalm K, Bernsel A, Hennerdal A, Illergård K, Enquist K, Kauko A, Cristobal S, von Heijne G, Lerch-Bader M, Nilsson I, Elofsson A. Membrane insertion of marginally hydrophobic transmembrane helices depends on sequence context. *J Mol Biol* 396 (2010), 221–229
- Hegde RS & Keenan RJ Tail-anchored membrane protein insertion into the endoplasmic reticulum. *Nat Rev Mol Cell Biol* 12 (2011) 787–798
- Helenius A, Trombetta ES, Hebert DN, Simons JF. Calnexin, calreticulin and the folding of glycoproteins. *Trends Cell Biol* 7 (1997) 193–200
- Hellman R, Vanhove M, Lejeune A, Stevens FJ, Hendershot LM. The in vivo association of BiP with newly synthesized proteins is dependent on the rate and stability of folding and not simply on the presence of sequences that can bind to BiP. *J Cell Biol* 144 (1999) 21–30
- Helmers J, Schmidt D, Glavy JS, Blobel G, Schwartz T. The β -subunit of the protein-conducting channel of the endoplasmic reticulum functions as the guanine nucleotide exchange factor for the β -subunit of the signal recognition particle receptor. *J Biol Chem* 278 (2003) 23686–90
- Hershey JWB. Translational control in mammalian cells. *Annu Rev Biochem* 60 (1991) 717–755
- Hessa T, Kim H, Bihlmaier K, Lundin C, Boekel J, Andersson H, Nilsson I, White SH, von Heijne G. Recognition of transmembrane helices by the endoplasmic reticulum translocon. *Nature* 433 (2005), 377–381
- Hessa T, Meindl-Beinker NM, Bernsel A, Kim H, Sato Y, Lerch-Bader M, Nilsson I, White SH, von Heijne G. Molecular code for trans-membrane-helix recognition by the Sec61 translocon. *Nature* 450 (2007), 1026–1030
- Hessa T, Reithinger JH, von Heijne G, Kim H. Analysis of transmembrane helix integration in the endoplasmic reticulum in *S. cerevisiae*. *J Mol Biol* 386 (2009) 1222–1228
- Hessa T, Sharma A, Mariappan M, Eshleman HD, Gutierrez E, Hegde RS. Protein targeting and degradation are coupled for elimination of mislocalized proteins. *Nature* 475 (2011) 394–7
- Higy M, Junne T, Spiess M. Topogenesis of membrane proteins at the endoplasmic reticulum. *Biochem* 43 (2004), 12716–12722
- Higy M, Gander S, Spiess M. Probing the environment of signal-anchor sequences during topogenesis in the endoplasmic reticulum. *Biochem* 44 (2005), 2039–2047
- Hizlan D, Robson A, Whitehouse S, Gold VA, Vonck J, Mills D, Kühäbrandt W, Collinson I. Structure of the SecY complex unlocked by a preprotein mimic. *Cell Rep* 1 (2012) 21–28

Hou B, Lin P-J, Johnson AE Membrane protein TM segments are retained at the translocon during integration until the nascent chain cues FRET-detected release into bulk lipid. *Mol Cell* 48 (2012) 398–408

Hunt JF, Weinkauf S, Henry L, Fak JJ, McNicholas P, Oliver DB, Deisenhofer J. Nucleotide control of interdomain interactions in the conformational reaction cycle of SecA. *Science* 297 (2002) 2018–26

Jameson JL, Ito M. Molecular basis of autosomal dominant neurohypophyseal diabetes insipidus. Cellular toxicity caused by the accumulation of mutant vasopressin precursors within the endoplasmic reticulum. *J Clin Invest* 99 (1997), 1897–1905

Janda CY, Li J, Oubridge C, Hernandez H, Robinson CV, Nagai K. Recognition of a signal peptide by the signal recognition particle. *Nature* 465 (2010) 507–10

Jendle J, Christensen JH, Kvistgaard H, Gregersen N, Rittig S. Late-onset familial neurohypophyseal diabetes insipidus due to a novel mutation in the AVP gene. *Clin. Endocrinol. (Oxf)* 77 (2012) 586–592

Johnson N, Vilardi F, Lang S, Leznicki P, Zimmermann R, High S. TRC40 can deliver short secretory proteins to the Sec61 translocon. *J Cell Sci* 125 (2012) 3612–3620

Jo S, Kim T, Iyer VG, Im W. CHARMM-GUI: A web-based graphical user interface for CHARMM. *J Comput Chem* 29 (2008) 1859–1865

Jonikas MC, Collins SR, Denic V, Oh E, Quan EM, Schmid V, Weibezahn J, Schwappach B, Walter P, Weissmann JS, Schuldiner M. Comprehensive characterization of genes required for protein folding in the endoplasmic reticulum. *Science* 323 (2009) 1693–97

Jomaa A, Boehringer D, Leibundgut M, Ban N. Structures of the *E. coli* translating ribosome with SRP and its receptor and with the translocon. *Nat. Commun.* 7 (2016) 10471

Jungnickel B, Rapoport TA. A posttargeting signal sequence recognition event in the endoplasmic reticulum membrane. *Cell* 82 (1995) 261–70

Junne T, Schwede T, Goder V, and Spiess M. The plug domain of yeast Sec61p is important for efficient protein translocation, but is not essential for cell viability. *Mol Biol Cell* 17 (2006) 4063–4068

Junne T, Kocik L, Spiess M. The hydrophobic core of the Sec61 translocon defines the hydrophobicity threshold for membrane integration. *Mol Biol Cell.* 15;21 (2010) 1662-70

Junne T, Spiess M. Integration of transmembrane domains is regulated by their downstream sequences. *J Cell Sci* 130 (2017) 372–381

Käser, Christine. Aggregation of provasopressin in the endoplasmic reticulum and in secretory granules at the trans-Golgi network. Master thesis (2016)

Kalbfleisch T, Cambon A, Wattenberg BW. A bioinformatics approach to identifying tail-anchored proteins in the human genome. *Traffic* 8 (2007) 1687–94

Kalies KU, Stokes V, Hartmann E. A single Sec61-complex functions as a protein-conducting channel. *Biochim Biophys Acta* 1783 (2008) 2375–2383

Karaoglu D, Kelleher DJ, Gilmore R. The highly conserved Stt3 protein is a subunit of the yeast oligosaccharyltransferase and forms a subcomplex with Ost3p and Ost4p. *J Biol Chem* 272 (1997) 32513–32520

Kauko A, Hedin LE, Thebaud E, Cristobal S, Elofsson A, von Heijne G. Repositioning of Transmembrane α -Helices during Membrane Protein Folding. *J Mol Biol* 397 (2010) 190-201

- Kedrov A, Kusters I, Krasnikov VV, Driessen AJM. A single copy of SecYEG is sufficient for preprotein translocation. *EMBO J* 30 (2011) 4387–97
- Kempf G, Wild K, Sinning I. Structure of the complete bacterial SRP Alu domain. *Nucleic Acids Res* 42 (2014) 12284–12294
- Kienzle C, von Blume J. Secretory cargo sorting at the trans-Golgi network. *Trends Cell Biol* 24 (2014) 584–93
- Kim PK, Janiak-Spens F, Trimble WS, Leber B, Andrews DW. Evidence for multiple mechanisms for membrane binding and integration via carboxyl-terminal insertion sequences. *Biochem* 36 (1997) 8873–82
- Kim PK, Hollerbach C, Trimble WS, Leber B, Andrews DW. Identification of the endoplasmic reticulum targeting signal in vesicle-associated membrane proteins. *J Biol Chem* 274 (1999) 36876–82
- Kocik, Lucyna; Junne, Tina; Spiess, Martin. Orientation of Internal Signal-Anchor Sequences at the Sec61 Translocon. *J Mol Biol*, 424 (2012), 368-78
- Kornfeld S and Mellman I. The biogenesis of lysosomes. *Annu Rev Cell Biol* 5 (1989), 483-525
- Kuliawat R, Arvan P. Protein targeting via the constitutive-like secretory pathway in isolated pancreatic islets: passive sorting in the immature granule compartment. *J Cell Biol* 118 (1992) 521-529
- Kurzchalia TV, Wiedmann M, Girshovich AS, Bochkareva ES, Bielka H, Rapoport TA. The signal sequence of nascent preprolactin interacts with the 54K polypeptide of the signal recognition particle. *Nature* 320 (1986) 634–6
- Kutay U, Ahnert-Hilger G, Hartmann E, Wiedenmann B, Rapoport TA. Transport route for synaptobrevin via a novel pathway of insertion into the endoplasmic reticulum membrane. *EMBO J* 14 (1995) 217–23
- Kyte J, Doolittle RF. A simple method for displaying the hydropathic character of a protein. *J Mol Biol* 157 (1982) 105-132
- Lakkaraju AK, Abrami L, Lemmin T, Blaskovic S, Kunz B, Kihara A, Dal Peraro M, van der Goot FG. Palmitoylated calnexin is a key component of the ribosome–translocon complex, *EMBO J* 31 (2012) 1823–1835
- Lee MC, Miller EA. Molecular mechanisms of COPII vesicle formation. *Semin Cell Dev Biol* 18 (2007), 424-434
- Lerch-Bader M, Lundin C, Kim H, Nilsson I, von Heijne G. Contribution of positively charged flanking residues to the insertion of trans-membrane helices into the endoplasmic reticulum. *Proc Natl Acad Sci USA* 105 (2008) 4127–4132
- Leznicki P, Clancy A, Schwappach B, High S. Bat3 promotes the membrane integration of tail-anchored proteins. *J Cell Sci* 123 (2010) 2170–78
- Lee AH, Iwakoshi NN, Glimcher LH. XBP-1 regulates a subset of endoplasmic reticulum resident chaperone genes in the unfolded protein response. *Mol Cell Biol* 23 (2003) 7448–7459
- Li W, Schulman S, Boyd D, Erlandson K, Beckwith J, Rapoport TA. The plug domain of the SecY protein stabilizes the closed state of the translocation channel and maintains a membrane seal. *Mol. Cell* 26 (2007) 511–21
- Liang H, VanValkenburgh C, Chen X, Mullins C, Van Kaer L, Green N, Fang H. Genetic complementation in yeast reveals functional similarities between the catalytic subunits of mammalian signal peptidase complex. *J Biol Chem* 278 (2003) 50932–50939

- Lilley BN, Ploegh HL. A membrane protein required for dislocation of misfolded proteins from the ER. *Nature* 429 (2004) 834–40
- Lin JL, Addison R. A novel integration signal that is composed of two transmembrane segments is required to integrate the *Neurospora* plasma membrane H⁺-ATPase into microsomes. *J Biol Chem* 270 (1995) 6935–6941
- Lin PJ, Jongsma CG, Liao S, Johnson AE. Transmembrane segments of nascent polytopic membrane proteins control cytosol/ER targeting during membrane integration. *J Cell Biol* 195 (2011 I) 41–54
- Lin PJ, Jongsma CG, Pool MR, Johnson AE. Polytopic membrane protein folding at L17 in the ribosome tunnel initiates cyclical changes at the translocon. *J Cell Biol* 195 (2011 II) 55–70
- Liu W, Xie Y, Ma J, Luo X, Nie P, Zuo Z, Lahrmann U, Zhao Q, Zheng Y, Zhao Y, Xue Y, Ren J. IBS: an illustrator for the presentation and visualization of biological sequences. *Bioinformatics* 31 (2015) 3359–3361
- Lycklama A Nijeholt JA, Bulacu M, Marrink SJ, Driessen AJM. Immobilization of the plug domain inside the SecY channel allows unrestricted protein translocation. *J Biol Chem* 285 (2010) 23747–23754
- Lycklama a Nijeholt JA, Wu ZC, Driessen AJM. Conformational dynamics of the plug domain of the SecYEG protein-conducting channel. *J Biol Chem* 286 (2011) 43881–43890
- Lyman SK, Schekman R. Interaction between BiP and Sec63p is required for the completion of protein translocation into the ER of *Saccharomyces cerevisiae*. *J Cell Biol* 131 (1995) 1163–1171
- Lundin C, Kim H, Nilsson I, White SH, von Heijne G. Molecular code for protein insertion in the endoplasmic reticulum membrane is similar for N(in)-C(out) and N(out)-C(in) transmembrane helices. *Proc Natl Acad Sci USA* 105 (2008) 15702–15707
- Mahamid J, Pfeffer S, Schaffer M, Villa E, Danev R, Cuellar LK, Forster F, Hyman AA, Plietzko JM, Baumeister W. Visualizing the molecular sociology at the HeLa cell nuclear periphery. *Science* 351 (2016) 969–972
- Maillard AP, Lalani S, Silva F, Belin D, Doung F. Deregulation of the SecYEG translocation channel upon removal of the plug domain. *J Biol Chem* 282 (2007) 1281–1287
- Maji SK, Perrin MH, Sawaya MR, Jessberger S, Vadodaria K, Rissman RA, Singru PS, Nilsson KP, Simon R, Schubert D, Eisenberg D, Rivier J, Sawchenko P, Vale W, Riek R. Functional amyloids as natural storage of peptide hormones in pituitary secretory granules. *Science* 325 (2009) 328–332
- Mariappan M, Li X, Stefanovic S, Sharma A, Mateja A, Keenan RJ, Hegde RS. A ribosome-associating factor chaperones tail-anchored membrane proteins. *Nature* 466 (2010) 1120–24
- Matsuoka K, Orci L, Amherdt M, Bednarek SY, Hamamoto S, Schekman R, Yeung T. COPII-coated vesicle formation reconstituted with purified coat proteins and chemically defined liposomes. *Cell* 93 (1998) 263–275
- Mason N, Ciuffo LF, Brown JD. Elongation arrest is a physiologically important function of signal recognition particle. *EMBO J* 19 (2000) 4164–74
- Mateja A, Szlachcic A, Downing ME, Dobosz M, Mariappan M, Hegde RS, Keenan RJ. The structural basis of tail-anchored membrane protein recognition by Get3. *Nature* 461 (2009) 361–66
- MacArthur MW, Thornton JM. Influence of proline residues on protein conformation. *J Mol Biol* (1991) 218 397–412

- MacCallum JL, Bennett WF, Tieleman DP. Distribution of amino acids in a lipid bilayer from computer simulations. *Biophys J* 94 (2008) 3393–3404
- MacCallum JL, Tieleman DP (2011) Hydrophobicity scales: A thermodynamic looking glass into lipid-protein interactions. *Trends Biochem Sci* 36 (2011) 653–662
- MacKerell AD, Bashford D, Bellott M, Dunbrack RL, Evanseck JD, Field MJ, Fischer S, Gao J, Guo H, Ha S, Joseph-McCarthy D, Kuchnir L, Kuczera K, Lau FT, Mattos C, Michnick S, Ngo T, Nguyen DT, Prodhom B, Reiher WE, Roux B, Schlenkrich M, Smith JC, Stote R, Straub J, Watanabe M, Wiórkiewicz-Kuczera J, Yin D, Karplus M. All-atom empirical potential for molecular modeling and dynamics studies of proteins. *J Phys Chem B* 102 (1998) 3586–3616
- Matlack KE, Misselwitz B, Plath K, Rapoport TA. BiP acts as a molecular ratchet during posttranslational transport of prepro-a factor across the ER membrane. *Cell* 97 (1999) 553–564
- McCormick PJ, Miao Y, Shao Y, Lin J, Johnson AE. Cotranslational protein integration into the ER membrane is mediated by the binding of nascent chains to translocon proteins. *Mol Cell* 12 (2003) 329–341
- Ménétret JF, Hegde RS, Heinrich SU, Chandramouli P, Ludtke SJ, Rapoport TA, Akey CW. Architecture of the ribosome-channel complex derived from native membranes. *J Mol Biol* 348 (2005) 445–457
- Menetret JF, Hegde RS, Aguiar M, Gygi SP, Park E, Rapoport TA, Akey CW. Single copies of Sec61 and TRAP associate with a nontranslating mammalian ribosome. *Structure* 16 (2008) 1126–37
- Meyer HA, Grau H, Kraft R, Kostka S, Prehn S, Kalies KU, Hartmann E. Mammalian Sec61 is associated with Sec62 and Sec63. *J Biol Chem* 275 (2000) 14550–57
- Miller JD, Tajima S, Lauffer L, Walter P. The beta subunit of the signal recognition particle receptor is a transmembrane GTPase that anchors the alpha subunit, a peripheral membrane GTPase, to the endoplasmic reticulum membrane. *J Cell Biol.* 128 (1995) 273-82.
- Misselwitz B, Staeck O, Rapoport TA. J proteins catalytically activate Hsp70 molecules to trap a wide range of peptide sequences. *Mol. Cell* 2 (1998) 593–603
- Molinari M, Helenius. Chaperone selection during glycoprotein translocation into the endoplasmic reticulum, *Science* 288 (2000) 331–333
- Morales R, Watier Y, Bocskei Z. Human Prorenin Structure Sheds Light on a Novel Mechanism of Its Autoinhibition and on Its Non-Proteolytic Activation by the (Pro)renin Receptor *J.Mol.Biol.* 421 (2012) 100-111
- Müller L, de Escauriaza MD, Lajoie P, Theis M, Jung M, Müller A, et al. 2010. Evolutionary gain of function for the ER membrane protein Sec62 from yeast to humans. *Mol Cell Biol* 21 (2017) 691–703
- Munishkina LA, Cooper EM, Uversky VN, Fink AL. The effect of macromolecular crowding on protein aggregation and amyloid fibril formation. *J Mol Recognit* 17 (2004) 456-64
- Nam SE, Paetzel M. Structure of signal peptide peptidase A with C-termini bound in the active sites: Insights into specificity, self-processing, and regulation. *Biochemistry* 52 (2013) 8811–8822
- Ng DT, Brown JD, Walter P. Signal sequences specify the targeting route to the endoplasmic reticulum membrane. *J Cell Biol* 134 (1996) 269–78
- Nicchitta CV, Blobel G. Luminal proteins of the mammalian endoplasmic reticulum are required to complete protein translocation. *Cell* 73 (1993) 989–998

- Nijenhuis M, Zalm R, Burbach JPH. Mutations in the Vasopressin Prohormone Involved in Diabetes Insipidus Impair Endoplasmic Reticulum Export but Not Sorting. *J Biol Chem* 274 (1999) 21200–21208
- Ngosuwan J, Wang NM, Fung KL, Chirico WJ. Roles of cytosolic Hsp70 and Hsp40 molecular chaperones in post-translational translocation of presecretory proteins into the endoplasmic reticulum. *J Biol Chem* 278 (2003) 7034–42
- Ninagawa S, Okada T, Sumitomo Y, Kamiya Y, Kato K, Horimoto S, Ishikawa T, Takeda S, Sakuma T, Yamamoto T, Mori K. EDEM2 initiates mammalian glycoprotein ERAD by catalyzing the first mannose trimming step. *J Cell Biol* 206 (2014) 347–56
- Oberai A, Ihm, Y, Kim S, Bowie JU. A limited universe of membrane protein families and folds. *Protein Sci* 15 (2006) 1723–1734
- Oiso Y, Robertson GL, Nørgaard JP, Juul KV. Clinical review: Treatment of neurohypophyseal diabetes insipidus. *J Clin Endocrinol Metab* 98 (2013) 3958–3967
- Ogg SC, Walter P. SRP samples nascent chains for the presence of signal sequences by interacting with ribosomes at a discrete step during translation elongation. *Cell* 81 (1995) 1075–84
- Oliver JD, van der Wal FJ, Bulleid NJ, High S. Interaction of the thiol-dependent reductase ERp57 with nascent glycoproteins. *Science* 275 (1997) 86–88
- Osborne AR, Rapoport TA, van den Berg B. Protein translocation by the Sec61/SecY channel. *Annu Rev Cell Dev Biol* 21 (2005) 529–550.
- Or E, Boyd D, Gon S, Beckwith J, Rapoport T. The bacterial ATPase SecA functions as a monomer in protein translocation. *J Biol Chem* 280 (2005) 9097–105
- Osborne AR, Rapoport TA. Protein translocation is mediated by oligomers of the SecY complex with one SecY copy forming the channel. *Cell* 129 (2007) 97–110
- Ota K, Sakaguchi M, von Heijne G, Hamasaki N, Mihara K. Forced transmembrane orientation of hydrophilic polypeptide segments in multispinning membrane proteins. *Mol. Cell* 2 (1998) 495–503
- Palade, G. Intracellular aspects of the process of protein synthesis. *Science* 189 (1975) 347–358
- Panzner S, Dreier L, Hartmann E, Kostka S, Rapoport TA. Posttranslational protein transport in yeast reconstituted with a purified complex of Sec proteins and Kar2p. *Cell* 19;81 (1995) 561–70
- Papanikolaou Y, Papadovasilaki M, Ravelli RB, McCarthy AA, Cusack S, Economou A, Petratos K. Structure of dimeric SecA, the Escherichia coli preprotein translocase motor. *J Mol Biol* 366 (2007) 1545–57
- Park E, Rapoport TA. Preserving the membrane barrier for small molecules during bacterial protein translocation. *Nature* 12;473 (2011) 239–42
- Park E, Rapoport TA. Mechanisms of Sec61/SecY-mediated protein translocation across membranes. *Annu Rev Biophys* 41 (2012) 21–40
- Pauling L, Corey RB. Configurations of polypeptide chains with favored orientations around single bonds: two new pleated sheets. *Proc Natl Acad Sci USA* 37 (1951) 729–740
- Pauling L, Corey RB, Branson HR. The structure of proteins: two hydrogen-bonded helical configurations of the polypeptide chain. *Proc Natl Acad Sci USA* 37 (1951) 205–211
- Pech M, Spreter T, Beckmann R, Beatrix B. Dual binding mode of the nascent polypeptide-associated complex reveals a novel universal adapter site on the ribosome. *J Biol Chem* 285 (2010) 19679–19687

- Pelham HR. The dynamic organisation of the secretory pathway. *Cell Struct Funct* 21 (1996), 413-419
- Pfeffer S, Dudek J, Gogala M, Schorr S, Linxweiler J, Lang S, Becker T, Beckmann R, Zimmermann R, Förster F. Structure of the mammalian oligosaccharyl-transferase complex in the native ER protein translocon. *Nat Commun* 5 (2014) 3072
- Phillips JC, Braun R, Wang W, Gumbart J, Tajkhorshid E, Villa E, Chipot C, Skeel RD, Kalé L, Schulten K. Scalable molecular dynamics with NAMD. *J Comput Chem* 26 (2005) 1781–1802
- Pilon M, Schekman R, Römisch K. Sec61p mediates export of a misfolded secretory protein from the endoplasmic reticulum to the cytosol for degradation. *EMBO J* 16 (1997) 4540–4548
- Plempner K, Bohmler S, Bordallo J, Sommer T. Mutant analysis links the translocon and BiP to retrograde protein transport for ER degradation. *Nature* 388 (1997) 891-5
- Pfeffer S, Dudek J, Zimmermann R, Förster F. Organization of the native ribosome–translocon complex at the mammalian endoplasmic reticulum membrane. *Biochim Biophys Acta* 1860 (2016) 2122–2129
- Plath K, Rapoport TA. Spontaneous release of cytosolic proteins from posttranslational substrates before their transport into the endoplasmic reticulum. *J Cell Biol* 151 (2000) 167–178
- Pitonzo D, Yang Z, Matsumura Y, Johnson AE, Skach WR. Sequence-specific retention and regulated integration of a nascent membrane protein by the endo-plasmic reticulum Sec61 translocon. *Mol Biol Cell* 20 (2009) 685–698
- Rabu C, Wipf P, Brodsky JL, High S. A precursor-specific role for Hsp40/Hsc70 during tail-anchored protein integration at the endoplasmic reticulum. *J Biol Chem* 283 (2008) 27504–27513
- Radzicka A, Wolfenden R. Comparing the polarities of the amino-acids - side-chain distribution coefficients between the vapor- phase, cyclohexane, 1-octanol, and neutral aqueous-solution. *Biochem* 27 (1988) 1664 – 1670
- Ramabaran N, Serpell L. Amyloid fibrils. *Prion* 2:3 (2008) 112-117
- Rapoport TA. Protein translocation across the eukaryotic endoplasmic reticulum and bacterial plasma membranes. *Nature* 450 (2007) 663-9
- Rapoport TA, Li L, Park E. Structural and mechanistic insights into protein translocation. *Annu Rev Cell Dev Biol* 33 (2017), 1.1-1.22
- Rodriguez Camargo DC, Tripsianes K, Buday K, Franko A, Gobl C, Hartlmuller C, Sarkar R, Aichler M, Mettenleiter G, Schulz M, Boddich A, Erck C, Martens H, Walch AK, Madl T, Wanker EE, Conrad M, de Angelis MH, Reif B. The redox environment triggers conformational changes and aggregation of hIAPP in Type II Diabetes. *Sci Rep* 7 (2017) 44041-44041
- Rothblatt JA, Deshaies RJ, Sanders SL, Daum G, Schekman R. Multiple genes are required for proper insertion of secretory proteins into the endoplasmic reticulum in yeast. *JCB* 109 (1989), 2641
- Rothman JE, Wieland FT. Protein sorting by transport vesicles. *Science* 272 (1996) 227–234
- Ruggiano A, Foresti O, Carvalho P. ER-associated degradation: Protein quality control and beyond. *J Cell Biol* 204 (2014) 869–879
- Ruiz-Canada C, Kelleher DJ, Gilmore R. Cotranslational and posttranslational N-glycosylation of polypeptides by distinct mammalian OST isoforms. *Cell* 136 (2009) 272–283

- Russel TA, Ito M, Ito M, Yu RN, Martinson FA, Weiss J, Jameson JL. A murine model of autosomal dominant neurohypophyseal diabetes insipidus reveals progressive loss of vasopressin-producing neurons. *J Clin Invest* 112 (2003), 1697-1706
- Rutkevich LA, Williams DB. Participation of lectin chaperones and thiol oxidoreductases in protein folding within the endoplasmic reticulum. *Curr Opin Cell Biol* 23 (2011) 157–166
- Rychkova A, Warshel A. Exploring the nature of the translocon-assisted protein insertion. *Proc Natl Acad Sci USA* 110 (2013) 495–500
- Sadlish H, Pitonzo D, Johnson AE, Skach WR. Sequential triage of trans-membrane segments by Sec61alpha during biogenesis of a native multispansing membrane protein. *Nat Struct Mol Biol* 12 (2005) 870–878
- Saparov SM, Erlandson K, Cannon K, Schaletzky J, Schulman S, Rapoport TA, Pohl P. Determining the conductance of the SecY protein translocation channel for small molecules. *Mol Cell* 25;26 (2007) 501-9
- Saraogi I, Akopian D, Shan SO. A tale of two GTPases in cotranslational protein targeting. *Protein Sci* 20 (2011) 1790-5
- Schäuble N, Lang S, Jung M, Cappel S, Schorr S, Ulucan Ö, Linxweiler J, Dudek J, Blum R, Helms V, Paton AW, Paton JC, Cavalié A, Zimmermann R. BiP-mediated closing of the Sec61 channel limits Ca²⁺ leakage from the ER. *EMBO J* 31 (2012) 3282–3296
- Schindler AJ, Schekman R. In vitro reconstitution of ER-stress induced ATF6 transport in COPII vesicles. *Proc Natl Acad Sci USA* 106 (2009) 17775
- Schuldiner M, Metz J, Schmid V, Denic V, Rakwalska M, Schmitt HD, Schwappach B, Weissman JS. The GET complex mediates insertion of tail-anchored proteins into the ER membrane. *Cell* 134 (2008) 634–45
- Schwartz T, Blobel G. Structural basis for the function of the β subunit of the eukaryotic signal recognition particle receptor. *Cell* 112 (2003) 793–803
- Schweizer A, Fransen JA, Bächli T, Ginsel L, Hauri HP. Identification, by a monoclonal antibody, of a 53-kD protein associated with a tubulo-vesicular compartment at the cis-side of the Golgi apparatus. *J Cell Biol.* 107 (1988) 1643-53
- Seppälä, S, Slusky JS, Lloris-Garcera P, Rapp M, von Heijne G. Control of membrane protein topology by a single C-terminal residue. *Science* 328 (2010) 1699-1700
- Sesso A, de Faria FP, Iwamura ES, Correa H. A three-dimensional reconstruction study of the rough ER-Golgi interface in serial thin sections of the pancreatic acinar cell of the rat. *J Cell Sci* 107 (1994) 517-528
- Shao S, Hegde RS. A Calmodulin-Dependent Translocation Pathway for Small Secretory Proteins. *Cell* 147,7 (2011) 1576 – 1588
- Shao S, Hegde RS. Target selection during protein quality control. *Trends Biochem Sci*, 41,2 (2016) 124-137
- Shen K, Zhang X, Shan S. Synergistic action between the SRP RNA and translating ribosome allows efficient delivery of correct cargos during cotranslational protein targeting. *RNA* 17 (2011) 892-902
- Simon SM, Blobel G. A protein-conducting channel in the endoplasmic reticulum. *Cell*. 65 (1991) 371-80

- Sipos L, von Heijne G. Predicting the topology of eukaryotic membrane proteins. *Eur J Biochem* 213 (1993) 1333–40
- Siwiak M, Zielenkiewicz P. A comprehensive, quantitative, and genome-wide model of translation. *PLOS Comput Biol* 6 (2010) e1000865
- Sommer N, Junne T, Kalies KU, Spiess M, Hartmann E. TRAP assists membrane protein topogenesis at the mammalian ER membrane. *Biochim Biophys Acta* 1833 (2013) 3104–3111
- Stefanovic S, Hegde RS. Identification of a targeting factor for posttranslational membrane protein insertion into the ER. *Cell* 128 (2007) 1147–59
- Stevenson J, Huang EY, Olzmann JA. Endoplasmic Reticulum-associated degradation and lipid homeostasis. *Annu Rev Nutr* 36 (2016) 511–42
- Stone TA, Schiller N, von Heijne G, Deber CM. Hydrophobic blocks facilitate lipid compatibility and translocon recognition of transmembrane protein sequences. *Biochem* 54 (2015) 1465–1473
- Stone TA, Schiller N, Workewych N, von Heijne G, Deber CM. Hydrophobic clusters raise the threshold hydrophilicity for insertion of transmembrane sequences in vivo. *Biochem* 55 (2016) 5772–5779
- Tabas I, Ron D. Integrating the mechanisms of apoptosis induced by endoplasmic reticulum stress. *Nat Cell Biol* 13 (2011) 184–90
- Teilum K, Hoch JC, Goffin V, Kinet S, Martial JA, Kragelund BB. Solution structure of human prolactin. *J Mol Biol* 351 (2005) 810–823
- Thomas Y, Bui N, Strub K. A truncation in the 14 kDa protein of the signal recognition particle leads to tertiary structure changes in the RNA and abolishes the elongation arrest activity of the particle. *Nucleic Acids Res.* 25 (1997) 1920–1929
- Thor F, Gautschi M, Geiger R, Helenius A. Bulk flow revisited: Transport of a soluble protein in the secretory pathway. *Traffic* 10 (2009) 1819–1830
- Thrower JS, Hoffman L, Rechsteiner M, Pickart CM. Recognition of the polyubiquitin proteolytic signal. *EMBO J* 19 (2000), 94–102
- Tripathi A, Mandon E, Gilmore R, Rapoport TA. Two alternative binding mechanisms connect the protein translocation Sec71-Sec72 complex with heat shock proteins. *J Biol Chem* 292 (2017) 8007–8018
- Tsukazaki T, Mori H, Fukai S, Ishitani R, Mori T, Dohmae N, Perederina A, Sugita Y, Vassilyev DG, Ito K, Nureki O. Conformational transition of Sec machinery inferred from bacterial SecYE structures. *Nature* 455 (2008) 988–991
- Tsukazaki T, Mori H, Echizen Y, Ishitani R, Fukai S, Tanaka T, Perederina A, Vassilyev DG, Kohno T, Maturana AD, Ito K, Nureki O. Structure and function of a membrane component SecDF that enhances protein export. *Nature* 474 (2011) 235–38
- Valent QA, Kendall KA, High S, Kusters R, Oudega B, Lührink J. Early events in preprotein recognition in *E. coli*: interaction of SRP and trigger factor with nascent polypeptides. *EMBO J* 14 (1995) 5494–5505
- Van den Berg B, Clemons WM Jr, Collinson I, Modis Y, Hartmann E, Harrison SC, Rapoport TA. X-ray structure of a protein-conducting channel. *Nature* 427 (2004) 36–44
- Van der Sluis EO, Driessen AJM. Stepwise evolution of the Sec machinery in proteobacteria. *Trends Microbiol* 14 (2006) 105–108

- Van Valkenburgh C, Chen X, Mullins C, Fang H, Green N. The catalytic mechanism of endoplasmic reticulum signal peptidase appears to be distinct from most eubacterial signal peptidases. *J Biol Chem* 274 (1999) 11519–11525
- von Heijne G. Patterns of amino acids near signal-sequence cleavage sites. *Eur J Biochem* 133 (1983) 17-21
- von Heijne G. The distribution of positively charged residues in bacterial inner membrane proteins correlates with the trans-membrane topology. *EMBO J* 5 (1986) 3021–3027
- von Heijne G. Control of topology and mode of assembly of a polytopic membrane protein by positively charged residues. *Nature* 341 (1989) 456–458.
- Voorhees RM, Hegde RS. Structures of the scanning and engaged states of the mammalian SRP-ribosome complex. *eLife* 4 (2015) e07975
- Voorhees RM, Hegde RS. Structure of the Sec61 channel opened by a signal sequence. *Science* 351 (2016) 88-91 (I)
- Voorhees RM, Hegde RS. Toward a structural understanding of co-translational protein translocation. *Curr Opin Cell Biol* 41 (2016), 91-99 (II)
- Wahlberg JM, Spiess M. Multiple determinants direct the orientation of signal-anchor proteins: the topogenic role of the hydrophobic signal domain. *J Cell Biol* 137 (1997) 555-562
- Wang F, Brown EC, Mak G, Zhuang J, Denic V. A chaperone cascade sorts proteins for posttranslational membrane insertion into the endoplasmic reticulum. *Mol Cell* 40 (2010) 159–71
- Walter P, Blobel G. Purification of a membrane-associated protein complex required for protein translocation across the endoplasmic reticulum. *Proc Natl Acad Sci USA* 77 (1980) 7112–16
- Walter P, Blobel G. Translocation of proteins across the endoplasmic reticulum III. Signal recognition protein (SRP) causes signal sequence-dependent and site-specific arrest of chain elongation that is released by microsomal membranes. *J Cell Biol.* 1981 91(1981) 557-61
- Walter P, Blobel G. Signal recognition particle contains a 7S RNA essential for protein translocation across the endoplasmic reticulum. *Nature* 299 (1982) 691–98
- Walter P, Ron D. The unfolded protein response: from stress pathway to homeostatic regulation. *Science* 334,6059 (2011) 1081-1086
- Wessels HP, Spiess M. Insertion of a multispanning membrane protein occurs sequentially and requires only one signal sequence. *Cell* 55 (1988), 61-70
- Westermarck GT. Amyloid proteins: the beta sheet conformation and disease, 2005. p. 723–54
- Wilce MCJ, Abiular MI, Hearn MTW. Physicochemical Basis of Amino Acid Hydrophobicity Scales: Evaluation of Four New Scales of Amino Acid Hydrophobicity Coefficients Derived from RP-HPLC of Peptides. *Anal Chem* 67 (1995) 1210–1219
- Whitley P, Nillson L, von Heijne G. Three-dimensional model for the membrane segment of *Escherichia coli* leader peptidase based on disulfide mapping. *Biochem* 32 (1993) 8534-8539
- Wimley WC, Creamer TP, White SH. Solvation energies of amino acid sidechains and backbone in a family of host-guest pentapeptides. *Biochem* 35 (1996) 5109–5124
- Wimley WC, White SH. Experimentally determined hydrophobicity scale for proteins at membrane interfaces. *Nat Struct Biol* 3 (1996) 842–848

- Wu CK, Hu B, Rose JP, Liu ZJ, Nguyen TL, Zheng C, Breslow E, Wang BC. Structures of an unliganded neurophysin and its vasopressin complex: Implications for binding and allosteric mechanisms. *Prot Sci* 10 (2001) 1869–1880
- Xie K, Hessa T, Seppälä S, Rapp M, von Heijne G, Dalbey RE. Features of transmembrane segments that promote the lateral release from the translocase into the lipid phase. *Biochemistry* 46 (2007) 15153–15161
- Xu Z, Knafels JD, Yoshino K. Crystal structure of the bacterial protein export chaperone SecB. *Nat Struct Biol* 7 (2000) 1172–77
- Xu Y, Cai M, Yang Y, Huang L, Ye Y. SGTA recognizes a non-canonical ubiquitin-like domain in the Bag6-Ubl4A-Trc35 complex to promote ER-associated degradation. *Cell Rep* 2 (2012) 1633-1644
- Yohannan S, Yang D, Faham S, Boulting G, Whitelegge J, Bowie JU. Proline substitutions are not easily accommodated in a membrane protein. *J Mol Biol* 341 (2004) 1–6
- Zhang X, Schaffitzel C, Ban N, Shan S. Multiple conformational changes in a GTPase complex regulate protein targeting. *Proc Natl Acad Sci USA* 106 (2009) 1754–1759
- Zhang X, Rashid R, Wang K, Shan S. Sequential checkpoints govern fidelity during co-translational protein targeting. *Science* 328 (2010) 757–60
- Zhang B, Miller TF. Hydrophobically stabilized open state for the lateral gate of the Sec translocon. *Proc Natl Acad Sci USA* 107 (2010) 5399–5404
- Zhang B, Miller TF. Direct simulation of early-stage Sec-facilitated protein translocation. *J Am Chem Soc* 134 (2012) 13700–13707 (I)
- Zhang B, Miller TF. Long-timescale dynamics and regulation of Sec-facilitated protein translocation. *Cell Rep* 2 (2012) 927–937 (II)
- Zimmer J, Nam Y, Rapoport TA. Structure of a complex of the ATPase SecA and the protein-translocation channel. *Nature* 455 (2008) 936–43
- Zimmer J, Rapoport TA. Conformational flexibility and peptide interaction of the translocation ATPase SecA. *J Mol Biol* 394 (2009) 606–12
- Zimmermann R, Zimmermann M, Wiech H, Schlenstedt G, Müller G, Morel F, Klappa P, Jung C, Cobet WW. Ribonucleoparticle-independent transport of proteins into mammalian microsomes. *J Bioenerg Biomembr* 22 (1990) 711-23

Curriculum Vitae

Name	Erhan Demirci
Address	Pappelweg 26 4310 Rheinfelden, Switzerland
Phone	+41 78 667 28 55
Email	erhandemirci@mailbox.org
Date of birth	April 9 th , 1985
Nationality	German

Education

November 2010 to September 2017

Universität Basel

PhD thesis under Prof. Dr. Martin Spiess, Department of Biochemistry, with the title "Functional Asymmetry within the Sec61 Translocon" and the addendum "Disulfide Loops of Peptide Hormones as a Motif for Protein Aggregation"

October 2009 to October 2010

Albert-Ludwigs-Universität Freiburg

Diploma thesis under Prof. Dr. Karl-Friedrich Fischbach, Department of Biophysics and Neurobiology, with the title "Differential Localization of Misexpressed IRM Proteins in the Olfactory System of *Drosophila melanogaster*".

October 2007 to October 2009

Albert-Ludwigs-Universität Freiburg

Advanced undergraduate studies of biology. Subjects: cell biology, biochemistry, genetics, neuropathology

October 2005 to September 2007

RWTH Aachen

Basic undergraduate studies of biology

Curriculum Vitae

Publication, Posters and Teaching

Demirci E, Junne T, Baday S, Bernèche S, Spiess M. (2013) "Functional Asymmetry within the Sec61 Translocon." *PNAS*, vol. 110, no. 47, 18856-18861

Posters Biozentrum Symposium 2012, 2014
 PhD Retreat of the Biozentrum, 2011, 2012, 2015

Teaching Assistant for teaching in neurogenetics (2010) and biochemistry (2010, 2011, 2014)
 Tutorial sessions for new students "Einführung in die Biologie" (2011)

Miscellaneous

Languages German (native), English (fluent), Turkish (basic)

Software Microsoft Office, Adobe Illustrator, Adobe Photoshop, Imaris, Zen, ImageJ, Huygens Suite, ImageQuant